ADAPTIVE ENERGY-AWARE REAL-TIME DETECTION MODELS FOR CARDIAC ATRIAL FIBRILLATION

by

Redjem Bouhenguel

A Dissertation Submitted to the Faculty of

The College of Engineering and Computer Science

in Partial Fulfillment of the Requirements for the Degree of

Doctor of Philosophy

Florida Atlantic University

Boca Raton, FL

December 2012

ADAPTIVE ENERGY AWARE REAL-TIME DETECTION MODELS FOR CARDIAC ATRIAL FIBRILLATION

by

Redjem Bouhenguel

This dissertation was prepared under the direction of the candidate's dissertation advisor, Dr. Imad Mahgoub, Department of Computer, Electrical Engineering & Computer Science, and has been approved by the members of his supervisory committee. It was submitted to the faculty of the College of Engineering and Computer Science and was accepted in partial fulfillment of the requirements for the degree of Doctor of Philosophy.

SUPERVISORY COMMITTEE:

Imad Mahgoub, Ph.D.
Dissertation Advisor

Mohammad Ilyas, Ph.D.

Mihaela Cardei, Ph.D.

Ed Callaway, Ph.D.

Borko Furht, Ph.D.
Chair, Department of Computer, Electrical Engineering & Computer Science

Mohammad Ilyas, Ph.D.
Dean, College of Engineering and Computer Science

Barry T. Rosson, Ph.D.
Dean, Graduate College

November 8, 2012
Date

ACKNOWLEDGEMENTS

This journey is made possible thanks to the support and encouragement from many individuals. Having caring and talented people along the way truly gave me all the drive and motivation I needed.

I would like to express my deepest gratitude to my dissertation advisor, Dr. Imad Mahgoub, whose infinite patience, unselfish guidance, thoughtful advice, and contagious enthusiasm made the journey memorable. Thanks to my committee members, Dr. Mohammad Ilyas, Dr. Mihaela Cardei, and Dr. Ed Callaway, for devoting their time to provide encouragement and constructive comments throughout the process. Additional thanks go to Dr. Mohammad Ilyas for his helpful insight and unwavering support. I also offer my deep appreciation to Jean Mangiaracina and Debra Szabo, for their help and guidance with the administrative process.

I am indebted to my wife, Debbie, for her patience and understanding, not to mention the long nights proofreading my publications and dissertation work. I am grateful to our two wonderful sons, Adam and Jason, who kept me focused, and remind me daily of the joy of learning, and discovery. I am forever delighted by their friendship, emotional support and technical contributions. Also, thanks to my parents-in-law, sister and her husband, brothers, and their families, and to my colleagues in the mobile computing lab.

Finally, I would like to acknowledge my late father who instilled in me the sense of "it is never too late."

The early work of this doctorate was supported by a Secure Telecommunications Grant from the U.S. Department of Defense.

ABSTRACT

Author:	Redjem Bouhenguel
Title:	Adaptive Energy-aware Real-time Detection Models for Cardiac Atrial Fibrillation
Institution:	Florida Atlantic University
Dissertation Advisor:	Dr. Imad Mahgoub
Degree:	Doctor of Philosophy
Year:	2012

Though several clinical monitoring ways exist and have been applied to detect cardiac atrial fibrillation (A-Fib) and other arrhythmia, these medical interventions and the ensuing clinical treatments are after the fact and costly. Current portable healthcare monitoring systems come in the form of Ambulatory Event Monitors. They are small, battery-operated electrocardiograph devices used to record the heart's rhythm and activity. However, they are not energy-aware; they are not personalized; they require long battery life, and ultimately fall short on delivering real-time continuous detection of arrhythmia and specifically progressive development of cardiac A-Fib. The focus of this dissertation is the design of a class of adaptive and efficient energy-aware real-time detection models for monitoring, early real-time detection and reporting of progressive development of cardiac A-Fib. The design realizes the personalized energy-aware models by using a baseline energy model and incorporating a real-time detection algorithm for

the onset of A-Fib using individual A-Fib risk factors, A-Fib incidence rates, and A-Fib prevalence circadian windows. We combine ubiquitous smartphone platforms, Bluetooth wireless personal area networking, and bio-sensing technology to derive personalized energy models that rival today's A-Fib monitoring devices. We compare the energy contributed from each energy-aware model to the energy from the baseline model known as the telemetry model. Given a low A-Fib risk factor, for an A-Fib incidence rate of 0.02, and a prevalence window of 4 hours, our energy-aware model reduces energy consumption by as much as 66%. We further extend the detection of A-Fib to the paroxysmal phase, and derive the total energy-aware model for the detection and reporting of A-Fib from its onset to its final stage. The design promises to have a greater positive public health impact from predicting A-Fib and providing a viable approach to meeting the energy needs of current and future real-time monitoring, detecting and reporting required in wearable computing healthcare applications that are constrained by scarce energy resources.

DEDICATION

To my wife, Debbie
And our sons, Adam and Jason

ADAPTIVE ENERGY-AWARE REAL-TIME DETECTION MODELS FOR CARDIAC ATRIAL FIBRILLATION

LIST OF TABLES

LIST OF FIGURES

CHAPTER 1

1. INTRODUCTION

A plethora of mobile applications ranging from games to network services to healthcare are growing in popularity and becoming an integral part of personal daily life. The quality and the performance of these mobile applications are constantly improving. The significant progress in mobile hardware technology, wireless personal area networking, wireless security and bio-sensing technology using Bluetooth has helped propel the smartphone platform into new areas of on-body healthcare monitoring and detection. Future wearable computing devices will have the ability to continuously sense, analyze and report medical ailments such as cardiac arrhythmia. They will also need to balance innovative interfaces, energy management, network resources, and privacy concerns. In addition, they must be ready, unrestrictive, not monopolizing of user attention, attentive to the environment, useful as a communication tool, personal, observable and easily controllable by the user. The devices have to be hands-free or espouse hands-limited portability; they can be event-triggered or can run continuously. They must be cost-effective to economically monitor a patient's health on a continuous basis and rival the more traditional, cumbersome and significantly more expensive, stationary monitoring system located in an emergency room or a hospital. They must be able to collect biomedical data continuously over a long period in advance of the start of a serious health problem. Today, the traditional healthcare monitoring system takes only a small snapshot

of data collected when a patient who is already sick, is admitted to the hospital or emergency room. The focus of this dissertation is the design of a class of adaptive and efficient energy-aware models for real-time monitoring, early detection and reporting of progressive development of cardiac A-Fib. Wearable devices face high performance requirements in the middle of energy constraint challenges. Studies and research suggest various methods to minimize power consumption in mobile devices. Study [1] suggests a trade-off between power-saving and detection accuracy or performance; they show how power can be saved at the loss of a small amount of accuracy by applying different techniques using a low power real-time epilepsy seizure detection algorithm. The authors of [2] describe a framework that is used to reduce the energy consumption of sensors by temporarily turning them off. In study [3], the battery life is extended by as much as 30% through a collaborative relationship between the operating system and applications. In [4], the authors propose ways to enable systems to trade computational accuracy for resources by scaling down the data or feature set for use on a remote healthcare system. The study reports significant resource savings for small amounts of utility degradation, e.g., 33% of bandwidth saving for only a 1% of accuracy degradation. In project [5], the battery life of a wireless healthcare system is optimized using a dynamic scheduling technique by efficiently assigning tasks to the available resources. The dissertation includes the implementation of a risk assessment algorithm and the design of an incidence based A-Fib detection scheme for wearable healthcare computing devices. Related work in biomedicine and information technology introduced various algorithms for diagnosing and detecting different types of arrhythmia, and developed cardiovascular disease prediction algorithms. The Framingham Heart study [6] developed a risk score to

calculate individual risk of developing atrial fibrillation and a development framework for researcher. The work by [7] developed a prediction model to detect tachycardia and send alerts to a designated care center for appropriate medical action. The research funded by the Health Technology Assessment Program addresses the accuracy of electrocardiogram (EKG a.k.a. ECG) for the diagnosis of A-Fib and the potential risk of A-Fib misinterpretation errors [8]. A mobile medical device, dubbed HeartSaver [9] was developed to monitor the onset of atrial fibrillation and other cardiac pathologies. Other related work deals with the classification of arrhythmia and the performance of machine learning algorithms such as OneR, J48 and Naïve Bayes [10] but does not address logistic regression, a machine learning algorithm adopted in this dissertation.

1.1 Motivation of the problem

Given the imminent healthcare crisis threatening the aging world population, especially in developed countries, current healthcare systems and services are inadequate and mal-structured. They are not fit to handle the necessary continuous healthcare monitoring for the aging millions. They cannot proactively diagnose or predict ailments because patients do not visit physicians frequently, and as a result, when they visit their doctor, problems have already begun.

Today, most hospitals and medical institutions offer excellent inpatient care for major chronic disease; however, they lack daily preventive care and interaction with their outpatients, especially before and after surgery or hospital discharge, when diagnosing some ailments such as cardiac A-Fib. The American College of Cardiology and the American Heart Association define A-Fib as a supraventricular tachyarrhythmia characterized by uncoordinated atrial activation accompanied by the deterioration of

atrial mechanical function. A-Fib is the most prevalent arrhythmia in the United States and accounts for more than 750,000 strokes per year [11]. The cost to treat A-Fib in the United States exceeds $6.4 billion per year [12]. Approximately four million Americans suffer from recurrent arrhythmias. Serious arrhythmia is responsible for 500,000 deaths annually [13]. Hospitals treat about 850,000 people annually for arrhythmia. The only outpatient interaction occurs when seeing doctors, but people visit doctors rarely or infrequently and typically visit them after problems have already started. The average patient's condition progressively deteriorates for five days before seeking emergency treatment [14]. Only a small snapshot of data is collected when a patient who is already sick, is admitted to the hospital or emergency room. Furthermore, current healthcare monitoring and detection systems are expensive, cumbersome and generally restricted to more populated areas.

Current portable healthcare monitoring systems come in the form of Ambulatory Event Monitors. They are small, battery-operated electrocardiograph devices used to record the heart's rhythm. These on-body healthcare devices fall short on delivering real-time continuous monitoring and detection, and are plagued by technological challenges, which are exacerbated by energy constraints, process optimization problems, data security risks and interference, among others. Developing and deploying new proactive healthcare technologies will alleviate the looming crisis by extending services from hospitals into homes all over the world. Typical wearable computing devices shown in Figure 1, will keep people out of overburdened hospitals and emergency rooms by continuously monitoring and providing feedback of a patient's physiological and vital signals. They

will sense, store and process the acquired data on the local, on-body network, or on a remote server.

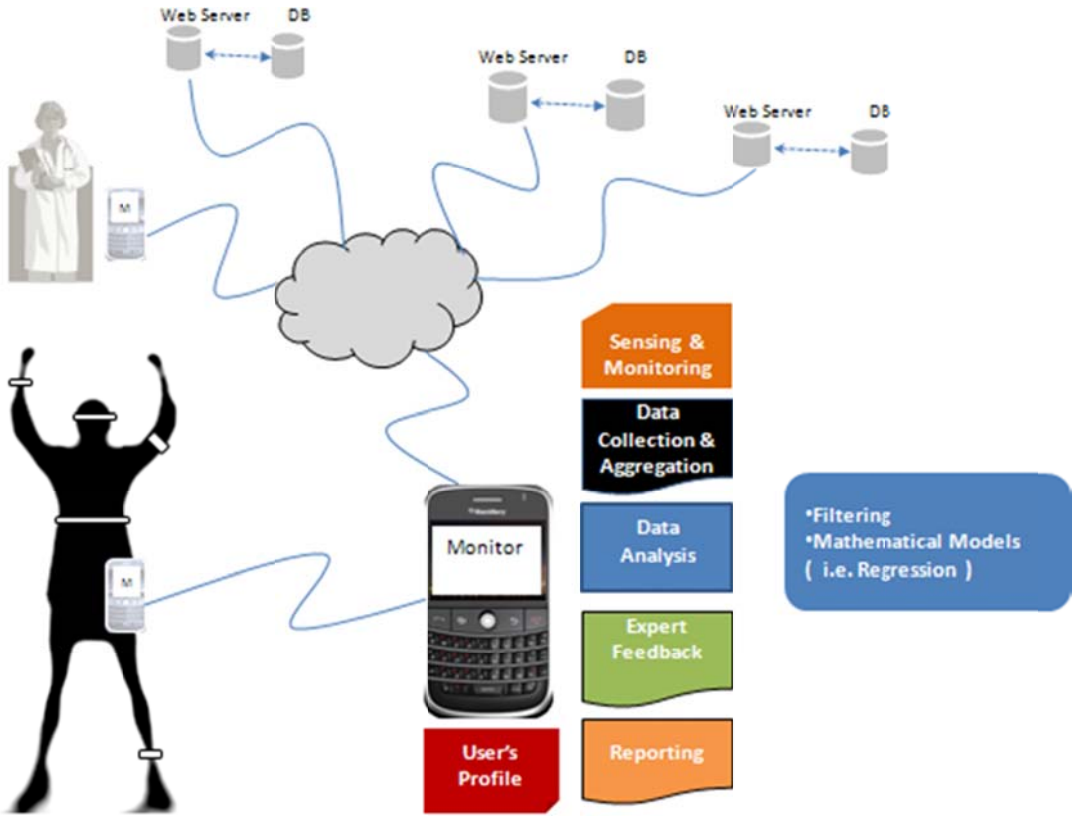

Figure 1: Monitoring and detecting A-Fib

1.2 Problem Statement

The goal of this dissertation is to deliver adaptive energy-aware models for the monitoring, detection and reporting of progressive development of A-Fib. These energy models would extend battery life in a wearable healthcare computing device.

The cost associated with the utilization of emergency rooms and hospitalization to treat A-Fib is exorbitant [15]. The average direct cost of a patient with A-Fib was estimated to be more than five times the cost of a non-AFIB individual [16]. Many healthcare providers are actively seeking cost-effective solutions to monitor symptoms suggestive of

cardiac arrhythmias, i.e., palpitations, dizziness, or syncope, a brief loss of consciousness caused by a temporary decrease in blood flow to the brain. Existing devices include Ambulatory Event Monitors (AEMs) and outpatient cardiac telemetry. In-progress development promises to deliver wearable healthcare computing devices that continuously monitor physiological patient information, analyze and report abnormal medical conditions. However, these niceties quickly drain the small device batteries. In order for these devices to be ubiquitously adapted, biomedical researchers and computer engineers need to solve central technological problems that deal with short battery life, energy management and energy optimization.

1.2.1 Current AEMs and outpatient cardiac telemetry face challenges

Today, cardiac arrhythmia is diagnosed under the supervision of a physician using various diagnostic methods and tools. Healthcare monitoring solutions are designed on a fixed hardware and software platform. They are not modular and are instead implemented as 'one size fits all'. Current healthcare monitoring solutions do not adjust or adapt to different users profiles or medical needs and analyses. Patients have to physically visit health centers to receive devices and be hooked up, which is a transportation hardship for many individuals who live in poor, remote areas. Current healthcare monitoring solutions are designed to work over a scheduled or pre-programmed period of time, but monitoring is ineffective for patients who experience infrequent symptoms outside the scheduled period. Moreover, arrhythmia of very short duration would be difficult to record. Existing event monitoring stores a limited number of events. The analysis feedback and results are delayed because EKG data and logged patient's daily activities are first downloaded to a computer. Certified technicians and doctors in remote medical centers review and

analyze the data before a full report is generated and communicated to the patient. These solutions are not seamless; they require patient interaction and device activation. The devices are carried by the patient and activated when symptoms are present in order to record the heart electrical impulses. The symptoms might last only a short period. The procedure becomes impractical when the patient is incapacitated during symptomatic periods.

1.2.1.1 Current solutions lack energy optimization

Energy optimization is not addressed in current solutions, and battery consumption is not efficiently budgeted. Mobile computing introduces healthcare application opportunities but provides new challenges. The major challenges stem from energy shortage, limited CPU speed, constrained resources such as cache and on-board memory, wireless data security and privacy risks, wireless network unpredictability, latency and interference. Mobile computing healthcare applications are steadily on the rise because mobile computing devices are getting less expensive, smaller and more wearable. Today healthcare wearable computing requires flexible user interface/interactivity, 'plug and play' functionality, and high performance computing. These requirements impose severe hardship on energy-constrained mobile computing environments.

1.3 Contributions

- The design of a class of adaptive and efficient energy-aware models for real-time early detection of cardiac A-Fib that incorporate a real-time detection algorithm, individual A-Fib risk factor, A-Fib incidence rate, and A-Fib prevalence circadian window. For example, given an A-Fib risk factor, an A-Fib incidence rate of 0.02,

and a prevalence window of 4 hours, the proposed energy-aware model reduces the energy consumption by as much as 66%.

- Bridging the gap between health science and engineering by introducing machine-learning techniques in deriving atrial fibrillation algorithms.
- The design of A-Fib classification/detection algorithms using J48, Naïve Bayes, and logistic regression. Future work may use other techniques such as support vector machines, neural networks, and Fast Fourier.
- The selection of best fit A-Fib detection algorithm using performance measurements and accuracy comparison. The logistic regression algorithm is slightly more accurate and is selected for its ease of portability and embedding in wearable devices.
- The recognition of the A-Fib incidence rate as it relates to the positive rate of the logistic regression detection algorithm. If the detection algorithm is as accurate as the cardiologist's interpretation of EKG readings, then having a detection positive rate equal to the clinical incidence rate gives our energy-aware model the best energy performance.
- The discovery that the duration and distribution of A-Fib episodes during a circadian cycle play important roles in scheduling the monitoring and detection of A-Fib.
- The assessment of individual A-Fib risk factors as they contribute to scheduling the monitoring and detection of A-Fib.

- The validation of the proposed energy-aware models using a commercial heart monitor device and demonstration of the efficiency of the proposed energy-aware models.

1.4 Organization

The dissertation goal is to design adaptive, energy-aware schemes for the detection and reporting of progressive development of cardiac A-Fib. It bridges both biomedical research and computer engineering. The dissertation is divided into two main parts: The first part includes chapters 2, 3 and 4, which contain medical and data mining literature surveys. The second part includes chapters 5, 6, 7, 8, 9 and 10, which contain the design of adaptive energy-aware models.

- Chapters 2, 3 and 4 contain technical and medical literature to provide an understanding of the heart's electrical system, EKG Interpretation, types of arrhythmia, current arrhythmia monitoring and detection methods, shortcomings of Holter Monitors, event monitors, and mobile outpatient cardiac telemetry. They survey machine-learning classification methods in healthcare, particularly the logistic regression model and its classification detection accuracy measurements. Studying the heart's electrical system and the intrinsic electrical activity of the heart under normal and abnormal heart rhythms is necessary for the interpretation of EKG information related to A-Fib and for determining predictors for A-Fib detection. Chapters 2, 3 and 4 are the subject of a book chapter titled "Cardiac Arrhythmia Monitoring and Detection Techniques in Wearable Healthcare Computing Device" [98].

- Chapters 5, 6, 7, 8, 9, and 10 present the design of adaptive energy-aware models for the real-time early detection and reporting of progressive development of cardiac A-Fib [92][93]. The design realizes the primary and hybrid energy models by incorporating features that include an A-Fib risk factor, an A-Fib incidence rate, a prevalence window, and an A-Fib detection algorithm. As a prerequisite to designing such energy models, the energy requirements for the current healthcare monitoring devices and the energy requirements for wearable healthcare computing devices are determined. Next, a telemetry energy model, which is used as a reference, and the wearable computing energy models are developed. Using the telemetry energy as reference, each energy model is compared to the telemetry energy model. The results are validated using a two-lead EKG Heart Monitor A102D7 device from Alive Technologies wirelessly connected to an Apple MacBook computer via Bluetooth.

CHAPTER 2

2. EKG INTERPRETATION AND ARRHYTHMIA MONITORING

Technical and medical literature surveyed provides an understanding of the heart's electrical system, EKG interpretation, types of arrhythmia, current arrhythmia monitoring and detection methods, and the shortcomings of Holter Monitors, event monitors, and mobile outpatient cardiac telemetry. Understanding how to detect cardiac arrhythmias and more specifically A-Fib, which is the focus of this dissertation, is a prerequisite to interpreting A-Fib detection results. Studying the heart's electrical system and the intrinsic electrical activity of the heart under normal and abnormal heart rhythms is necessary for the interpretation of EKG information related to A-Fib and for determining predictors for A-Fib. Current portable battery-operated arrhythmia monitoring devices such as Holter monitors, event monitors, and Mobile Cardiac Outpatient Telemetry monitors are analyzed in order to pinpoint their shortcomings concerning energy awareness and detection of arrhythmia. Just as important, applying data mining and machine-learning classification methods to healthcare monitoring and detection help predict A-Fib.

2.1 Understanding the electrical system of the heart and arrhythmia

The following sections survey literature explaining the internal electrical system of the heart and the different types of cardiac arrhythmias. First, we look at a normal cardiac

sinus rhythm, then, learn how the heart activities are monitored and recorded on an EKG. We identify A-Fib as being the most common cardiac arrhythmia as well as one of the most dangerous.

2.1.1 Understanding the heart's electrical system

Understanding the heart's internal electrical system helps in understanding arrhythmia. The heart's electrical system controls the rate and rhythm of the heartbeat. With each heartbeat, an electrical signal starts at the top of the heart and propagates to the bottom of the heart. As the signal travels, it causes the heart to contract and pump blood.

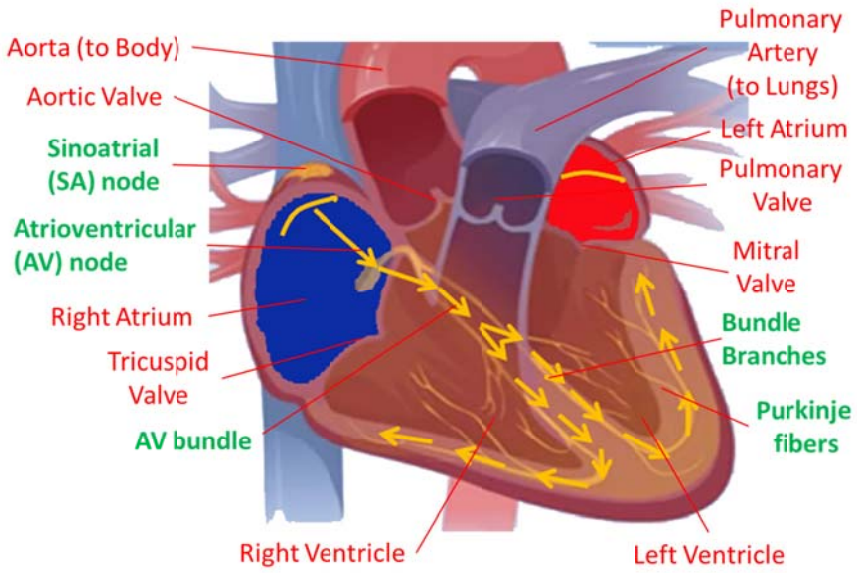

Figure 2: Chambers and valves of the heart

The heart muscle, or myocardium (Greek: myos = muscle, kardia = heart; Latin -ium = diminutive), naturally contracts when it is electrically stimulated. The heart (see Figure 2) has four chambers: right atrium, right ventricle, left atrium and left ventricle. The interior of the heart muscle is made up of cells (myocytes). When the heart is at rest, myocytes are negatively charged (polarized), whereas when the heart contracts the myocytes become positively charged (depolarized) [17]. Some cells form heart connective tissue

and other cells grow into heart valves. Muscle cells give the heart its ability to beat and pump blood throughout the body. A single cell beats when a complex series of gates – called ion channels - open and close in an organized manner. If the myocyte cells do not beat in unison, heart arrhythmias can occur. Three ions, sodium ion (Na^+), calcium ion (Ca^{++}) and potassium ion (K^+), maintain the cardiac electrical system. The controlled movement of Na^+ ions, Ca^{++}ions, and K^+ ions provides the cardiac functions and physiology. The sodium ions are responsible for initiating the myocyte depolarization as well as the electrical conduction through the myocardium. The calcium ions are responsible for the heart contractions. The potassium ions are responsible for the re-polarization as well as the maintenance of the reference potential. The conduction system keeps the heart beating in a normal rhythm and allows the continuous exchange of oxygen-rich blood with oxygen-poor blood. Each electrical signal begins in a group of cells called the sinus node, or sino-atrial (SA) node, located in the right atrium (the upper right chamber of the heart). A normal, healthy adult heart at rest beats 60 to 100 times a minute. The electrical signal (see Figures 2, 3 and 4), generated in the SA node, travels through special pathways in the right and left atria and causes the atria to contract and pump blood into the heart's two lower chambers, the ventricles. When the electrical signal reaches the atrio-ventricular (AV) node, located between the atria and the ventricles, it is delayed to wait for the ventricles to fill with blood. Next, the electrical signal leaves the AV node and travels along a pathway known as the Bundle of His. The Bundle of His divides into a right bundle branch and a left bundle branch. The signal goes down the right bundle branch and left bundle branch to the ventricles, causing them to contract and pump blood out to the lungs and the rest of the body. The ventricles then

relax, and the heartbeat process starts all over again in the SA node. A problem with any part of this process can cause an arrhythmia.

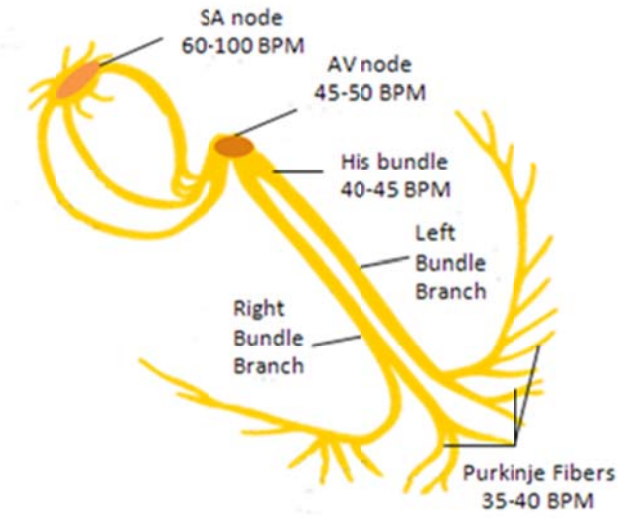

Figure 3: Understanding the heart's electrical system

Doctors occasionally identify heart arrhythmias during a routine check-up. In some people, arrhythmias do not provide any signs or symptoms, while in others; the signs and symptoms of heart arrhythmias are very noticeable and may cause some distress**.** The common symptoms of arrhythmia include a feeling of tiredness or light-headedness, palpitations, pain in the chest, shortness of breath, and loss of consciousness.

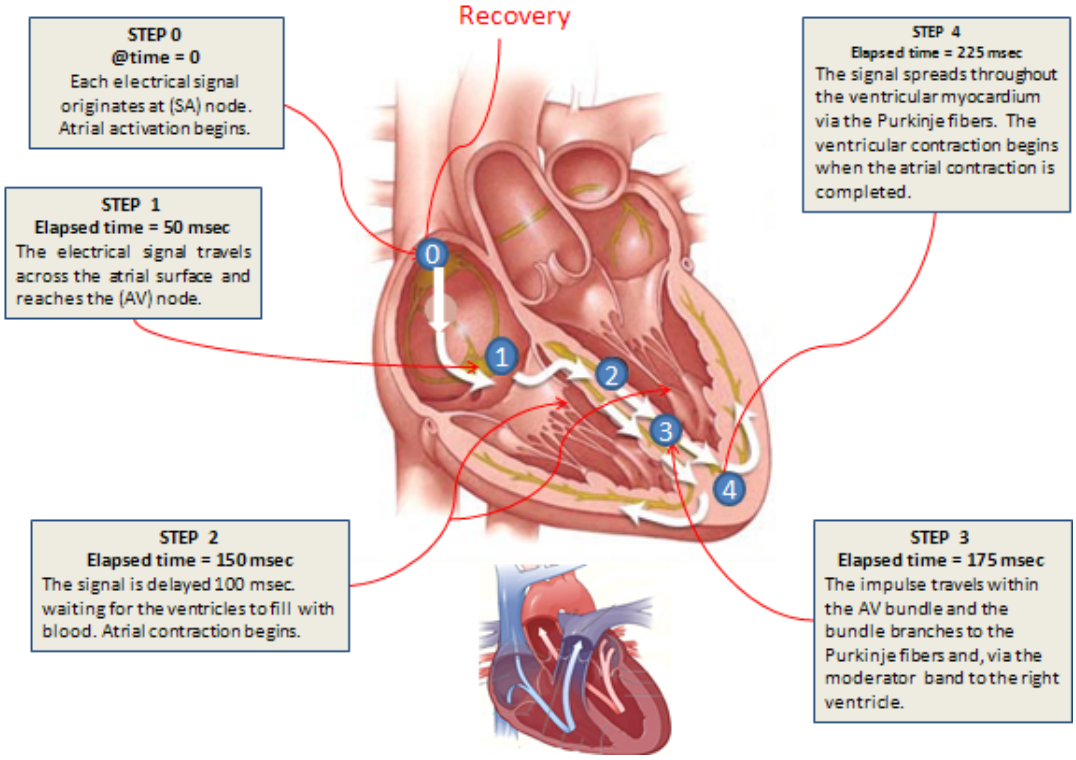

Figure 4: Intrinsic electrical activity of the heart [104]

2.1.2 Normal heart rhythm

A normal heartbeat begins when an electrical signal is sent by a tiny cluster of cells called the sinus node. The signal then traverses the atria and passes through the atrio-ventricular node. Next, the signal travels through the ventricles, causing them to contract and pump out blood. The process recovers and repeats. Figure 5 explains a normal heart rhythm process.

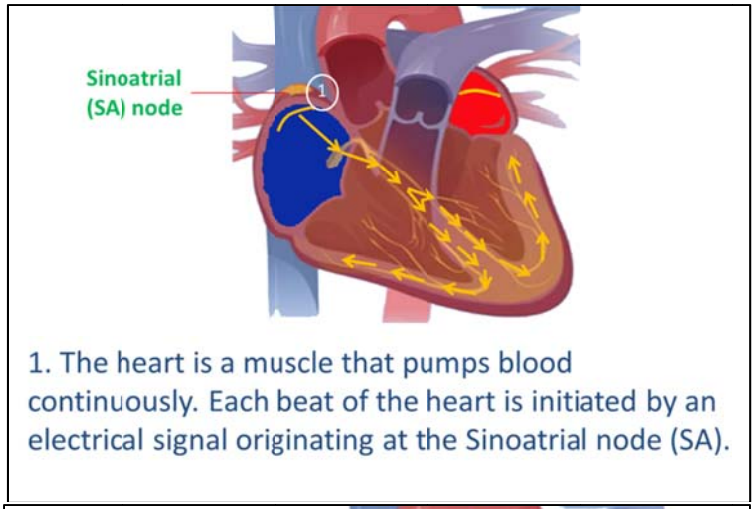

1. The heart is a muscle that pumps blood continuously. Each beat of the heart is initiated by an electrical signal originating at the Sinoatrial node (SA).

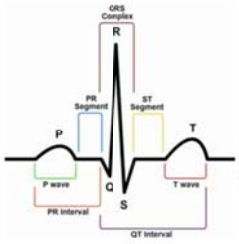

EKG Diagram

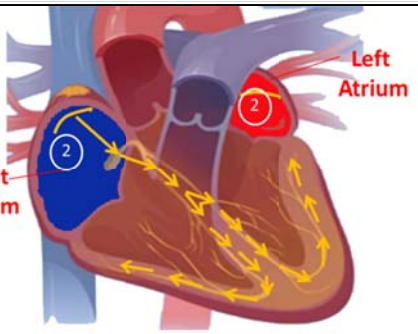

2. When the right atrium is full of blood, the signal spreads across the cells of the left and right atria causing the atria to contract.

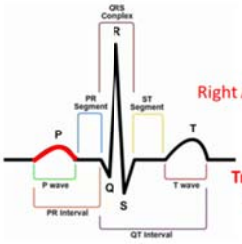

Atrial Depolarization

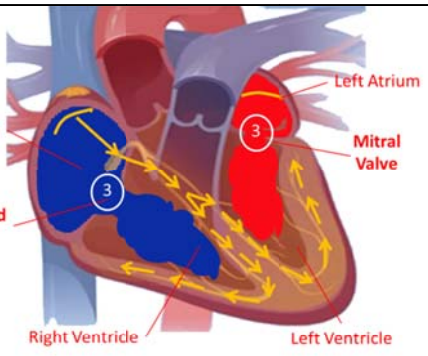

3. The blood is squeezed through the open valves from the atria into both ventricles. The contraction of the atria is indicated by the P wave on the EKG.

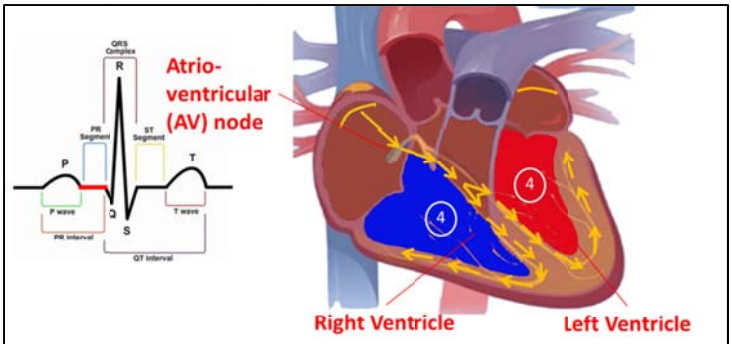

4. The signal reaches the atrioventricular (AV) node. There is a 100 msec delay to allow the ventricles to fill with blood, represented by the line segment between P and Q wave.

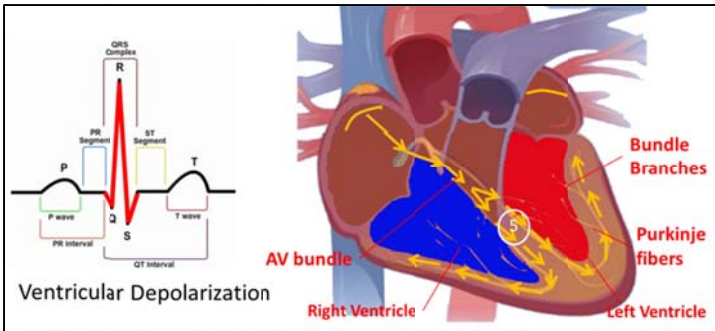

5. The signal travels through the left and right branches to the Purkinje fibers and spreads across the ventricles. Both ventricles contract. The left ventricle contracts slightly before the right ventricle.

- The contraction of the left ventricle is indicated by the R wave.
- The contraction of the right ventricle is marked by the S wave.

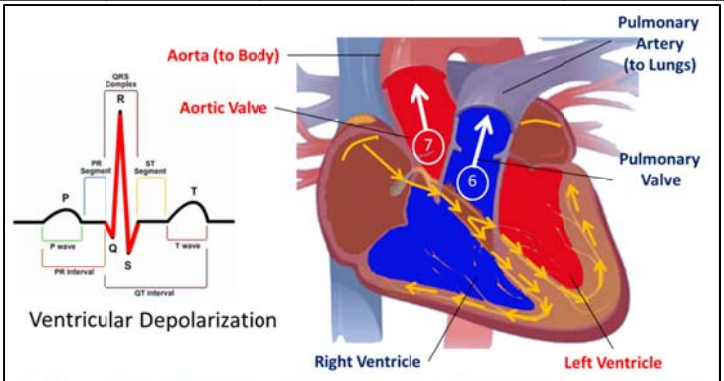

6. The contraction of the right ventricle forces blood through the pulmonary valve to the lungs.

7. The contraction of the left ventricle forces blood through the aortic valve to the rest of the body.

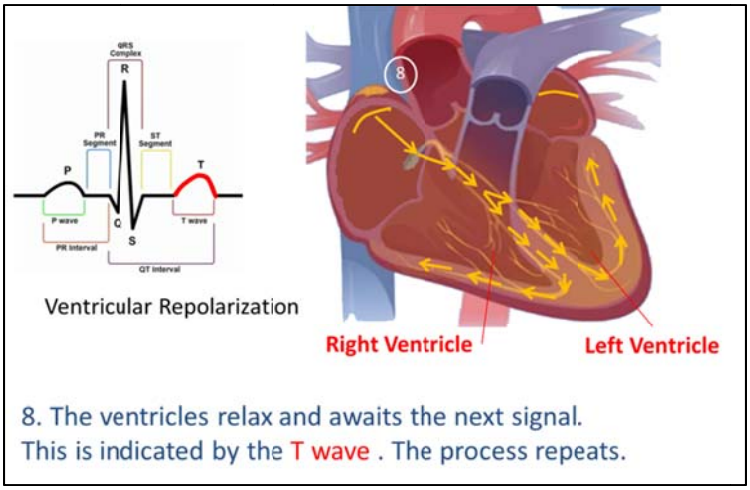

Figure 5: Normal heart rhythm

2.1.3 EKG Interpretation

The standard 12-lead electrocardiogram is a depiction of the heart's electrical activity recorded from electrodes placed on specific locations on the body and translated into line tracings on graph paper (see Table 1 for an example of electrocardiogram electrodes placement). It plots the relative timing of a traveling impulse through the atria, AV conduction system and ventricles on graph paper. The standard EKG is made up of 12 separate leads: six limb leads and six chest leads. A limb lead records signals from electrodes connected to a left leg, a right arm and a left arm. A chest lead records signals through suction cup electrodes positioned at six different positions on the chest. The conditional standard for reading the EKG using the three locations for electrodes was originally used by Willem Einthoven [99]. The EKG is recorded on 1 mm by 1 mm graph paper (see Figures 6 and 7). It utilizes a long strip or a large sheet. Every fifth line is a heavy line forming a square of 5 by 5 smaller squares. The graph has a time axis and an amplitude (voltage) axis. A cardiac event is displayed as a wave that has height and depth. The wave has either an upward or downward deflection or direction, and an

amplitude or magnitude. Segments of baseline may have elevation or depression. All measurements are in millimeters (mm).

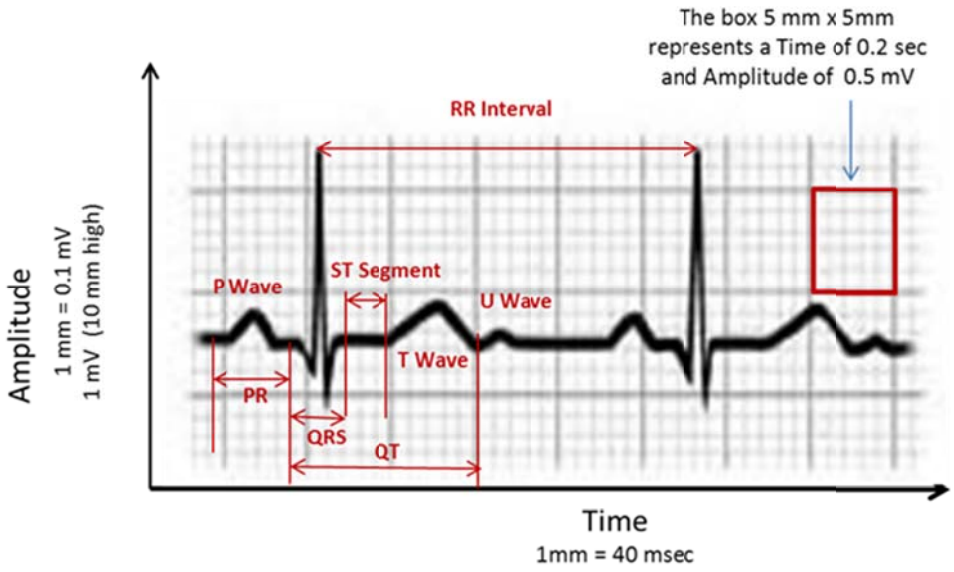

Figure 6: EKG waves and intervals

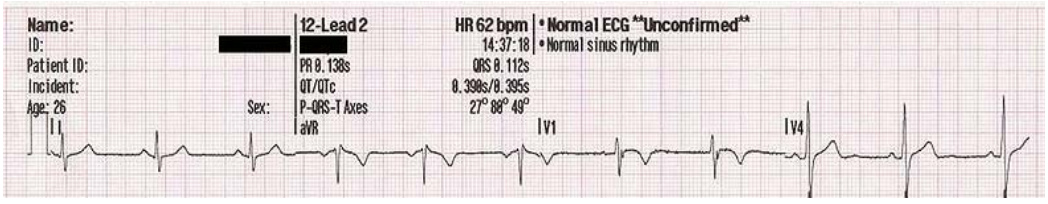

Figure 7: The EKG is recorded on 1 mm by 1 mm graph paper [17]

The EKG waves and intervals explained below are used to describe the heart electrical signals (see Figure 6 and 7):

- P wave: The P wave represents the wave of depolarization that spreads from the SA node throughout the atria, and is usually between 0.08 and 0.1 seconds in duration. Atrial rate is calculated by determining the time interval between P waves.

- PR interval: The PR interval is the period from the onset of the P wave to the beginning of the QRS complex, which normally ranges from 0.12 to 0.20 seconds. This interval represents the time between the onset of atrial depolarization and the onset of ventricular depolarization.
- QRS complex: The QRS complex represents ventricular depolarization consisting of the Q, R, and S waves. Normally, the QRS interval is 0.06 to 0.10 sec.
- QT interval: The QT interval is the time between onset of ventricular depolarization and end of ventricular repolarization. The QT interval (< 0.44 sec) must be corrected for heart rate using the $QTc = \frac{QT}{\sqrt{RR}}$ where QT_c is the corrected QT interval; R-R interval is the time between 2 QRS complexes.
- ST segment: The ST segment represents completed ventricular myocardial depolarization. Normally, it is horizontal along the baseline of the PR (or TP) intervals or slightly off baseline.
- T wave: The T wave reflects ventricular repolarization. It usually takes the same direction as the QRS complex (concordance); opposite polarity (discordance) may indicate past or current infarction.
- The U wave's origin is not clearly understood but the consensus is it probably represents "after depolarization" in the ventricles.
- The PP interval is the duration of the atrial cycle; it is an indicator of the atrial rate.

Electrode label (in the USA)	Electrode placement
RA	On the right arm, avoiding bony prominences.
LA	In the same location that RA was placed, but on the left arm this time.
RL	On the right leg, avoiding bony prominences.
LL	In the same location that RL was placed, but on the left leg this time.
V1	In the *fourth* intercostal space (between ribs 4 & 5) just to the *right* of the sternum (breastbone).
V2	In the *fourth* inter-costal space (between ribs 4 & 5) just to the *left* of the sternum.
V3	Between leads V2 and V4.
V4	In the fifth inter-costal space (between ribs 5 & 6) in the mid- clavicular line (the imaginary line that extends down from the midpoint of the clavicle (collarbone).
V5	Horizontally even with V4, but in the anterior axillary line. (The anterior axillary line is the imaginary line that runs down from the point midway between the middle of the clavicle and the lateral end of the clavicle; the lateral end of the collarbone is the end closer to the arm.)
V6	Horizontally even with V4 and V5 in the mid axillary line. (The mid axillary line is the imaginary line that extends down from the middle of the patient's armpit.)

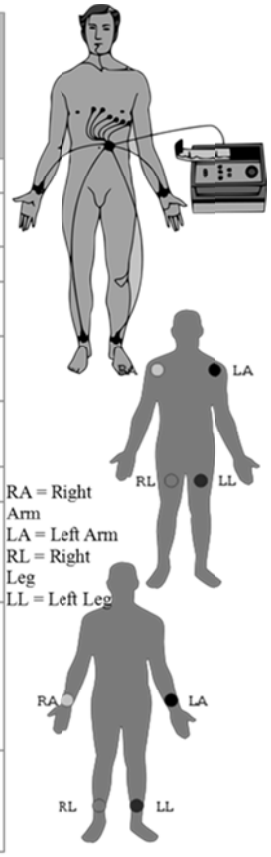

Table 1: Example of electrocardiogram electrodes placement

The 12-lead electrocardiogram is carefully measured and analyzed in order to determine abnormalities of the waveforms. Usually, the analysis of the waveforms is performed in the order in which they appear: P waves, QRS complexes, ST segments, T waves, and U waves. The physician examines the P wave width and height, checks the QRS complex width, the ST segments elevation and/or depression, the T wave height and direction, and the U wave size and direction.

Though there are cases when atrial and ventricular rates are different, the phrase "heart rate" typically refers to ventricular contractions but determining rates for both atrial and ventricular rates is important. Using the EKG rhythm strip with recording taken from Lead II, the atrial rate is determined by measuring the time intervals between P waves (P-

R intervals) [18]. Similarly, ventricular rate is determined by measuring the time intervals between the QRS complexes, or by measuring the R-R intervals (see Figure 8).

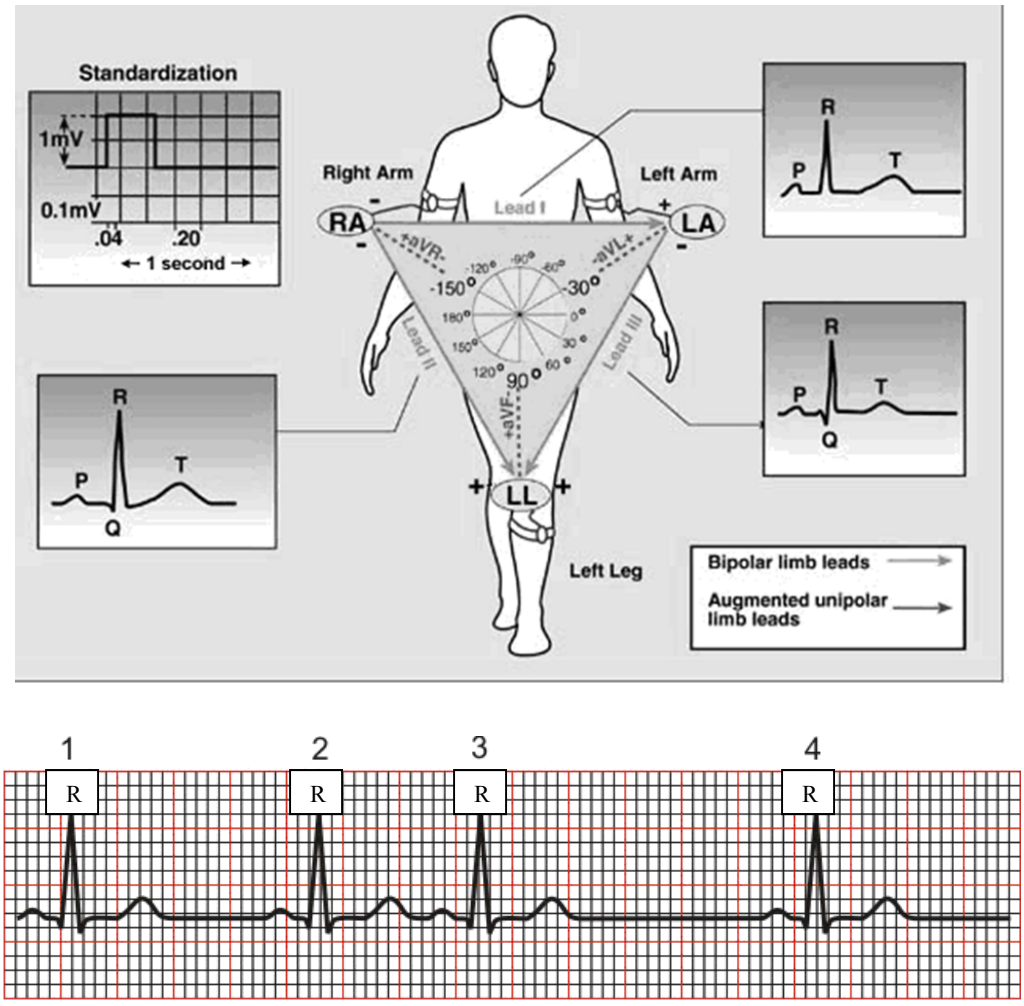

Figure 8: Example of standard limb EKG leads and EKG record strip [101]

Ventricular rate measurements: Assuming the recording EKG strip speed of 25 mm/sec, the following rates: 1500-300 - 150 - 100 - 75 - 60 may be used to calculate a heart rate: *Method 1*: divide 1500 by the number of small squares between two R waves. The rate between beats R1 and R2 in the above tracing is 68 beats per minute, i.e. 1500/22.

Method 2: divide 300 by the number of large squares (red boxes in this diagram) between two R waves. The rate between beats R1 and R2 in the above tracing is 68 beats per minute, i.e. 300/4.4.

Method 3: count the number of large squares between two R waves with the following rates: 300 - 150 - 100 - 75 - 60. For example, if there are four large squares between two R waves, then the rate is 75 beats per minute. Extrapolation is sometimes needed between squares.

Atrial rate measurement: Atrial rate measurements are calculated similarly to the ventricular rate however, the P waves are used.

If the heart is in sinus rhythm and if there is a P wave for every QRS complete then the atrial rate is equal to the ventricular rate.

If the rhythm is not consistent, that is the distances between the R waves are different, a time-averaged rate over a 10 second interval or longer is calculated. Using the EKG recording strip above where the recording time scale is 25 mm per second, the rate is 75 beats per minute if there are 12.5 beats in 10 seconds [17] [101].

2.1.4 Understanding cardiac arrhythmia and A-Fib

Cardiac arrhythmia, a common and mostly harmless condition, is defined by the presence of irregular heartbeats. For many people, the experience usually goes unnoticed. They feel as if the heart has skipped a beat, or has given an unexpected flutter. However, some arrhythmia can be extremely dangerous and require medical treatment. Today, cardiac arrhythmia is diagnosed under the supervision of a physician using various diagnostic methods and tools. Arrhythmia could be due to strong emotions, excessive exercise,

Coronary Artery Disease (CAD), electrolyte (i.e., Sodium or Potassium) imbalances in the blood, changes in the heart muscle, injury from heart attack and the post-heart surgery healing process. Sudden cardiac death (SCD) is a major cause of mortality in industrialized nations [100]. People, especially the young, usually die from SCD asymptomatically. Fatal arrhythmias are due to either genetic defects and/or mechanical dysfunction and ischemic events (reduced blood supply to the heart). Patients who survive life threatening ventricular arrhythmias remain at high risk of fatal arrhythmia. The bad news: treatment for SCD has not progressed.

2.1.5 Types of Arrhythmia

Arrhythmia [19] varies in severity, point of origin, and the speed at which it causes the heart to beat. Arrhythmia can be generally classified into three types, based on the heart rate: Tachycardia, Bradycardia, and premature heartbeats. Tachycardia occurs when a heartbeat is regular (i.e., sinus rhythm) but the rate is more than 100 beats per minute. Bradycardia takes place when a heartbeat is regular but the rate is less than 60 beats per minute. Premature heartbeats are revealed as an extra beat between two normal heartbeats; they are generally not unsafe and do not damage the heart.

These arrhythmias are not necessarily dangerous unless they occur unexpectedly. During an aerobic exercise or while having an anxiety attack, the normal heart rate is expected to be greater than 100 beats per minute.

2.1.5.1 Atrial Arrhythmia:

These types of arrhythmia originate in the atria such as the A-Fib, the Atrial Flutter, and the Supra-Ventricular Tachycardia (SVT).

2.1.5.1.1 A-Fib:

The American College of Cardiology and the American Heart Association define A-Fib as a supraventricular tachyarrhythmia characterized by uncoordinated atrial activation accompanied by the deterioration of atrial mechanical function [19] [20]. On an EKG diagram, A-Fib is characterized by the absence of P waves replaced by rapid oscillations or irregular waves that vary in size, shape, and timing [20]. Normal rhythm begins in the sino-atrial node but in A-Fib the electrical signals originate in a different part of the atria where they become uncoordinated, with an irregular pattern (see Figure 9).

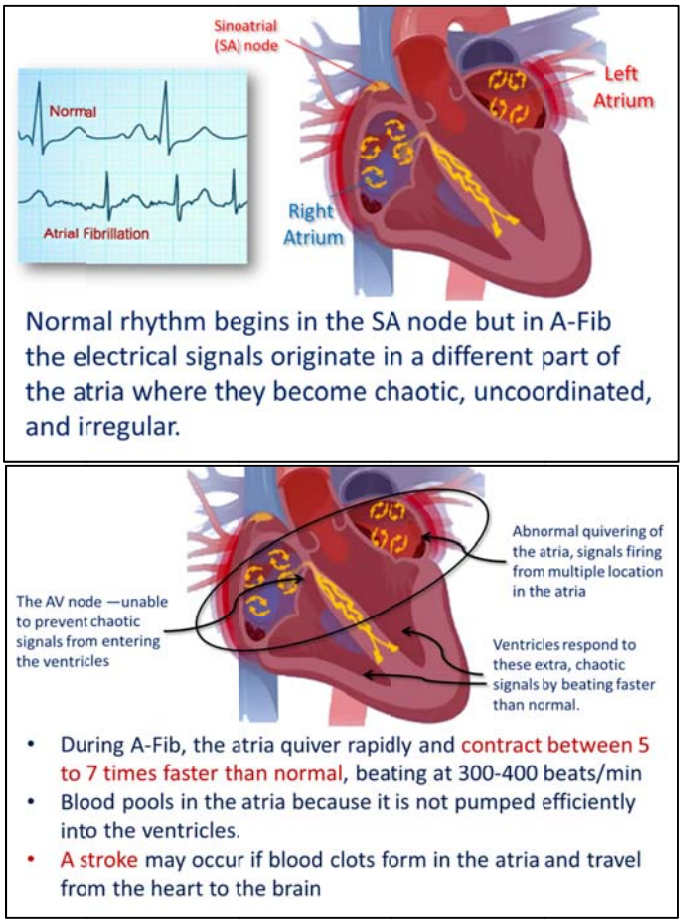

Figure 9: A-Fib activity

The atria pump the blood at an unusually fast and irregular rate without the heart fully contracting. The heart's two small upper chambers or atria quiver instead of beating effectively. The heart may beat at about 300-400 beats per minute and contract between five to seven times faster than normal. Blood may pool and clot because it is not pumped completely out of the atria. A blood clot in the atria may end up lodged in an artery in the brain, resulting in a stroke. A-Fib, a potentially dangerous condition, may lead to chronic fatigue, heart rhythm problems, congestive heart failure and in extreme cases, a stroke.

A-Fib Type	Defining Characteristics
First A-Fib detected	Only one diagnosed episode that lasts longer than 30 seconds when the heart is in and out of normal sinus rhythm.
Paroxysmal or intermittent A-Fib	– The heart is in and out of normal sinus rhythm. – Episodes of A-Fib come and go on their own. – Episodes typically last less than 24 hours but can last up to seven days before they terminate spontaneously.
Persistent A-Fib	– Episodes last longer than seven days. – Episodes do not go away on their own. – Medical treatment is necessary to restore normal sinus rhythm.
Longstanding persistent A-Fib	– Episodes of A-Fib are continuous. – Episodes last longer than one year.
Permanent A-Fib	A person's irregular heartbeat does not return to normal sinus rhythm, even with medical treatment.

Table 2: Progressive development of A-Fib

A-Fib is responsible for about 15 percent of the strokes occurring in people with A-Fib. A-Fib is a condition found in 2.2 million Americans [21] but a study conducted by the Mayo Clinic in Minnesota estimates that A-Fib would affect 15.9 million by 2050 [22]. The likelihood of developing A-Fib increases with age. Three to five percent of people over age 65 have A-Fib [21][22]. After the first A-Fib is detected, there are four

predominant types of A-Fib: Paroxysmal, persistent, longstanding persistent and permanent (see Table 2).

2.1.5.1.2 Atrial Flutter:

Atrial Flutter is similar to A-Fib, except there is only a single electrical wave that circulates very rapidly in the atria. The heart beats irregularly and rapidly, between 230–380 beats per minute [19] [20].

2.1.5.1.3 Supra-Ventricular Tachycardia (SVT):

Usually not harmful, Supra-Ventricular (or Supraventricular) Tachycardia is a type of tachycardia that originates either in the atria or in the middle region. It makes the heart beat very fast in a regular rhythm for periods of time [19] [20].

2.1.5.1.4 Premature Atrial Contraction (PAC):

Premature Atrial Contraction (PAC) is a type of tachycardia that is common in children and teenagers. PAC starts in the atria causing premature beats or extra beats that result in irregular heart rhythms [19] [20].

2.1.5.1.5 Sick Sinus syndrome:

Sick Sinus syndrome occurs when the heart rhythm may switch between having bradycardia (a slow heartbeat rate) and tachycardia (a fast heartbeat rate) because the sino-atrial node does not fire the signals properly [19] [20].

2.1.5.1.6 Sinus Arrhythmia:

Sinus Arrhythmia is a condition in which the heart rate varies with breathing.

2.1.5.1.7 Sinus Tachycardia:

Sinus Tachycardia occurs when the heart experiences transient rapid heartbeat such as in response to fever, excitement, anxiety, stress, or exercise.

2.1.5.1.8 Wolff-Parkinson-White (WPW) syndrome:

Wolff-Parkinson-White (WPW) syndrome is the name given to episodes when there are abnormal pathways for the electrical signals to travel between the atria and ventricles. The electrical impulses go down one pathway from the atria to the ventricles and then return to the atria through the other pathway, often accompanied with a fast heart rate [19] [20].

2.1.5.2 Ventricular Arrhythmias:

Ventricular Arrhythmias originate in the ventricles. They are typically fatal and therefore require immediate medical attention [19] [20].

2.1.5.2.1 Ventricular Tachycardia (VT):

Ventricular Tachycardia (VT) is a rapid heartbeat that originates in the ventricles. The heart beats at a rate of more than 100 beats per minute, with at least three irregular heartbeats in a row [19] [20].

2.1.5.2.2 Premature Ventricular Contraction (PVC):

Premature Ventricular Contraction is a type of arrhythmia that originates in one of the ventricles. It is caused by extra, abnormal heartbeats that disrupt the regular heart rhythm, sometimes causing a feeling of a skipped beat. PVCs are very common in normal children and teenagers [19] [20].

2.1.5.2.3 Ventricular Fibrillation:

Ventricular Fibrillation is a type of arrhythmia triggered by chaotic electrical activity, which leads to rapid, unsynchronized ventricular contractions. The heart pumps little or no blood during this episode of Ventricular Fibrillation, resulting in the patient's collapse or even sudden death [19] [20].

2.1.6 Arrhythmia treatments

Drugs that treat arrhythmia are called anti-arrhythmic drugs. They affect ion channels involved in the movement, suppressing arrhythmia by altering the movement of sodium, calcium and potassium ions going in and out of the cell. As a result, they affect the electrical activity of pacemaker and non-pacemaker cells.

The following sections survey literature on current arrhythmia testing methodology and current portable healthcare monitoring systems. The different types of portable arrhythmia testing devices and shortcomings are described.

2.1.7 Current arrhythmia monitoring and detection methods

Today, cardiac arrhythmia may be diagnosed under the supervision of a physician using various methods and tools. Passive and active tests may be scripted to detect cardiac arrhythmia ranging from blood tests, to electrocardiogram tests, to Holter monitoring, etc. Passive tests are intended to check for cardiac arrhythmia during periods of normal activity. Active tests are designed to induce arrhythmia in a closely monitored situation so that it can be observed by a physician. Current portable healthcare monitoring systems come in the form of Ambulatory Event Monitors (AEMs). They are small, portable electrocardiograph (EKG) devices that are used to record the heart's rhythm (Figure 10).

2.1.7.1 Holter monitor

A Holter monitor is a portable EKG recorder that is worn during normal daily activities (including sleeping) over a period lasting typically 24 to 48 hours, in order to determine whether there is a problem with the heart. The Holter monitor test offers a more comprehensive picture of the heart's health than the regular EKG, which monitors the heart's electrical activity during a short session in a doctor's office. Its electrodes are

placed on the skin of patient's chest. Leads from the electrodes are connected to an electronic box that is worn on a belt or carried with a shoulder strap. The electrical heart impulses are continuously recorded and stored. A patient wearing a Holter monitor keeps a diary of the daily activities and occurring symptoms, such as chest palpitations, rapid heartbeats, feeling of dizziness or faintness. The logged activities and symptoms are communicated to a physician. The data is downloaded to a computer and checked for any heart rhythm abnormalities. A full report, including a printout of abnormal heart rhythms, is generated.

2.1.7.2 Event monitor

Event monitoring is a diagnostic alternative to Holter monitoring in patients who experience infrequent symptoms (less frequently than every 48 hours) suggestive of cardiac arrhythmias (i.e., palpitations, dizziness, pre-syncope, or syncope). Electrodes are placed on the skin of patient's chest. Leads from the electrodes are connected to an electronic box, which is worn on a belt or shoulder strap. When a patient feels symptoms, he depresses a button to activate the recorder. The monitor records the heart electrical impulses for 60 seconds prior to the button being pushed and up to 40 seconds afterwards. The event monitor can store up to three events. The recorded data is ultimately transmitted either to a physician's office or to a central recording station. If the reading indicates arrhythmia, the patient will be instructed to go to the emergency room.

2.1.7.3 Mobile Outpatient Cardiac Telemetry

Mobile Cardiac Outpatient Telemetry (MCOT) allows continuous heartbeat monitoring lasting a few days. This device consists of a small sensor attached to three electrode pads, worn either as a pendant on a chain around the neck or on a belt clip. The sensor sends

each heartbeat to a handheld monitor. When the monitor detects a heart rhythm problem, it automatically transmits EKG information to the CardioNet [23] monitoring center. At the CardioNet center, certified cardiac technicians analyze each transmission, respond appropriately to each event and transmit diagnostic reports to the authorized physician. The patient may use the touch screen on the CardioNet monitor to transmit the EKG from any felt symptom to the CardioNet monitoring center. Integrated symptom and EKG data can help doctors rule in, or rule out, cardiac causes for symptoms such as dizziness and fainting.

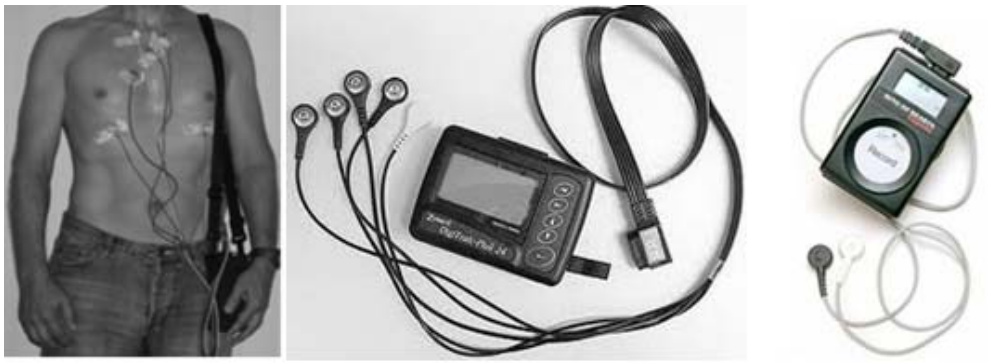

Figure 10: Holter monitor (left and middle), Event monitor (right)

2.1.7.4 Shortcomings of monitoring

Holter and Event monitors have shortcomings. They are ineffective for patients who experience infrequent symptoms outside the typical monitoring period of 24 to 48 hours. These types of monitors require a patient's activation and interaction, which is impractical when the patient is incapacitated during symptomatic periods.

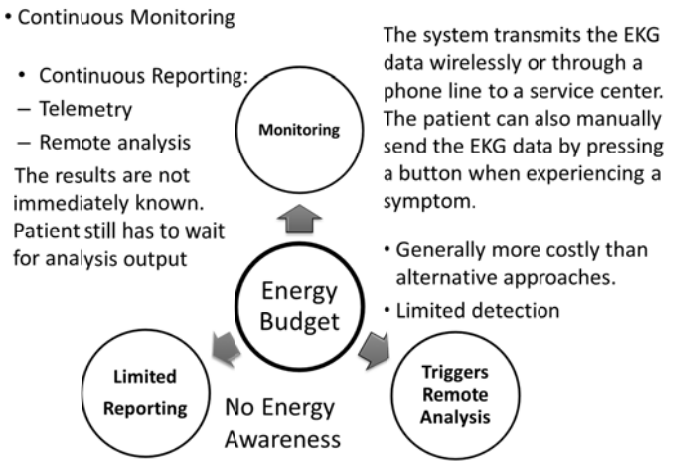

Figure 11: Mobile Outpatient Cardiac Telemetry represented in the scheme

In addition, the patient has no knowledge of the state of his health while wearing the monitor. Only a snapshot of recordings is sent to the monitoring center and the results are not immediately known. The patient has to wait for the results of the data analysis and medical recommendations performed by a remote care center.

Mobile Outpatient Cardiac Telemetry is generally more costly than alternate approaches. The device is not practical for patients who experience infrequent (less frequently than every 48 hours) symptoms suggestive of cardiac arrhythmias (i.e., palpitations, dizziness, pre-syncope, or syncope). Figure 11 summarizes some of the concerns using telemetry devices.

2.1.7.5 Echocardiogram

The echocardiogram test creates moving pictures of the beating heart. It sends sound waves into the heart muscle, which are then bounced back to the monitoring device. An Echocardiogram provides information about how well the heart chambers and valves are functioning, determines the shape and the size of the heart, and identifies areas of defective heart muscle and poor blood flow.

2.1.7.6 Electrophysiological study (EPS)

An electrophysiological study is a more invasive procedure; it is used to assess serious arrhythmia. During an electrophysiological test, a thin flexible wire or catheter is passed to the heart by going through peripheral veins or peripheral arteries. The cardiac electrical signals are recorded at various points to detect the point of origin of tachycardia. The wire can be used to trigger an arrhythmia by electrically stimulating the heart. This process helps the doctor to determine whether medication can stop the arrhythmia.

2.1.7.7 Esophageal electrophysiological procedure

The esophageal electrophysiological procedure records cardiac electrical signals by inserting a thin, supple, and flexible plastic tube through a nostril and positioning it in the esophagus. An electric stimulator is used to make the heart beat faster and trigger an arrhythmia.

2.1.7.8 Treadmill testing

Treadmill testing requires the patient to walk or jog on an exercise treadmill. It is prescribed for patients who are suspected of experiencing arrhythmia. The heart rate and rhythm are monitored while the patient is exercising on a treadmill.

2.1.7.9 Blood tests

Blood tests measure the sodium, potassium and thyroid hormone levels.

2.1.7.10 Electrocardiogram (EKG)

The Electrocardiogram (EKG) records the cardiac electrical activity and other information about the heart's structure and health status, such as rhythm and rate, by connecting electrodes to the surface of the skin. Sensors or electrodes from the EKG machine are placed on the skin to detect the heart's electrical activities. The different

signals emanating from the heart are recorded on scrolling paper and/or memory devices for further analysis.

2.2 Wireless privacy and interference concerns

Advances in wireless sensor and networking technologies have been extended to wearable computing systems. They provide a multitude of opportunities in the development and integration of pervasive wireless communication for new and existing specialized technologies in monitoring, data collection, and real-time analysis and reporting. Today, healthcare applications can utilize wireless technologies such as Bluetooth, Zigbee, RFID, UWB, Wireless Local Area Networks (WLAN), Wireless Metropolitan Area Networks (WMAN), and Wireless Wide Area Networks (WWAN). Although some of these wireless network solutions are acceptably secure, the nature of the wireless ad hoc and the device addressing schemes still make them vulnerable to possible attacks and privacy risks [24].

2.2.1 Bluetooth technology

In a Personal Area Network (PAN), Bluetooth frees mobile workers and allows them to work unhindered while managing multiple devices.

Bluetooth operates in the unlicensed 2.4 gigahertz (GHz) to 2.4835 GHz ISM (Industrial, Scientific, and Medical) frequency band. This bandwidth is commonly used by other technologies such as the IEEE 802.11b/g WLAN standard, making it prone to interference. The Bluetooth standard aims at guaranteeing reliability and robustness in the presence of such interference through the utilization of Frequency-Hopping Spread Spectrum (FHSS) and Error Correction techniques. Such a claim generated increasing demand from the industrial, military and healthcare worlds and motivated research

groups to perform specific environmental field tests on wireless communication involving Bluetooth units. Several tests have concluded that Bluetooth is reliable enough in industrial applications for monitoring conditions. Bluetooth robustness stems from FHSS technique, which makes the protocol particularly robust in an environment where interference from other radiating sources exists. Today, compared to other personal electronics devices currently allowed in use on passenger airplanes during flight, Bluetooth is classed as an intentional radiator. The test results show that the levels of intentional emissions as well as spurious emissions from Bluetooth devices did not interfere with the aircraft systems while in flight [25].

Bluetooth technology protocol supports voice and data communication. It provides built-in security, serial and TCP/IP networking integration in both one-to-one and one-to-many networking topologies. The protocol is regulated by governments worldwide. A plethora of modern mobile devices incorporates Bluetooth technology to track and monitor individual social interaction and location [26]. Bluetooth technology positions itself well in the Wireless Personal Area Network (WPAN) and in the Body Area Network (BAN).

2.2.2 Bluetooth in wearable computing applications

Bluetooth architecture offers built-in security features that accommodate the simplest of applications. It also provides adequate support for the most demanding security requirements imposed on various Bluetooth healthcare applications. Bluetooth is a low-cost, low-power technology, primarily used in short-range radio frequency (RF) communication. It is used to establish wireless ad hoc or peer-to-peer (P2P) communication between a wide variety of devices for the transfer of voice and data in a personal area network. Bluetooth technology is pervasive in many consumer devices,

including smartphones, headsets, personal digital assistants (PDA), laptops, automobiles, printers, and wearable healthcare computing devices, among others.

A wearable computing Bluetooth network topology is comprised of a piconet and scatternet topologies. A Bluetooth device operating in master mode can communicate with up to seven slave devices. Piconet (see Figure 12) is a Bluetooth network that contains one master and at least one slave within range sharing the same channel. When Bluetooth devices come within range of each other, they automatically connect to each other. One of them is the master and the rest are slaves. The master Bluetooth device controls all the wireless traffic. It sends its own unique device address (similar to an Ethernet address) and the value of its internal clock. This information helps the network to calculate the frequency-hop sequence.

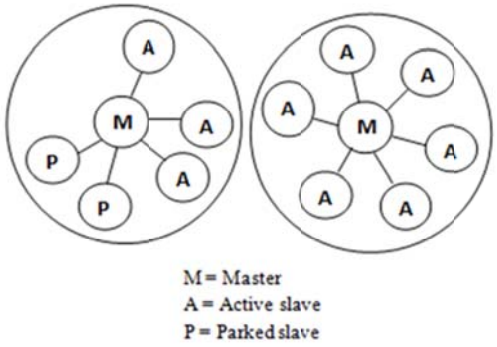

Figure 12: Bluetooth piconets

The slaves on the other hand, take commands from the master. Slave devices in a piconet can assume the following power-saving modes: active, sniff, hold or parked.

Bluetooth device address is preconfigured with a unique 48-bit number (IEEE 802 hardware or MAC address) [27]. A 3-bit address number is used to indicate whether a Bluetooth device is active in a piconet, and an 8-bit address is used to indicate a parked

Bluetooth device. Each piconet can include one master and up to seven slaves. Multiple piconets can cover the same area.

A Bluetooth device can be a member of multiple overlapping piconets. When connections exist between a group of piconets, a scatternet is formed. A Bluetooth device can be master in only one piconet but a slave in many different piconets. Master and slave roles can be switched between Bluetooth devices in a piconet.

2.2.3 Bluetooth security methodology

Bluetooth provides security in three ways:

- It uses pseudo-random frequency hopping to solve the problem of interference from other signals after transmitting or receiving a packet.
- It utilizes authentication to restrict connectivity to devices. Authentication is initiated when the device is in security mode 2 or in security mode 3.
- It employs encryption to use secret keys where only authorized users can make data intelligible again.

A. Frequency-hopping scheme

Bluetooth uses frequency-hopping spread spectrum (FHSS) when transmitting signals (see Figure 13). It hops (i.e., changes) between Bluetooth devices using 79 different radio channels using frequencies of approximately 1600 times per second for data/voice links and 3200 times per second during page and inquiry scanning [24].

A channel is used for a very short period (e.g. 625 microseconds for data/voice links), followed by a hop marked by a pre-determined pseudo-random sequence to another channel as shown in Figure 13. The frequency-hopping scheme enables the Bluetooth device to avoid interference with other devices. Bluetooth also allows for radio link

power control, a low power consumption adaptation output scheme, where devices can negotiate and adjust their radio power consumption relative to the transmitted signal intensity. The Bluetooth power control feature blocks any potential adversary to pose a threat to a Bluetooth piconet. The combination of a frequency-hopping scheme and radio link power control provide Bluetooth with some additional protection from eavesdropping and malicious access.

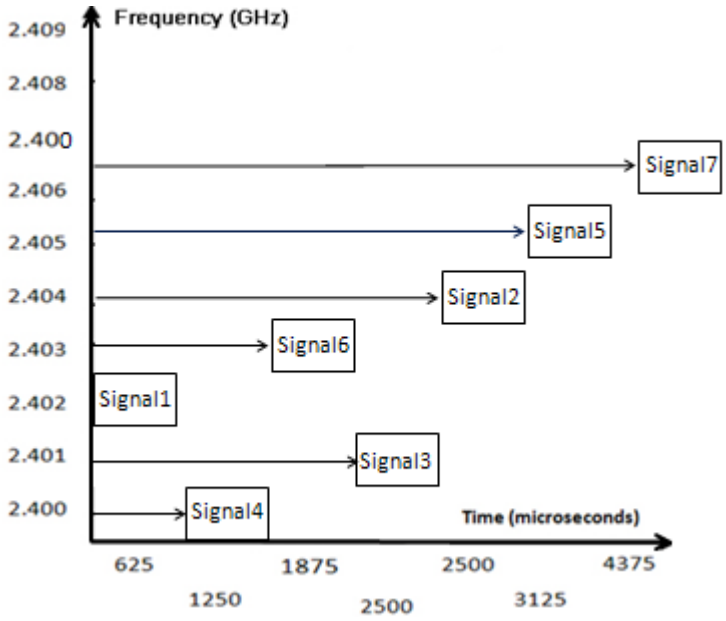

Figure 13: Bluetooth Frequency Hopping Spread Spectrum [27]

Because Bluetooth devices use the ISM band in its entirety, and transmit from a fixed frequency in very short periods, they guarantee that any interference will be short-lived. This makes it very difficult for an eavesdropping device to predict which frequency will be used next by the Bluetooth devices. The Bluetooth specification ensures that connected devices agree on the next frequency to use by first defining a master-slave relationship between Bluetooth devices, and second by specifying an algorithm, that uses device-specific information to calculate random frequency-hop sequences. Spread

spectrum transmissions are less affected by outside signal interference since any noise interference is likely to influence only a small portion of the signal and not impact the entire signal. Bluetooth security is implemented in the generic access profile through two methods, an authentication process and a choice of security modes. Bluetooth technology arrived with security key types namely, the authentication generation keys, and the ciphering keys.

B. Authentication and Ciphering

Security in Bluetooth uses symmetric key cryptographic mechanisms for authentication, link encryption, and key generation. In Bluetooth, an authentication mechanism called *link key* is used to determine that a link is established. The result of a successful pairing between two Bluetooth devices will generate a link key that the two devices will use for authentication and a link encryption. Bluetooth uses two types of link keys: temporary keys and semi-permanent keys. The latter is composed of unit keys and combination keys. A unit key is a link key that is generated by a specific Bluetooth device and used as a link key with another Bluetooth device. It is used when there is full trust among the devices that are paired with the same unit key. Since Bluetooth version 1.2, unit keys have been deprecated. On the other hand, a combination key is a link key that a device generates in combination with another Bluetooth device. Besides the combination and the unit keys, there are two other key types called temporary keys: the initialization key and the master key. The initialization key exists temporarily during the pairing of two devices. The master key is a link key generated by a master prior to the setup of an encrypted broadcast communication. There are three other link keys of interest, called ciphering keys: the encryption key K_C, the constrained encryption key K'_C and the

payload key K_P. The encryption key K_C is the main key that controls the ciphering. This key may have too many bits that exceed an allowed key length, at which point K_C is replaced by the constrained encryption key K'_C [28].

C. Security Modes

All Bluetooth-enabled devices implement the Generic Access Profile. This profile defines a security model that includes three security modes:

1) Security Mode 1:

- Mode 1 is an insecure mode of operation. It provides no security.
- When a Bluetooth device is in security mode 1, no security procedure is initiated.
- Devices operating in this mode are able to pair with devices operating in the same mode because neither device implements security controls.

2) Security Mode 2:

- Mode 2, known as service-level enforced security, provides security at the service level, after the channel has been established. This mode enables applications to run in parallel and have different access policies.
- When a Bluetooth device is in security mode 2, no security procedure is initiated before a channel establishment request has been received or a channel establishment procedure has been initiated by itself.
- Devices operating in this mode enforce service level security at the L2CAP layer and above by invoking a combination of authorization and authentication schemes.

3) Security Mode 3:

- Mode 3, known as link-level enforced security, provides security at the link level before the channel is established.
- Link encryption is enforced by devices operating in mode 3 at the LMP layer.

4) Security Mode 4:

Security Mode 4 calls for Bluetooth services to use an authenticated link key, an unauthenticated link key, or no security at all. In this mode, Secure Simple Pairing (SSP) is used to simplify the pairing process, and protect against passive eavesdropping and man-in-the-middle attacks by utilizing a public key cryptography. Secure Simple Pairing offers four association models: Numeric Comparison, Passkey Entry, Just Works, and Out of Band.

In the Numeric Comparison model, both pairing devices display a six digit number and allow the user to enter a "yes' response if the numbers match. A "no" response makes the pairing fail. A Passkey Entry association model is offered for Secure Simple Pairing of two Bluetooth devices where one device has input capability such as Bluetooth enabled keyboard and the second device has no input capability. A six-digit number is entered into the device with the keyboard capability and shown to the other device with the display-only capability. Both Numeric Comparison and Passkey Entry association models do not incorporate the six-digit number into the link key generation, therefore an attacker finds no value to the six-digit number. The Just Works association model is applicable where either one or both pairing devices lack a display for viewing the six-digit number or a keyboard for inputting it. In this case, the user is forced to accept the pairing connection without being able to verify the six-digit number allowing for man-in-the-middle protection to fail. Finally, the Out of Band association model supports a wireless

technology alternative to Bluetooth such as Near Field. This model performs device pairing by having the user accept the pairing by pushing a button on the device following tapping one device against the other. Except for the Just Works association model, all of the association models described above provide authenticated link keys.

D. Trust Levels and Service Levels

Bluetooth provides two levels of trust and three levels of service security. The two levels of trust are trusted and un-trusted. A trusted Bluetooth device has full access to all services, whereas an un-trusted device does not have an established relationship with another Bluetooth device, and as a result receives restricted access to services.

The three levels of Bluetooth service security deal with authorization, authentication, and encryption. Service Level 1 requires both authorization and authentication. Automatic access is granted only to trusted units; as for un-trusted devices, manual authorization is required. Service Level 2 requires authentication only; authorization is not necessary. Service Level 3 requires no authentication, access is granted automatically to all devices.

E. Bluetooth potential security risks

Bluetooth protocol is a Personal Area Network (PAN) protocol used in devices that communicate wirelessly with one another when within 300 feet. Bluetooth is designed to run in a peer-to-peer short-range wireless network. If the security of Bluetooth is compromised, and if one or more devices in the network are used as gateways to other connected networks, it could expose the devices or their attached networks. Bluetooth supports third party extensions. The security of a device or local network connected to these extensions could be compromised if these extensions do not use proper security and authentication procedures.

CHAPTER 3

3 APPLYING MACHINE LEARNING METHODS TO PREDICT A-FIB

Classification is learning a function that maps (classifies) a data item into one of several predefined classes [29].

”A computer program is said to learn from experience E with respect to some task T and some performance measure P, if its performance on T, as measured by P, improves with experience E” [30]. Data mining is a task used to discover unknown rules, patterns and relationships hidden in vast amount of raw data that is available as datasets stored in databases [31]. Machine learning is the study of methods and algorithms that learn and improve their performance with experience. Few machine learning algorithms and statistical approaches have been applied in medical applications; for example, algorithmic and statistical approaches for finding biomarkers that could be potential factors causing prostate cancer among African American men [32], classification of electrocardiogram arrhythmias using neural networks [33], EKG arrhythmia classification based on logistic model tree [34], and analysis of EKG signals using self-organizing maps (SOM). Much of the related work dealing with classification of cardiac arrhythmia has been based on neural networks, Markov chain models and support vector machines (SVMs).

Although several clinical ways exist and have been applied to treat arrhythmia, these medical interventions and clinical treatments come after the fact and are expensive. Moreover they do not come without risks to the patients [35]; there would be a greater

positive public health impact from predicting arrhythmia and preventing heart attacks. This detection can be regarded as a general classification/prediction problem.

3.1 Data mining overview

Data became ubiquitous, and new technologies have made retrieval of large amounts of data easy and fast. Uncovering meaningful information and hidden patterns from the data remain keys to the success of research. The goal of data mining is to extract knowledge and hidden patterns from the data. "Data mining is the process of extracting valid, previously unknown, comprehensible, and actionable information from large databases and using it to make crucial business decisions." [36]. Data mining relies on technologies such as statistics, machine learning, and databases, to facilitate the uncovering of information from the data. Statistics is concerned with parameters and characteristics of the data whereas machine learning derives models and patterns from the data. Database technology stores and manages data for selective data retrieval. Data mining is not an exact science. Human interaction is sometimes required to decipher ambiguities during the four phases of data mining process: data collection, data pre-processing, data mining and information evaluation and interpretation. Classical data mining tasks such as classification, clustering, and association are used repeatedly in bioinformatics. The following overview will review each task (Figure 14 illustrates a graphical representation and visualization of the data mining process).

3.2 Data cleaning and data pre-processing

Biomedical data is highly distributed and sometimes uncontrollably generated. Data may contain information that simply does not make sense and must be cleaned. Data cleaning defined as a pre-processing step is an essential procedure in data mining to ensure

accuracy, completeness, and consistency of data [37]. Understanding the data and how it was gathered before proceeding with data cleaning helps eliminate outliers and data corruption.

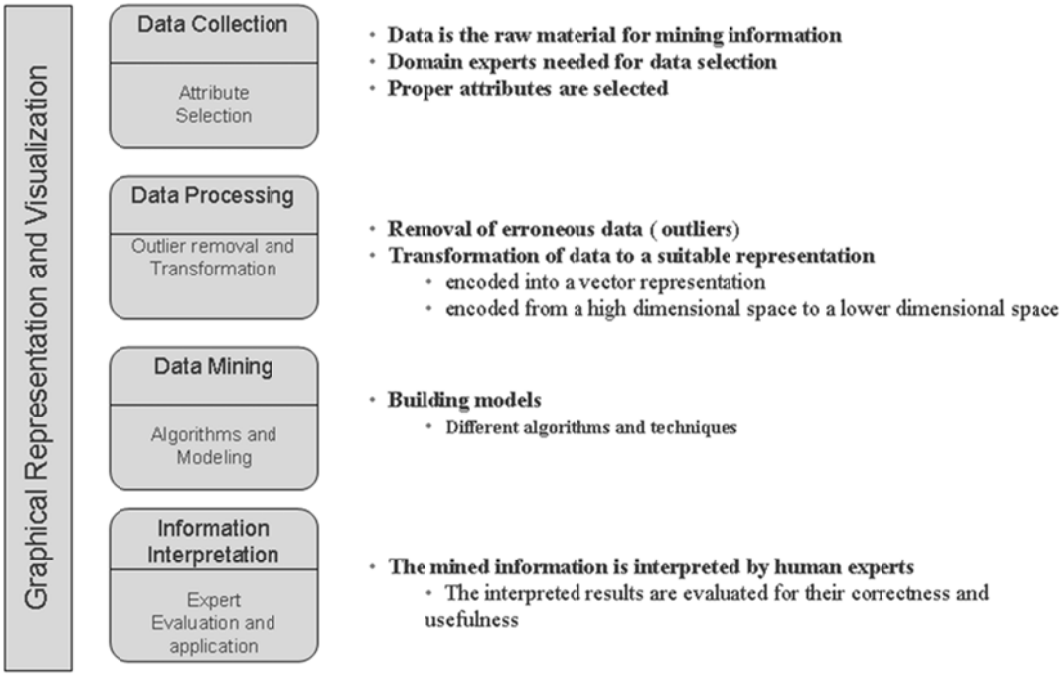

Figure 14: The four phases of a data mining process

3.3 Preparing the dataset

The dataset is partitioned using cross-validation. The training set is used to train the learning algorithm, and the induced decision rules are tested on the test set.

3.4 Cross-Validation

The model is to be first built and evaluated using 10-fold cross-validation on the fit data set, and then validated using the test data set. In 10-fold cross-validation, the dataset is divided into 10 subsets of (approximately) equal size. The dataset is trained 10 times, each time leaving out one of the subsets to use for testing. The basic idea is to use 90% of the dataset to build a model and 10% to test the performance of the model. The simplest

cross-validation is the holdout method where the two datasets, referred to as the training set and the test set are used in a single evaluation but this method allows for high variance and dependency in the dataset. A solution to this problem is the k-fold cross-validation where k is the number of subsets and where the model is built repeatedly each time for k-1 subsets. The remaining subset is used as a test dataset. The cross validation errors are computed for each of the k test subsets and then averaged to give the k-fold estimate of the cross-validation errors. Cross-validation is preferred over percentage split-sample for small data sets [38] [39].

3.5 Classification

Classification is a data-mining task that defines the class or group where each data instance belongs. A classification model requires at least two pre-defined classes. The attributes of a training data set constitute the input to the classification model. The pre-defined class defines the output where the different instances belong. A classification model requires supervised learning. In supervised classification, data is labeled i.e., belonging to a specific class [66].

3.6 Clustering

Clustering, also referred to as segmentations, is a technique that divides the data into natural groups, i.e., similar data is put into the same clusters or categories [66]. Unlike classification and association learning covered in the next section, clustering is unsupervised learning. The number of clusters is not known in advance. Iterative distance-based clustering technique such as the k-means, which employs the Euclidean distance, can be used to form clusters. An example of clustering is illustrated by examining how Amazon.com groups customers in clusters, based on the books they buy.

Customers in the same clusters are recommended the most commonly purchased book in the cluster because these customers appear to share the same taste in reading. A problem with clustering is deciding on an appropriate arbitrary number of clusters. This is a trial and error process. The user inputs the number of clusters. If the results are not satisfactory, another cluster number is chosen. Different clustering methodologies such as probabilistic clustering, top-down and bottom-top hierarchical clustering are available. The top-down hierarchical approach separates the data into different clusters based on the similarity measurement criteria. It starts with one single cluster housing all the data and ends up with each data sample being a single cluster. The bottom-top approach starts with the data being grouped into separate clusters containing a single data sample and end up with all data grouped into one cluster.

3.7 Association

Association rules, sometimes referred to as affinity analysis, search for dependencies between a data subset and the rest of the data set. They can predict any attribute or a combination of attributes. The association rule A => B means that when A exists B also exists with high probability. The Market Basket Analysis is an example of an association rule. Beer => chips implies that people who bought beer on Saturday night also bought chips. The association rule A => B exists when both the support and confidence of the rule is larger than the respective threshold. Support (a.k.a. coverage) of an association rule is defined as the number of instances for which it predicts correctly; while confidence (a.k.a. accuracy) of an association rule is the number of instances that it predicts correctly, expressed as a proportion of all instances to which it applies.

3.8 Other data mining

In text mining, the mined data is text. Keywords or phrases are used to find related documents in the database. Advanced text mining utilizes classification, association and clustering techniques. Similarity measures identify relationships between documents and terms. Text mining is useful when searching and retrieving large amounts of biomedical information.

Similarly, graphics mining technology is helpful in retrieving protein structures in bioinformatics. It retrieves graphics from databases.

3.9 Detection performance measurement

In this section, we focus on the binary classification of arrhythmia, in which a classifier yields two discrete results: positive, or presence of arrhythmia and negative, or absence of arrhythmia. Given an EKG record, a binary classification has four possible outcomes: number of True Negatives (TN), number of False Positives (FP), number of True Positives (TP), and number of False Negatives (FN), and correspondingly four possible rates: True Negative rate (tn), False Positive rate (fp), True Positive rate (tp), and False Negative rate (fn).

3.9.1 Specificity and sensitivity

Detection rates are measured in terms of specificity and sensitivity.

Specificity or true negative rate designated as tn measures the proportion of negatives that are correctly identified (i.e. the percentage of arrhythmia-free people who are correctly identified as not having arrhythmia). It is the ability of a test to identify correctly those patients without the disease (TN rate) [40].

$$\text{Specificity or } tn = \frac{\text{TN}}{\text{TN} + \text{FP}} 100\%$$

A specificity equal to 100% means no negatives are incorrectly classified as positive. A positive result in a high specificity test is used to confirm the presence of arrhythmia. The specificity test alone does not necessarily express how well the test recognizes the presence of arrhythmia. The sensitivity is also needed.

Sensitivity or true positive rate designated as tp (a.k.a. the recall rate in data mining) measures the proportion of actual positives (people having arrhythmia) which are correctly identified. It is the ability of a test to identify correctly those patients with the disease (tp) [40].

$$\text{Sensitivity or } tp = \frac{\text{TP}}{\text{TP} + \text{FN}} 100\%$$

Sensitivity equal to 100% signifies that the test identifies all actual positives. All instances suggestive of arrhythmia are recognized as having arrhythmia present. Compared to a high specificity test, negative results in a high sensitivity test are used to rule out the presence of arrhythmia.

If 1,000 patients diagnosed to have arrhythmia present are tested, and 640 test positive, then the test would suggest 64% sensitivity. On the other hand, if 1,000 patients that are known not to have arrhythmia are tested and 950 come back with a negative result, then the test suggests 95% specificity. A very highly specific test is not likely to give a false positive result. A positive finding should therefore indicate the presence of arrhythmia. Likewise a highly sensitive test rarely misses, thus a negative result should signify the absence of arrhythmia.

Both sensitivity and specificity are needed in the binary classification, as sensitivity alone does not indicate how well the test predicts the negative instances and specificity alone does not specify how well the test recognizes positive instances.

3.9.2 Type I and Type II errors

A theoretical, optimal detection can realize 100% sensitivity (i.e. predict all instances belonging to the arrhythmia group as having arrhythmia) and 100% specificity (i.e. not predict anyone from the healthy group as having arrhythmia). If each instance is correctly classified, then the values of the detection parameters are equal to one. These two measures are closely related to the concepts of Type I and Type II errors.

Type I error, a.k.a. α error or false positive, occurs when a model classifies a patient as having arrhythmia when in fact the patient does not have arrhythmia. This is described by poor specificity. Type II error, a.k.a. β error or false negative, occurs when a model classifies a patient as not having arrhythmia when the patient has arrhythmia. This is characterized by poor sensitivity. A model that offers a good balance between Type I and Type II errors with Type II error as low as possible is the goal for our model selection.

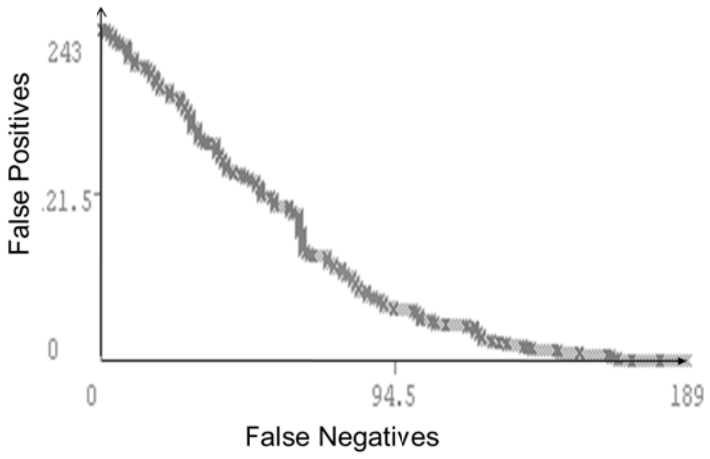

Figure 15: An example of false positives versus false negatives

A test with a high specificity has a low Type I error rate. A test with a high sensitivity has a low Type II error rate. There is an inverse relationship between False Positives versus False Negatives as depicted in Figure 15. As Type I error rate goes up, Type II error rate goes down.

For the overall error rate, the false positive rate, and the false negative rate, the best performance measure values are the lowest. For the F-measure, the best values are the highest values.

Type II or False Negative rate designated as fn (i.e. when a positive instance is wrongly classified as negative),

$$fn = \frac{\text{FN}}{\text{FN} + \text{TP}} 100\%$$

and Type I error or False Positive rate (i.e. when a negative instance is wrongly classified as positive).

$$fp = \frac{\text{FP}}{\text{FP} + \text{TN}} 100\%$$

are significant issues in medical diagnostics. False negative test results may provide patients and doctors a falsely reassuring message that arrhythmia is absent, when it is actually present. This may lead to inappropriate or inadequate treatment of the disease and sometimes unforgiving consequences to the patient. In statistical hypothesis testing, the False Negative rate is known as β. On the other hand, False Positive arrhythmia results may produce unnecessary worries and lead to needless financial expenses. The false positive rate is represented as α, significance level in statistics.

3.9.3 ROC for the evaluation of arrhythmia classification performance

Receiver Operating Characteristics curves (or ROC curves) have been used in biomedical informatics [41]. They are useful in expressing the sensitivity versus specificity of classifiers (see Figure 16). The ROC curve plot displays the FP rate on the X-axis (1-Specificity) and the TP rate (Sensitivity) on the Y-axis. Each point on the ROC curve represents a sensitivity/specificity pair corresponding to a particular decision threshold. The area under the ROC curve measures how well a particular parameter can distinguish between two diagnostic groups (such as presence of a disease/ absence of a disease). It plays an important role in the evaluation and analysis of class imbalance. It provides an effective approach to characterize the performance of classifiers [42] [43] [44].

To judge how well a classifier performs, the area under the curve (a.k.a. AUC) is a good indicator. The closer an ROC curve is to the upper left hand corner [45] [46] the better the performance of the classifier. When comparing the performance of two classifiers, the classifier with the corresponding ROC curve that is located closer to the upper left hand corner and above the ROC curve of another classifier produces better global performance. For example, classifier ‘a’ outperforms classifier ‘b’ as shown in the Figure 16. The perfect classifier has an area under the ROC curve equal to 1. Its ROC curve runs from point (0, 0) to point (1, 1) bending towards (0, 1). An ROC curve with an area of 0.5 follows a diagonal path from (0, 0) to (1, 1). A typical ROC curve lies in the upper left of the plot, and the corresponding AUC is between 0.5 and 1.0. The bigger the area is and the closest to 1, the better the classifier performance.

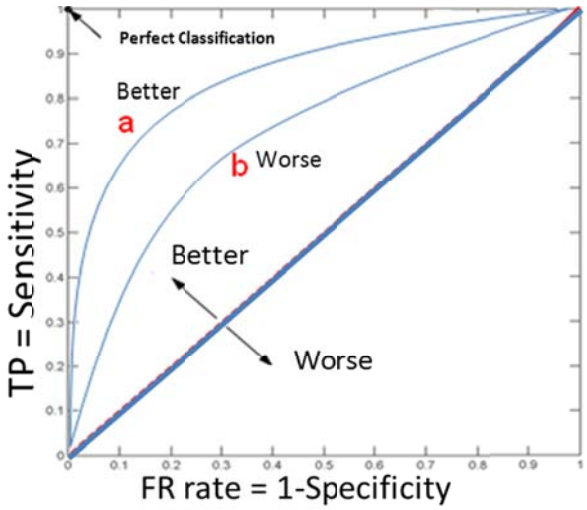

Figure 16: Specificity versus Sensitivity Curve

When considering the results of a particular test in two populations, one population with a disease, the other population without the disease, there is no clear separation between the two groups. The distribution of the test results will overlap, as shown in Figure 17.

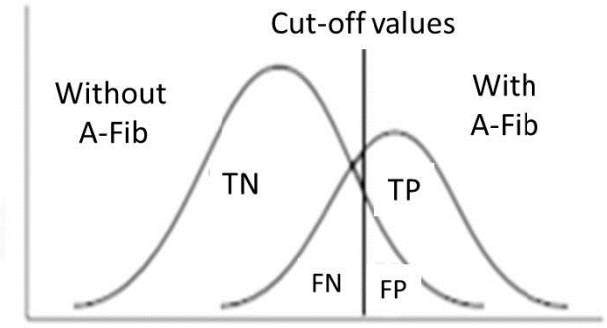

Figure 17: Example of A-Fib test results

Figure 18 shows the possible cut-off points in the test:

- Some cases with the disease that are correctly classified as positive (TP),
- Some cases with the disease that are incorrectly classified as negative (FN).
- Some cases without the disease that are correctly classified as negative (TN),
- Some cases without the disease that are incorrectly classified as positive (FP).

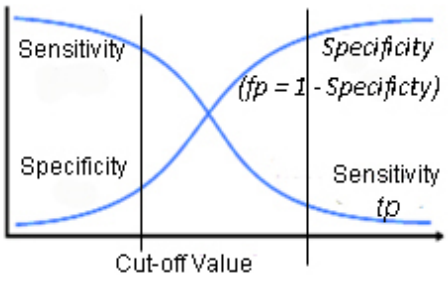

Figure 18: Sensitivity-Specificity trade-off

When opting for a high cut-off value, the false positive measure will decrease with increased specificity ($fp = 1 - specificity$) and the true positive measure or sensitivity will decrease. On the other hand, when selecting a lower criterion value, the true positive measure or sensitivity will increase and the false positive measure will also increase, and therefore the true negative measure and specificity will decrease.

3.9.4 Outcomes of a test

The confusion matrix (see Table 3) for our binary classification model (present, absent) is a 2x2 matrix that displays the counts of the four types of detections that will help us measure the classifier performance.

Confusion Matrix		**Actual**		
		Positive Arrhythmia is present	**Negative Arrhythmia is absent**	
Predicted	**Arrhythmia is present. (Positive)**	TP	FP (Type I Error)	Positive Predictive Value $= \frac{\text{TP}}{\text{TP} + \text{FP}}$
	Arrhythmia is absent. (Negative)	FN (Type II Error)	TN	Negative Predictive Value $= \frac{\text{TN}}{\text{TN} + \text{FN}}$
	Positive Likelihood Ratio	Sensitivity $= \frac{\text{TP}}{\text{TP} + \text{FN}}$	Specificity $= \frac{\text{TN}}{\text{TN} + \text{FP}}$	Negative Likelihood Ratio

	$= \frac{\text{Sensitivity}}{1 - \text{Specificity}}$			$= \frac{1 - \text{Sensitivity}}{\text{Specificity}}$

Table 3: Confusion matrix

- Sensitivity is the probability that a result is predicted to be positive when the disease is present.
- Specificity is the probability that a result is predicted to be negative when the disease is not present.
- Positive likelihood ratio is the ratio between the probability of a positive test result given the presence of the disease and the probability of a positive test result given the absence of the disease, Sensitivity / (1-Specificity).
- Negative likelihood ratio is the ratio between the probability of a negative test result given the presence of the disease and the probability of a negative test result given the absence of the disease, (1-Sensitivity) / Specificity.
- Positive predictive value is the probability that the disease is present when the test is positive.
- Negative predictive value is the probability that the disease is not present when the test is negative.

3.9.5 Overall classification accuracy and the overall classification error

Classification accuracy of a model is measured in terms of Type I and Type II errors. Both the overall classification accuracy and the overall classification error defined below can be used to evaluate the performance of a classifier, but when the costs of misclassifications of the different classes are uneven, this measure may be unacceptable.

In order to take into account the unevenness of misclassification costs when evaluating a classifier, one may explore the following metrics: error types, tp, fp, fn, tn, $F-measure$, and area under the ROC curve.

$$\text{Overall Accuracy } = \frac{\text{TP} + \text{TN}}{\text{TP } + \text{ TN} + \text{ FP} + \text{FN}}$$

$$\text{Overall Error rate } = 1 - \text{Overall Accuracy} = \frac{\text{FP} + \text{FN}}{\text{TP } + \text{ TN} + \text{ FP} + \text{FN}}$$

Both the overall accuracy and the overall error rate are poor performance metrics. Both metrics favor the majority class and penalize the minority class. Accuracy places more emphasis on the common classes than on rare classes. For example, given a two-class problem with distribution 90:10, the performance of the classifier on the majority class will be counted nine times more than the performance on the minority class. Accuracy leads to poor minority-class performance. Minority class has lower precision and recall than majority class. Recall and precision are inversely related (see Figure 19).

Recall (a.k.a. effectiveness) is a metric which is the same as True Positive Rate metric and defined as the proportion of positives that are correctly predicted positives. It is the ratio of the number of relevant records retrieved, to the total number of relevant records in the database, and is usually expressed as a percentage. In binary classification, recall is called sensitivity. It is trivial to achieve recall of 100% by returning all documents in response to any query. Therefore, recall alone is not enough but one must also measure the number of irrelevant document, for example by computing the precision.

$$\text{Recall } = \frac{\text{TP}}{\text{TP } + \text{ FN}} 100\%$$

Precision (a.k.a. efficiency) refers to the proportion of instances predicted to be of the positive class when actually they are from the positive class. It is the ratio of the number

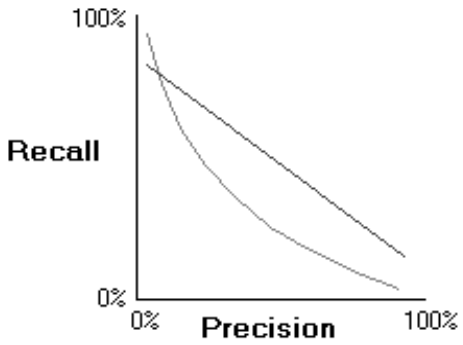

Figure 19: Recall and precision are inversely related.

of relevant records retrieved to the total number of irrelevant and relevant records retrieved. It is usually expressed as a percentage.

$$\text{Precision} = \frac{\text{TP}}{\text{TP} + \text{FP}} 100\%$$

Because both Precision and Recall are defined with respect to the Positive (rare) class, rare cases/classes can be appropriately assessed using these two metrics. Many systems have used a variation of both metrics like Geometric Mean (G_{Mean}) and F-Measure

The G_{Mean} tends to maximize the accuracies of both classes while keeping them balanced.

$$G_{Mean} = \sqrt{\text{Recall} \times \text{Precision}}$$

The $F_{Measure}$ is defined with respect to the Recall metric and the Precision metric. It indicates the combined relative importance of both metrics.

$$F_{Measure} = \frac{(1 + \text{Beta}^2)\text{Precision} \times \text{Recall}}{(\text{Beta}^2 \times \text{Recall} + \text{Precision})}$$

A larger Beta gives more weight to Recall. Two commonly used $F_{Measure}$ values are the F_2 measure (Beta =1) and $F_{0.5}$. F_2 measure emphasizes Recall twice as much as Precision, and the $F_{0.5}$ measure weights Precision twice as much as Recall.

CHAPTER 4

4 A-FIB PREDICTORS AND DETECTION CHALLENGES

A-Fib is the most common cardiac arrhythmia [47] [48]. A-Fib prevalence varies between 1.1 per 1,000 patients at age 40, and 105 at age 90 [49]. A-Fib symptoms start with the fast and irregular heart rate, palpitations, racing or heart-skipping sensations. The patient may have shortness of breath, lightheadedness, chest discomfort or fatigue. The important risk of A-Fib is blood clots and stroke due to uncoordinated upper chambers contractions. It can be diagnosed by reading and interpreting an electrocardiogram record in a primary care setting, whether by a general practitioner, a referred cardiologist, interpretative software, or a practice nurse during a routine screening visit or scheduled check-up. Traditionally, a 24-hour Holter monitor, or for longer periods an "event monitor", are worn by the patients in order to capture the first episode of A-Fib. A-Fib affects 2.5 million people in the United States or close to 1% of the total population [12]. The Manitoba study [50] and the Framingham Heart study [51] draw attention to the significance of the higher frequency of A-Fib with advancing age. Patients with A-Fib have a 1.5 to 2 fold increase in mortality rate when compared with the general population as suggested by Framingham Heart study data [6] [52]. Early recognition of A-Fib is difficult because most people are not aware of this silent rhythm disturbance [53]. Today, frequent monitoring and screening of patients allow for early detection of arrhythmia.

At least one-third of the A-Fib episodes go undetected [8] because either people are not screened often or a general practitioner or a practice nurse misses the A-Fib diagnosis. Few studies have addressed the misdiagnosis of A-Fib from an electrocardiogram (EKG) and the potential risk of A-Fib misinterpretation errors. Knight et al. [54] concluded that A-Fib is more often misdiagnosed by internists than cardiology fellows and cardiologists. Mant et al. [55] discovered that general practitioners correctly detected A-Fib 80% (true positive) of the time when interpreting 12-lead EKG data and misinterpreted 8% (false positive) of sinus rhythm cases as A-Fib. One of the major misdiagnosis confuses A-Fib with atrial flutter [56].

4.1 Predictors of A-Fib

A-Fib is the most prevalent arrhythmia in the United States and accounts for more than 750,000 strokes per year [11]. According to classification guidelines used by cardiologists and electro-physiologists, for the management of patients with A-Fib [57], after the first A-Fib is detected, there are four types of A-Fib: Paroxysmal, persistent, longstanding persistent, and permanent. A-Fib is termed progressive. Once a patient is diagnosed with a paroxysmal A-Fib he or she will eventually migrate to persistent A-Fib. Similarly, a patient diagnosed with persistent A-Fib will drift to longstanding persistent A-Fib and in time to permanent A-Fib [58]. The EKG waves and intervals represented in Figure 20 are used to describe the predictors of A-Fib.

From Section 2.1.3, the QRS interval is the duration of the ventricular muscle depolarization. The P wave is a record of the electrical activity or the sequential activation (depolarization) through the right and left atria. The PR interval is the time interval measured from the beginning of the P wave (atrial depolarization) to the onset of

the QRS complex (ventricular depolarization). The RR interval is the duration of the ventricular cardiac cycle; it is an indicator of the ventricular rate. The PP interval is the duration of the atrial cycle; it is an indicator of the atrial rate.

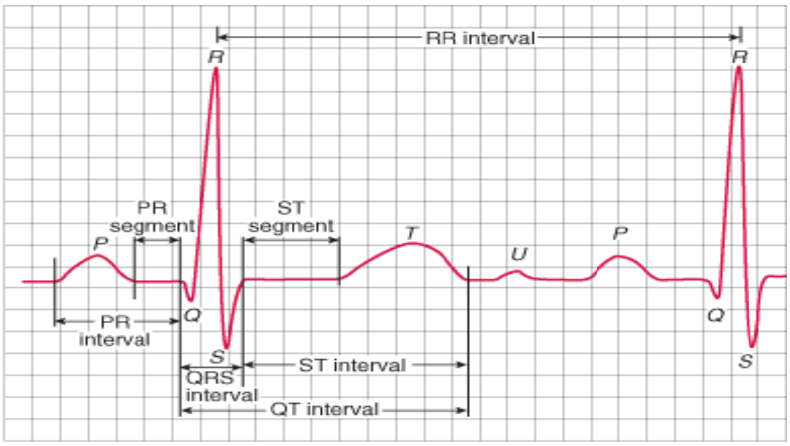

Figure 20: Typical EKG record.

A strong indicator of A-Fib presence is the absence of P waves on the EKG plot and an erratic noise-like activity in their place combined with irregular R-R intervals [20] (see Figure 21). Sometimes when the heart rate is too fast, irregular R-R intervals may be difficult to determine [50]. In addition, wide QRS complexes may be present with rapid ventricular response.

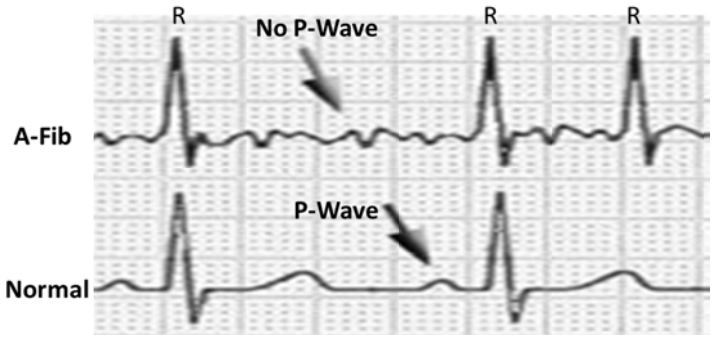

Figure 21: A-Fib depicted by the presence of the P-Wave [20]

Other factors that may contribute to A-Fib: Age, Gender, Body Mass Index (BMI), Systolic Blood Pressure (SBP), Treatment for Hypertension (TH), Significant Heart

Murmur (SHM), Prevalent Heart Failure (PHF), PR Interval, QRS duration, and Heartrate [6] .

4.2 A-Fib Telemetry Data Analysis

Telemetry is widely accepted in healthcare for remotely collecting and sending vital data to a monitoring station for analysis and interpretation of all types of arrhythmia in outpatients. Today, when prescribed by a physician, telemetry may be applied continuously for few days in the hope of capturing episodes of A-Fib. Telemetry may also be user-triggered by the patient as soon as he or she feels symptoms of A-Fib (such as heart palpitations). Using triggered events to start an A-Fib telemetry monitoring device runs the risk of missing the first 30 seconds of A-Fib. Moreover, triggering events might not be possible if the user is incapacitated.

The telemetry model continuously senses EKG signals, transmits EKG data, receives EKG records, and reports EKG information to a healthcare center for further diagnostics and analysis by a doctor or a healthcare specialist. The telemetry report includes all positive and negative results. We assume that telemetry EKG interpretations are conducted by a cardiologist or a cardio-physiologist who are experts at EKG readings; thus all judgments of what constitutes A-Fib are going to be assumed to be as accurate as possible. Unfortunately, not every physician is a cardiologist, so general practitioners are often the first to interpret EKG readings during a general screening evaluation. General practitioners introduce human errors when interpreting EKG readings leading to a false positive rate of 8% and a false negative rate of 20% [54].

CHAPTER 5

5 DEVELOPING A-FIB RISK FACTOR AND DETECTION ALGORITHMS

Several clinical methods of treating arrhythmia exist. These medical interventions and clinical treatments come after the fact and are expensive. Moreover, the average patient's condition progressively deteriorates for five days before seeking emergency treatment. The longer the heart remains out of rhythm, the more difficult for the doctor to restore the normal sinus rhythm to the heart. Knowing one's A-Fib risk factor and using an A-Fib detection algorithm will alleviate most of the aforementioned problems and one may plan an early and appropriate course of action to treat arrhythmia and A-Fib in particular.

5.1 Developing A-Fib risk factor

The risk of developing A-Fib may depend on several factors—some associated with lifestyle and some from heredity. Many of these factors behave nonlinearly, complicating accurate A-Fib risk assessment. Standardizing the prediction of A-Fib from mere clinical diagnoses is difficult [59]. Few studies have addressed the misdiagnosis of A-Fib from an electrocardiogram (EKG) [8] and the potential risk of A-Fib misinterpretation errors. Data mining techniques and statistical methods such as the Cox proportional hazards model [60] and the logistic regression model are used in many epidemiological studies.

The Cox Proportional Hazards Model is a multivariate statistical method used to compare survival in two different groups and determines the contribution of different variables on

survival. The Framingham Heart study in the United States and the Prospective Cardiovascular Münster (PROCAM) study in Europe used the Cox model to develop standardized risk factor assessments that may complement clinical practice. The Cox proportional-hazards regression is used to analyze the effect of risk factors on survival. The probability of the end game (onset of A-Fib) is called the hazard. The covariates and their corresponding coefficients (listed in Table 4) responsible for predicting A-Fib risk in people aged between 45 and 95 years old are extracted from the Framingham Heart study [6][51]: Age, Age2, Gender, Body Mass Index (BMI), Systolic Blood Pressure (SBP), Treatment for Hypertension (TH), Significant Heart Murmur (SHM), Prevalent Heart Failure (PHF), Gender*Age^2, and Age*PHF, PR Interval ($PR_{interval}$). We can express the hazard or risk of getting A-Fib at time t as:

$$H(t) = H_0(t) * e^{\sum_{i=1}^{k} \beta_i X_i}$$

We can linearize this model by dividing both sides of the equation by $H_0(t)$ and then taking the natural logarithm of both sides:

$$\ln\left(\frac{H(t)}{H_0(t)}\right) = \sum_{i=1}^{k} \beta_i X_i$$

$$\sum_{i=1}^{k} \beta_i X_i = \beta_1 Gender + \beta_2 Age + \beta_3 BMI + \beta_4 SBP + b_5 TH + \beta_6 SHM + \beta_7 PHF + \beta_8 Age^2 + \beta_9 Gender * Age^2 + \beta_{10} Age * SHM + \beta_{11} Age * PHF + \beta_{12} PR_{interval}$$

The quantity $H_0(t)$ is the baseline or underlying hazard function. It is practically the probability of getting A-Fib when all the other covariates are set equal to zero. The baseline hazard function is analogous to the intercept in linear regression. The regression

coefficients β1 to β12 provide the model with the proportional change or contribution from each covariate. The derived Cox proportional hazards equation is described below:

$$\ln(H(t)/(H_0(t)) = \sum_{i=1}^{k} \beta_i X_i = 1.994060\, Gender + 0.150520 Age + 0.019300\, BMI + 0.006150\, SBP + 0.424100\, TH + 3.795860\, SHM + 9.428330\, PHF - 0.000380 Age^2 - 0.000280\, Gender * Age^2 - 0.042380\, Age * SHM - 0.123070\, Age * PHF + 0.070650\, PR_{Interval}$$

Where $H_0(10) = 0.96337$ is the 10 year baseline survival or cumulative hazard function at time t = 10 years extracted from the Framingham Heart study [6] [51]. The values of the means for each covariate are tabulated below:

Covariate	Xbar		Covariate	Xbar
Gender	0.4464		SHM	0.0281
Age	60.9022		PHF	0.0087
BMI	26.2861		Age^2	3806.90
SBP	136.1674		Gender*Age^2	1654.66
TH	0.2413		Age*SHM	1.8961
$PR_{interval}$	16.3901		Age*PHF	0.61

Table 4: A-Fib risk covariates coefficients

The probability of getting A-Fib or having a risk is:

$$P(AFib) = 1 - H_0^{\,exp(\sum_{i=1}^{k} \beta_i X_i - \sum_{i=1}^{k} \beta_i Xbar_i)}$$

For example, we calculate the risk factor of a male person who is 70 years old, weighing 70 kg, with a body mass index of 22.96, a systolic blood pressure of 130, with no hypertension, a $PR_{interval}$ measuring 16 mms, with no significant heart murmur, and no previous heart failure.

Comparing to the mean values of the 10-year study from the Framingham Heart study [6] [51] we get:

$$\sum_{i=1}^{k} \beta_i X_i - \sum_{i=1}^{k} \beta_i Xbar_i = 11.669 - 10.786 = 0.883$$

$$e^{(\sum_{i=1}^{k} \beta_i X_i - \sum_{i=1}^{k} \beta_i Xbar_i)} = e^{0.883} = 2.418$$

The predicted risk factor is:

$$k = 1 - H_0^{e^{(\sum_{i=1}^{k} \beta_i X_i - \sum_{i=1}^{k} \beta_i Xbar_i)}} = 1 - 0.96337^{2.418} = 0.0863$$

The predicted Risk Factor is 0.0863 compared to a risk for a person of the same age and gender with BMI 20 to 24.9, Normal SBP (120 to 129), No Treatment for Hypertension, $PR_{interval}$ 16, No significant murmur or prevalent heart failure.

Risk Factor	Units	0.021	0.083	0.1788	0.1003
Age	years	50	**70**	70	70
Gender	M,F	M	M	M	**F**
Body Mass Index (BMI) $Weight/height^2$	kg/m^2	24	24	**35**	35
Systolic Blood Pressure (SBP)	mmHg	120	120	**150**	150
Treatment for Hypertension (TH)	yes/no	no	no	**yes**	yes
Significant Heart Murmur (SHM)	yes/no	no	no	no	no
Prevalent Heart Failure (PHF)	yes/no	no	no	no	no
$PR_{interval}$	mm	16	16	16	16

Table 5: Examples of risk factors

In Table 5, we fix values for some covariates while varying other covariates. Varying the age value from 50 to 70 while keeping the rest of the covariates fixed increases the A-Fib risk factor from 0.021 to approximately four times, 0.083. Similarly, everything else being the same, switching the gender from male to female, drops the A-Fib risk factor from 0.1788 to 0.1003.

A-Fib risk factors may be classified in three categories made up of risk ranges such as $k < 0.05$, $0.05 < k < 0.15$, $k > 0.15$. Knowing the A-Fib risk factor of a patient allows one to prescribe an A-Fib monitoring schedule (see Table 6). A high A-Fib risk factor may suggest more frequent monitoring compared to a low A-Fib risk factor.

Risk Factor Category	Risk Factor Range
Risk factor category 1 would be for a user who is healthy, athletic; this is similar to wearing a sports watch.	$k < 0.05$
Risk factor category 2 would be for a user who wants to monitor A-Fib daily during an AM/PM windows.	$0.05 \leq k < 0.15$
Risk factor category 3 is for the chronic case where a user monitors continuously with the data and detection results transmitted to a care center.	$k \geq 0.15$

Table 6: Risk factor category

5.2 Developing A-Fib detection algorithm

There would be a greater positive public health impact from predicting arrhythmia risk and detecting it to prevent heart attacks. Few machine learning algorithms and statistical approaches have been applied in medical applications; for example, classification of EKG arrhythmias using neural networks [29], EKG arrhythmia classification based on logistic model tree [61], and analysis of EKG signals using self-organizing maps (SOM). In this section, we concentrate on the design of a real-time early detection algorithm. We compare accuracy of machine learning schemes such as J48, Naïve Bayes, and Logistic Regression and choose the best algorithm to classify A-Fib from EKG medical data.

5.2.1 Classification and analysis environment

The Waikato Environment for Knowledge Analysis (WEKA) software environment for Machine Learning [62] is used to analyze the dataset and classify cardiac arrhythmia types. WEKA contains tools for data pre-processing, classification, regression, clustering,

association rules, and visualization. It is also well suited for developing new machine learning schemes. Figure 22 displays a screen shot of the WEKA tool.

5.2.2 Cardiac A-Fib dataset

The input dataset used in the analysis is a combination of data retrieved from a repository located at the University of California in Irvine, California [63] and MIT-BIH A-Fib database [64]. The A-Fib dataset consists of 304 instances, (224 instances free of A-Fib and 80 instances with A-Fib, containing seven attributes and two classes described in Tables 7 and 8 and Figures 22 and 23).

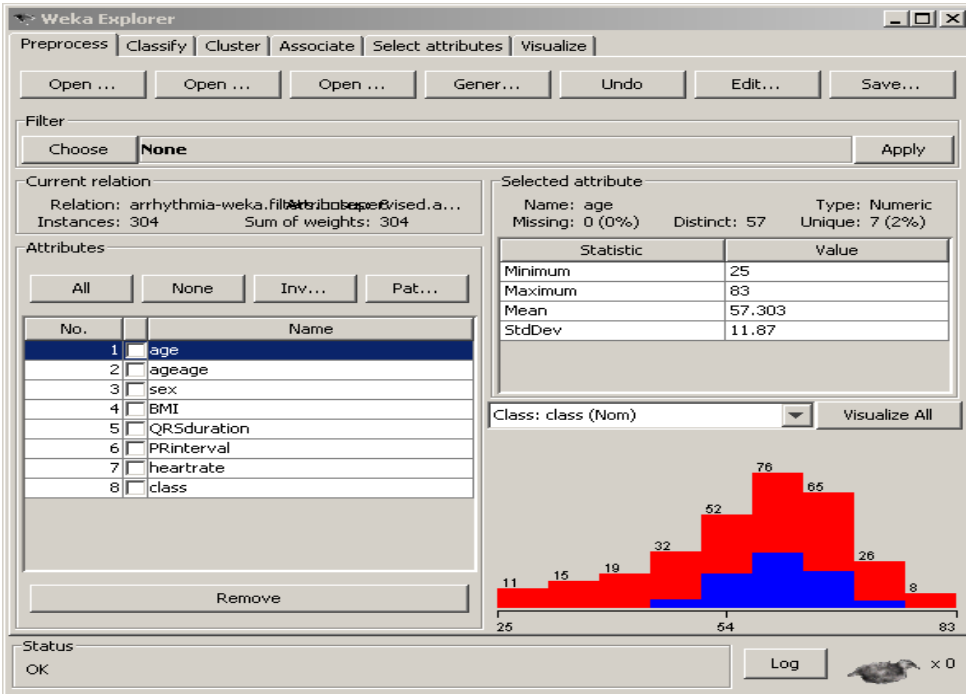

Figure 22: Screen shot of WEKA tool [62]

The dataset describes the attributes for diagnosing cardiac A-Fib where each instance or patient is classified into two categories: presence of A-Fib and absence of A-Fib. Few instances in the dataset were deleted because they contained omitted entries. The names

and ID numbers of the patients that took part in the cardiac arrhythmia study were removed from the dataset.

	Variable	Description	Value
1	Age	Age in years, linear	real
2	Age^2	Age^2 in $years^2$	real
3	Gender	Gender (0 = male; 1 = female), nominal	{0, 1}
4	BMI	Kg/m^2, Linear	real
5	QRSduration	Average of QRS duration in msec., linear	real
6	$PR_{interval}$	Average duration between onset of P and Q waves in msec., linear	real
7	Heartrate	Number of heart beats per min, linear	real
8	Class	{A-Fib present, A-Fib absent}	binary

Table 7: List of selected attributes for the detection of A-Fib

Class	Type	Number of Instances
01	A-Fib Absent	224
02	A-Fib Present	80

Table 8: Absent and present A-Fib classes in the pre-processed dataset

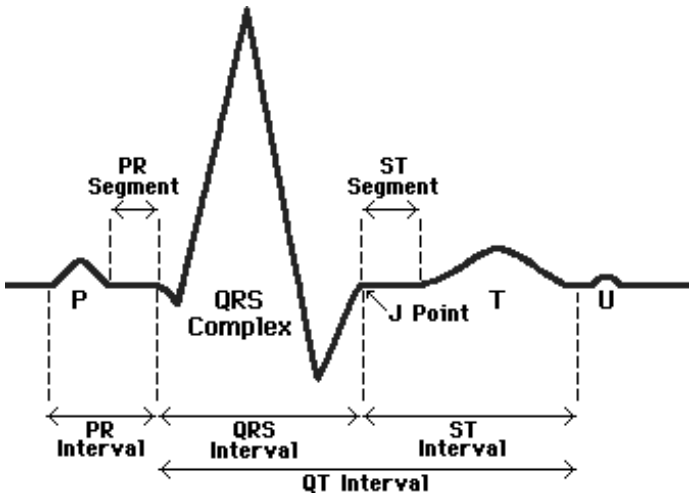

Figure 23: Typical EKG record

The objective of the analysis is to predict the absence (indicated by normal EKG) or the presence of cardiac A-Fib (see Figure 23). The cardiologist's classification is used as a reference. The aim is to minimize the error, i.e. the difference between the cardiologist's results and those obtained from the dataset analysis.

5.2.3 Classification of A-Fib

Classification is a popular data mining technique that is used to extract the relationships that exist among the various attributes and may be hidden in the data. The detection results were extracted from running WEKA tool using a dataset containing 304 instances using 10-fold cross validation to predict the detection of the presence or absence of arrhythmia.

The training dataset sports two classes, presence of A-Fib and absence of A-Fib. The idea behind this A-Fib classification is that when a new patient record is presented, it can be automatically determined whether the patient is having A-Fib or not. Classification has been used in statistics, data mining, and machine learning [65] [66].

In this dissertation, logistic regression is applied to the same dataset to classify a cardiac arrhythmia. The resulting detection accuracy will be compared to the accuracy obtained from the three applied machine learning techniques (i.e. OneR, J48, and Naïve Bayes algorithms) in the paper by Soman and Bobbie [10]. The number of attributes is reduced with the aim to yield only a marginal decrease in the accuracy. The approach will guarantee an energy-aware classification detection algorithm that is adequately accurate but consumes as little energy as optimally possible. Therefore, the criterion for the chosen classification detection algorithm is a trade-off between the highest level of accuracy achieved and the minimum number of possible attributes. The following sections explore classification algorithms using J48, Naïve Bayes, and Logistic Regression. We choose the best algorithm to classify A-Fib by deriving the accuracy of predicting the presence/absence of cardiac A-Fib. The resulting classification detection algorithm is portable to a Bluetooth-enabled wearable computing device. We will derive

the overall accuracy as well as Type I and Type II misclassification errors, sensitivity rate, and specificity rate in later sections.

5.2.4 Classification of A-Fib using the J48 decision tree classifier

Decision trees are tree-like graphs with human-readable and interpretable rules where each branch node represents a choice between a number of alternatives, and each leaf node represents a classification or decision. Some of decision tree classifiers are C4.5, C5.0, J48, NBTree, SimpleCart, REPTree and others [66]. J48 classifier is an implementation of the C4.5 decision tree learner in WEKA. The C4.5 implementation produces rule-sets and a decision tree model. These models are human readable, easy to understand and straightforward. J48 generates decision trees, the nodes of which evaluate the significance of individual features, such as age, gender, BMI, QRSduration, $PR_{interval}$, and heartrate. The decision trees are constructed in a top-down fashion starting from the main root and selecting the most significant feature at each branch. Tables 9, 10 and Figure 24 show the results of J48 decision tree results.

```
=== Run information ===

Scheme:     weka.classifiers.trees.J48 -C 0.25 -M 2
Relation:   arrhythmia-weka.filters.unsupervised.attribute.Remove-R4
Instances:  304
Attributes: 7
Classes: 2
Test mode:    10-fold cross-validation
```

Figure 24 displays the resulting J48 pruned tree

```
PR_interval <= 0
|   heartrate <= 68: NOAF (6.0)
|   heartrate > 68: AF (87.0/7.0)
PR_interval > 0: NOAF (211.0)

Number of Leaves:     3
Size of the tree:     5
```

=== Detailed Accuracy by Class ===

	TP Rate	FP Rate	Precision	Recall	F-Measure	ROC Area	Class
	0.975	0.036	0.907	0.975	0.940	0.979	AF
	0.964	0.025	0.991	0.964	0.977	0.979	NOAF
Weight Avg.	0.967	0.028	0.969	0.967	0.967	0.979	

Correctly Classified Instances	**294**	**96.7105 %**
Incorrectly Classified Instances	**10**	**3.2895 %**

Table 9: J48 classification classes

a	b	Classified as
78	2	a = Present
8	216	b = Absent

Table 10: J48 classification confusion matrix

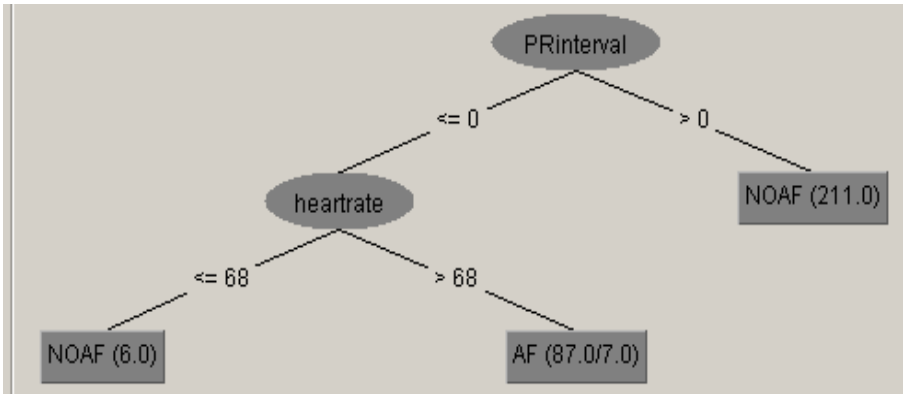

Figure 24: J48 A-Fib decision tree

5.2.5 Classification of A-Fib using Naïve Bayes classifier

A Naïve Bayes classifier is based on the Bayes' theorem and all the attributes are assumed independent given a class membership. In most real-world applications, this conditional

independence assumption fails, however the algorithm tends to perform well in many class predictions. Tables 11 and 12 show results Naïve Bayes classifier.

=== Run information ===

Scheme: weka.classifiers.bayes.NaiveBayes
Relation: arrhythmia-weka.filters.unsupervised.attribute.Remove-R4
Instances: 304
Attributes: 7
Classes: 2

Test mode: 10-fold cross-validation

Naïve Bayes Classifier

Attribute	Class AF (0.26)	NOAF (0.74)
age		
mean	60.5893	56.1967
std. dev.	6.3297	13.1467
weight sum	80	224
precision	1.0357	1.0357
ageage		
mean	3687.0911	3322.257
std. dev.	743.3334	1410.1275
weight sum	80	224
precision	111.8571	111.8571
sex		
0	17.0	96.0
1	65.0	130.0
[total]	82.0	226.0
BMI		
mean	29.2111	26.2917
std. dev.	4.2079	4.8099
weight sum	80	224
precision	1.6538	1.6538
QRSduration		
mean	91.2467	89.6563
std. dev.	16.4217	17.3387

weight sum	80	224
precision	2.1803	2.1803
$PR_{interval}$		
mean	0	153.8372
std. dev.	0.5698	45.627
weight sum	80	224
precision	3.4186	3.4186
heartrate		
mean	91.9031	73.31
std. dev.	17.3869	12.4025
weight sum	80	224
precision	1.2615	1.2615

=== Detailed Accuracy By Class ===

	TP Rate	**FP Rate**	**Precision**	**Recall**	**F-Measure**	**ROC Area**	**Class**
	1	0.049	0.879	1	0.936	0.989	AF
	0.951	0	1	0.951	0.975	0.989	NOAF
Weight Avg.	0.964	0.013	0.968	0.964	0.965	0.989	

Correctly Classified Instances	**293**	**96.3816 %**
Incorrectly Classified Instances	**11**	**3.6184 %**

Table 11: Naïve Bayes classification classes

a	**b**	**Classified as**
80	**0**	**a = Present**
11	**213**	**b = Absent**

Table 12: Naïve Bayes classification confusion matrix

5.2.6 Classification of A-Fib using logistic regression

Regression analysis is used to find a model that best fits the observation data. The logistic function is bounded by 0 and 1. It is a statistical modeling technique, a form of regression where the dependent variable or class is categorical and the independent variables are continuous, discrete and/or categorical. Generally, the dependent or response variable is

dichotomous, such as presence/absence or success/failure. When the dependent variable takes more than two ordered categories, a multinomial logistic regression is applied.

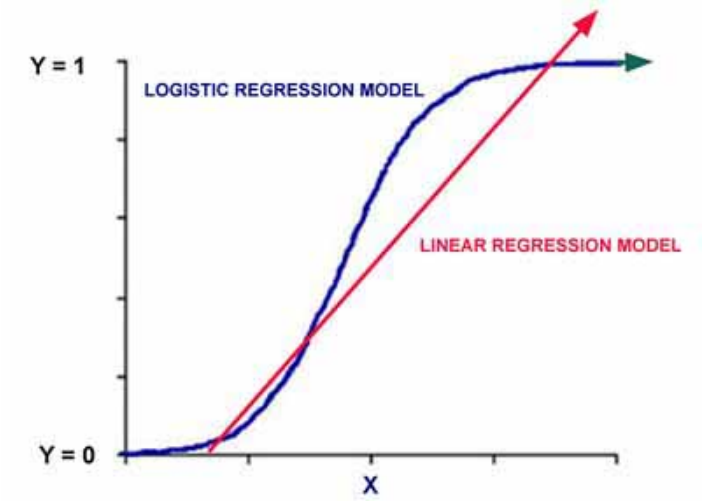

Figure 25: Logistic regression compared to linear regression

The dependent variable or class in logistic regression is said to be dichotomous (a.k.a. Bernoulli or binary) when it takes only two values, a value 1 with a probability of success p and a value 0 with probability of failure (1-p). When the logistic regression is applied to cases where the dependent variable has more than two choices, it is known as multinomial [67] [68]. Logistic regression makes no assumption about the distribution of the independent variables. Unlike linear regression, logistic regression does not require the relationship between the predicting variables and response variable to be normally distributed nor linearly related (see Figure 25). Logistic regression determines the relative effect of independent variables on the dependent variable or class and their statistical significance. This effect is usually explained in terms of odds ratios where the odds of an event x that occurs with probability p is defined as: $\text{odds}(p) = \frac{p}{1-p}$. The odds function maps probabilities p of an event (where p is between 0 and 1) to values between 0 and infinity (see Figure 26).

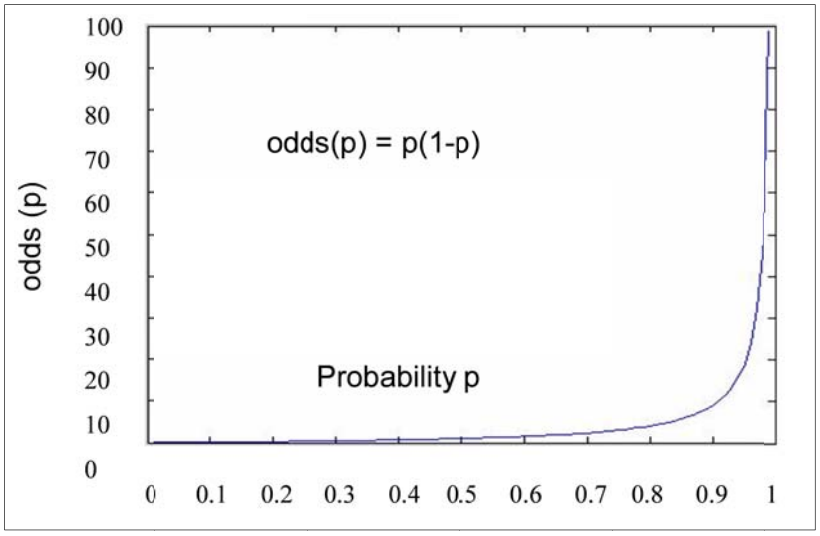

Figure 26: The odds function maps probabilities (0 to 1) to values (0 to infinity)

Logistic regression predicts the natural logarithm of the odds of the dependent event, called the logit function. In a binary logistic regression where dependent value is either 0 or 1, the event is equal to 1 and the reference category is equal to 0. For multinomial logistic regression, the event is equal to the value of interest and the reference category is equal to 1. In the case where there are only two classes, the logistic regression replaces the original target value: $p(1|x_1, x_2, \dots, x_k)$ which is constrained to [0, 1] interval with $\ln\left(\frac{p(1|x_1,x_2,\dots,x_k)}{1-p(1|x_1,x_2,\dots,x_k)}\right)$ which is called the logit transformation and can lie anywhere in [-∞, ∞] interval.

$$\text{logit}\big(p(1|x_1, x_2, \dots, x_k)\big) = \ln\left(\frac{p(1|x_1, x_2, \dots, x_k)}{1 - p(1|x_1, x_2, \dots, x_k)}\right)$$

$$= \ln(\text{odds}\big(p(1|x_1, x_2, \dots, x_k)\big))$$

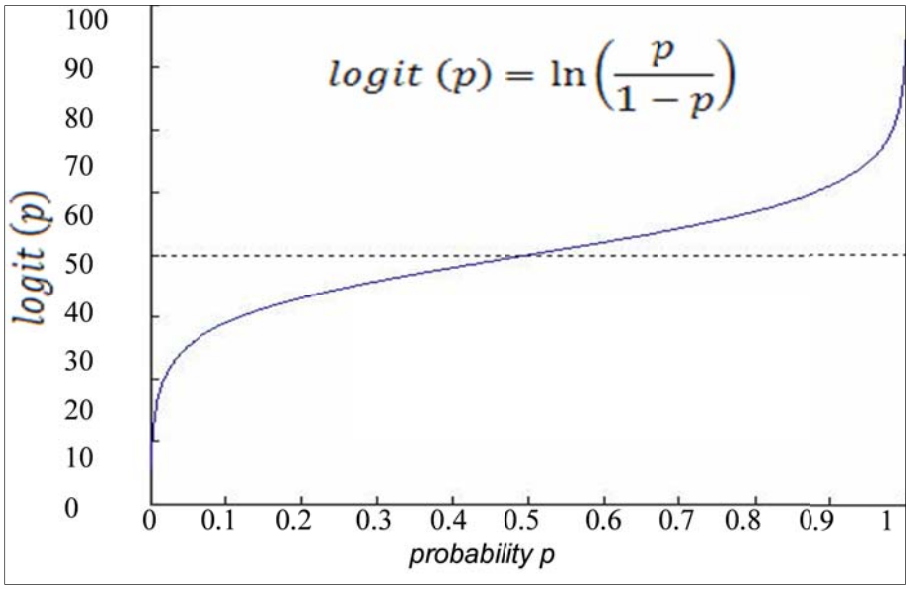

Figure 27: Logit function

The logit function has all the desired properties of a linear regression and still allows the response variable to follow a binomial distribution where the values of the probability p are bounded to values between 0 and 1 (See Figure 27). The linear expression of the logit(p) for input variable p is:

$$\text{logit}\big(p(1|x_1, x_2, \ldots, x_k)\big) = b_0 + b_1x_1 + b_2x_2 + \cdots + b_kx_k$$

Where:

$$\text{logit}(p) = \ln\big(\text{odds}(\text{event})\big) = \ln\left(\frac{p}{1-p}\right)$$

b_0 is a constant and the "b_k" terms are the logistic regression coefficients, also called parameter estimates. An alternative form of the logit(p) is:

$$\ln\left(\frac{p}{1-p}\right) = b_0 + b_1x + b_2x_2 + \cdots + b_kx_k$$

$$\text{odds} = \frac{p}{1-p} = e^{\,b_0 + b_1x + b_2x_2 + \cdots + b_kx_k}$$

Which becomes:

$$p(1|x_1, x_2, \ldots, x_k) = \frac{1}{1+e^{-(b_0 + b_1 x + b_2 x_2 + \cdots + b_k x_k)}}$$

Classification:

In summary, linear regression predicts:

$$\text{class} = 1 \text{ if } p(1|x_1, x_2, \ldots, x_k) > 0.5$$

$$\text{otherwise, class} = 0$$

The following section describes the test results pertaining to a logistic regression method involving the detection of the presence or absence of A-Fib using a 7-attribute case and a 10-fold cross-validation (see Tables 13 and 14). We derive the logistic regression coefficients, overall accuracy (see Table 15), Type I and Type II misclassification errors, sensitivity rate, specificity rate, and confusion matrix (see Tables 16 and 17).

Table 13 describes the attributes selected and their derived coefficients.

	Variable	Description	Value
1	Age	Age in years, linear	real
2	Age^2	Age^2 in $years^2$	real
3	Gender	Gender (0 = male; 1 = female), nominal	{0, 1}
4	BMI	Kg/m^2, Linear	real
5	QRSduration	Average of QRS duration in msec., linear	real
6	$PR_{interval}$	Average duration between onset of P and Q waves in msec., linear	real
7	Heartrate	Number of heart beats per min, linear	real
8	Class	{A-Fib present, A-Fib absent}	binary

Table 13: A-Fib attributes

Tables 14, 15, 16 and 17 show the results of A-Fib logistic regression classification.

=== Run information ===

Scheme: weka.classifiers.functions.Logistic -R 1.0E-8 -M -1
Relation: arrhythmia-weka.filters.unsupervised.attribute.Remove-R4

Instances: 304
Attributes: 7
Classes: 2
Test mode: 10-fold cross-validation

Class	Type	Number of instances
01	A-FIB present	80
02	A-FIB absent	224

Table 14: Classification classes of A-Fib

Logistic Regression Coefficients	
Variable	**Coefficient**
Age	0.8203
Age^2	-0.0062
Gender	4.7368
BMI	-0.0471
QRSduration	0.0982
$PR_{interval}$	-0.1776
Heartrate	0.0657
Intercept	-41.1751

Odds Ratios	
Variable	**Value**
Age	2.2712
Age^2	0.9938
Gender	114.0704
BMI	0.954
QRSduration	1.1032
$PR_{interval}$	0.8372
Heartrate	1.0679

Correctly Classified Instances	296	97.3684 %
Incorrectly Classified Instances	8	2.6316 %

TP	FP	Precision	Recall	F-Measure	ROC Area	Class
0.988	0.031	0.919	0.988	0.952	0.986	**A-Fib present**
0.969	0.013	0.995	0.969	0.982	0.986	**A-Fib absent**
0.974	0.017	0.975	0.974	0.974	0.986	**Weight Ave.**

Table 15: A-Fib results summary from WEKA tool

The confusion matrix for our binary classification model (A-Fib is present, A-Fib is absent) is a 2x2 matrix that displays the counts of the four types of detections that will help measure the classifier performance.

a	b	Classified as
79	**1**	a = A-Fib present
7	**217**	b = A-Fib absent

Table 16: A-Fib confusion matrix from WEKA tool results

Confusion Matrix		**Actual A-Fib**	
		A-Fib Positive (Present)	A-Fib Negative (Absent)
Predicted A-Fib	A-Fib Present. (Positive)	TP=79 Sensitivity $\frac{\text{TP}}{\text{TP+FN}}$ 98.7%	FP=7 (Type I Error) $\frac{\text{FP}}{\text{TN + FP}}$ 3.1%
	A-Fib Absent (Negative)	FN=1 (Type II Error) $\frac{\text{FN}}{\text{TP + FN}}$ 1.3 %	TN=217 Specificity $= \frac{\text{TN}}{\text{TN + FP}}$ 96.9%

Table 17: A-Fib detailed confusion matrix

Positive Predictive Value $\frac{\text{TP}}{\text{TP + FP}} = 91.9\ \%$	Positive Likelihood Ratio $\frac{\text{Sensitivity}}{1 - \text{Specificity}} = 38/1$
Negative Predictive Value $= \frac{\text{TN}}{\text{TN + FN}} = 99.5\ \%$	Negative Likelihood Raio $= \frac{1 - \text{Sensitivity}}{\text{Specificity}} = 1/1$

$$\text{Positive rate } = \frac{\text{TP + FP}}{\text{TN + FP + TP + FN}} = 28.3\ \%$$

$$\text{Negative rate} = \frac{\text{TN} + \text{FN}}{\text{TN} + \text{FP} + \text{TP} + \text{FN}} = 71.7\%$$

Note: more data for the classification of A-Fib may be needed to corroborate the false positive rate of 3.1%.

True positive rate = TP / (TP + FN) = 79 / (79 + 1) = .988

True negative rate or specificity = TN / (TN+FP) = 217 / (217+7) = .969

False positive rate (α) = FP / (FP + TN) = 7 / (7 + 217) = 0.031 = 1 – specificity

False negative rate (β) = FN / (TP + FN) = 1 / (79 + 1) = 0.013= 1 – sensitivity

Power = sensitivity = 1 – β = 1-.013 = 0.987

Positive Likelihood ratio = sensitivity / (1 – specificity) = .987/ (1 – .969) = 38 / 1

Likelihood ratio negative = (1 – sensitivity) / specificity = (1 – .987) / .969= 1 / 1

Positive rate = (TP + FP) / (TP + FP + TN + FN)

Negative rate = (TN + FN) / (TP + FP + TN + FN)

Positive predictive value (PPV): probability that the disease is present when the test is positive (expressed as a percentage).

Negative predictive value (NPV): probability that the disease is not present when the test is negative (expressed as a percentage).

The derived logistic regression algorithm is selected as the A-Fib detection algorithm. It identifies the instances with the A-Fib disease with 98.8% sensitivity, and identifies those without the disease with 96.9% specificity. A specificity of 96.9% leads to a false positive result of 3.1%. A sensitivity of 98.8% means that the classifier does not

recognize all actual positives. A sensitivity of 100% implies that the test extracted all actual positives whereas in a high specificity test, negative results are used to rule out the disease.

The outcomes of the Logistic Regression include True Positive and False Positive results. They may be triggered at A-Fib incidence rates reported by the Manitoba studies [50] in Section 4.

A-Fib is predicted present if probability p (A-Fib is Present | Age, Age^2, Gender, BMI, QRSduration, $PR_{interval}$, Heartrate) > 0.5

Otherwise, A-Fib is absent.

$$\text{logit}(p) = -41.175 + 0.820\ \text{Age} - 0.006\ \text{Age}^2 + 4.737\ \text{Gender} - 0.047\ \text{BMI} + 0.098\ \text{QRSduration} - 0.178\ \text{PR}_{\text{interval}} + 0.066\ \text{Heartrate}$$

And

$$p = 1 / (1 + e^{-\text{logit}(p)})$$

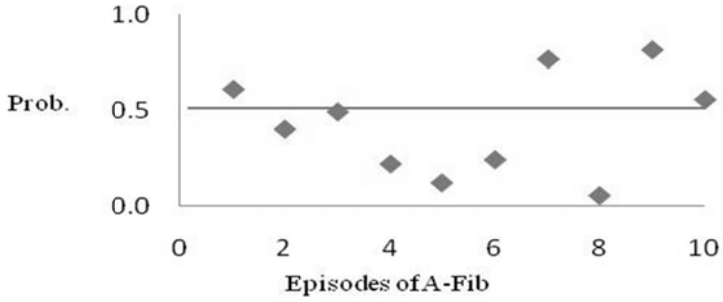

Figure 28: Probability of A-Fib prediction

The A-Fib detection algorithm is triggered by the onset of A-Fib. The incidence rate of A-Fib is higher in older people. Suggested studies [59] reveal that clinical measurement of sensitivity (True Positive rate) of 80% and specificity (True Negative rate) of 92% when A-Fib is diagnosed by internists and general practitioners instead of cardiologists. Our logistic regression classification of A-Fib has a measurement of sensitivity of 98.8%

and specificity of 96.9%. The false positive results, usually interpreted as false alarms, contribute to wasted or needless energy spent in transmitting inaccurate information. In this analysis the logistic regression algorithm with a False Positive rate of 3.1% (see Figure 10, Confusion matrix of A-Fib logistic regression) rivals the clinical measurement of False Positive rate of 8% diagnosed by internists and general practitioners.

Both the overall classification error rate and the overall classification accuracy are:

$$\text{Overall Error rate} = \frac{FP+FN}{TP + TN + FP + FN} = 2.63\%$$

$$\text{Overall Accuracy} = \frac{TP+TN}{TP + TN + FP+FN} = 97.37\%$$

The area under the ROC curve measures how well a particular parameter can distinguish between two diagnostic groups (such as presence of a disease/absence of A-Fib). The bigger the area is and the closest to 1, the better the classifier performance. The area under the ROC curve for the derived logistic regression model is 0.986.

5.2.7 Comparing accuracies in J48, Naïve Bayes and logistic regression

Three machine learning techniques, J48, Naïve Bayes algorithms, and logistic regression analysis are explored to test for the detection of the presence or absence of A-Fib: A 7-attribute case and a 10-fold cross-validation are used. The differences in accuracies from all three machine-learning algorithms are not significant (see Table 18). Though there are other methods to classify A-Fib, we select logistic regression for its simpler programmable implementation into mobile devices. The results of the experiment in terms of accuracy or number of correctly classified instances on the dataset between J48, Naïve Bayes and logistic regression are illustrated in Table 18:

Test Criteria	Algorithms Detecting A-Fib		
	J48	Naïve Bayes	logistic regression
Accuracy	96.71%	96.38%	97.37 %

Table 18: Comparing accuracy of J48, Naïve Bayes and logistic regression

5.2.8 The impact of Type I error and Type II error on A-Fib classification

False positive outcomes, known as Type I error, are classification results that predict the patient as having A-Fib when actually the patient does not have the disease, usually interpreted as a false alarm. They contribute to wasted or needless energy spent in transmitting inaccurate information. Clinical results suggest the A-Fib specificity is 92%.

$$\text{False positive rate} = 1 - \text{specificity} = 1 - 0.92 = 0.08$$

In an ideal classification, the positive rate would be the same as the incidence rate. If the positive rate is less than the incidence rate then the number of positive results reported by the classification algorithm is underestimated. Likewise, if the positive rate is greater than the incidence rate, the classification algorithm is exaggerating the number of positive results. The false positive results embedded in the positive results may prove to be costly and may erode the algorithm accuracy and confidence. A false positive rate in a classification should be as small as possible, preferably zero. Our proposed classifier is 97.37% accurate, and its False Positive error rate is 3.1% compared to the clinical False Positive rate of 8%.

On the other hand, failing to detect A-Fib and predicting the patient as not having A-Fib when the patient actually has the disease is serious and costly; this is known as Type II or

false negative error. The goal of any classification is to minimize the false negative. Clinical measurement results have an A-Fib sensitivity of 80%,

$$\text{False negative rate} = 1 - \text{sensitivity} = 1 - 0.80 = 0.20$$

Our proposed model has a false negative rate of 1.3%.

Ideally a classification system would consist of sensing EKG signals, transmitting EKG signals to the master device, receiving EKG by the device, classifying received data, and reporting the results that are guaranteed to be 100% True Positive (TP). In other words, there would be no False Positive (FP) results in the monitored data. In real life, the classification scheme would correctly classify the presence or absence of A-Fib with some accuracy and would transmit the positive results of the classifier when arrhythmia is present at the positive rate r_p. The classification positive rate plays an important role in the validity of the energy reduction scheme. If the positive rate is equal to the incidence rate then if the classification detection algorithm correctly classifies 100 % of the episodes of A-Fib then one concludes that the classification positive rate is made up of all True Positive results and no False Positives. Because classification rarely classifies 100% of the instances correctly, the goal in classification remains to minimize both the False Negative and the False Positive results. Minimizing the latter reduces the unnecessary transmission of information.

Further studies involving larger A-Fib datasets are needed to corroborate the results. As shown in later sections, the classification schemes using an incidence rate and prevalence window delivers better results in energy consumption than the telemetry model but has a risk of introducing False Positive results. Moreover, the classification model accuracy, the False Positive and the False Negative rates are also better than those obtained in a

clinical setting where practitioners and nurses interpret EKG data during patient screenings and/or during medical physical exam visits (see Table 19).

	Error Type	
FP = Type I error and FN = Type II error	**FP**	**FN**
Telemetry Device:		
• Telemetry by Cardiologist	reference	reference
Manual EKG readings during Screening and doctor visits:		
• General practitioner EKG interpretation	0.08	0.20
Wearable Computing Device:		
• Detecting A-Fib	0.031	0.013

Table 19: Error types summary

CHAPTER 6

6 ENERGY MODELS FOR MONITORING AND DETECTING THE FIRST EPISODE OF A-FIB

Today telemetry is widely accepted in healthcare for remotely collecting and sending vital data to a monitoring station for analysis and interpretation of all types of arrhythmia in outpatients. Mobile outpatient cardiac telemetry devices typically are not energy-aware; they consume battery energy continuously and necessitate outpatients to replace batteries often, sometimes daily. Moreover the device is not practical for patients who experience infrequent (less frequently than every 48 hours) symptoms suggestive of cardiac arrhythmias (i.e., palpitations, dizziness, pre-syncope, or syncope). As a prerequisite to this design, we first identify and calculate the energy requirements for the current telemetry and for the wearable healthcare computing devices. Next, we develop a reference energy model, then the proposed wearable computing energy models. Using the telemetry energy as reference, we compare each proposed energy model to the telemetry energy model by calculating the percent of relative energy reduction contributed from each proposed energy model. We adapt an evolutionary approach to the design of the proposed energy models (see Figure 29): we develop three primary energy models which incorporate the following features one at the time: an A-Fib detection algorithm, an A-Fib positive rate, an A-Fib incidence rate, and a prevalence window. Then by using the three

primary models, we generate a hybrid model by combining the three features with the aim to achieve the most efficient energy model for the detection and reporting of progressive development of cardiac A-Fib to be used in battery operated wearable healthcare computing devices.

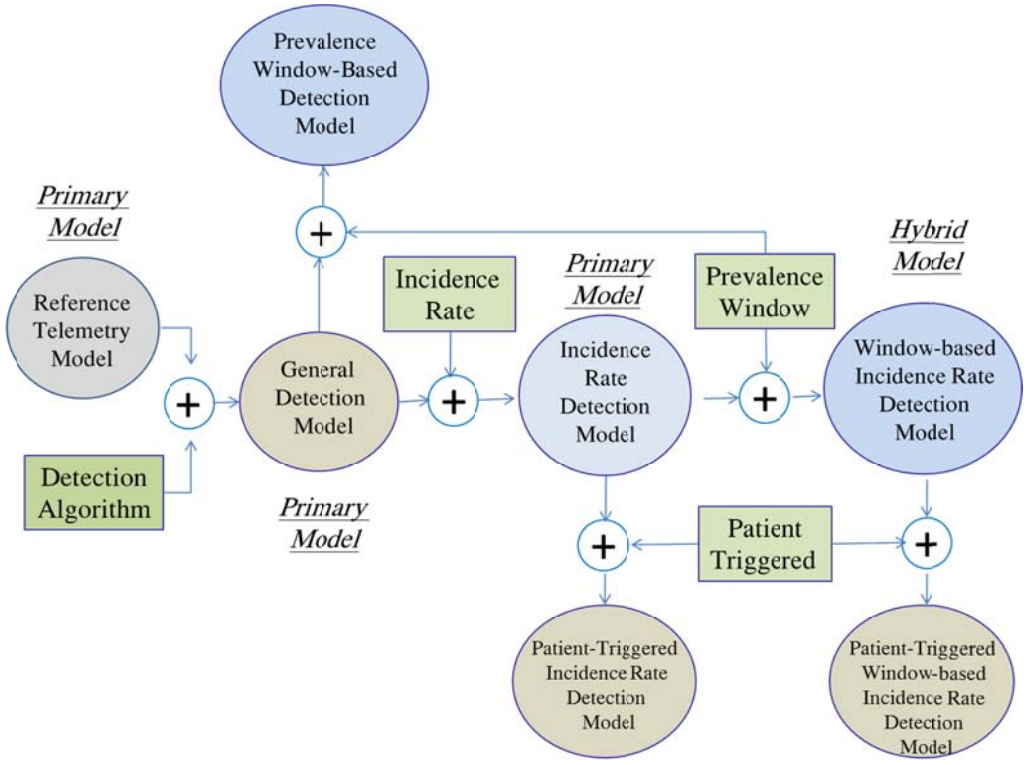

Figure 29: Telemetry and proposed detection energy models

Preliminary results showed that some proposed energy models performed better, i.e. consume less energy than the telemetry energy model. The performance varied from model to model depending on which feature and combination of features were used in the primary and hybrid models.

The following sections present the energy requirements of telemetry and wearable computing devices followed by the proposed energy models.

6.1 Energy requirements of wearable healthcare computing devices

Excluding the operating system and support, wearable healthcare monitoring devices are comprised of three main parts: sensing, detection, and reporting. In an energy-constrained environment, one cannot afford to run each component continuously. One must make judicious use of the energy that is available and run components in an optimized scheme. The operation of continuously sensing, analyzing, detecting, and reporting affects energy consumption. Furthermore, the combination of wearable mobility, a high performance requirement in ever-increasing healthcare applications, and high quality user-interactivity place severe resource demands on an already energy-constrained environment. Current healthcare systems must budget energy consumption in order to deliver optimum results, keep battery lifetime high and monetary expenditure low.

The proposed schemes are energy-aware of the timely importance as to when to process sensing, versus reporting, versus detection and any combination thereof. Though the proposed energy-aware budgeting schemes could be applied to a variety of healthcare detection and monitoring applications, their intent here would be for the detection and reporting of cardiac arrhythmia and more specifically, A-Fib. The schemes allow the wearable devices to be automatic, scalable, adaptive, and user-transparent as the user may be engaged in daily activities or even incapacitated. Wearable computing devices using wireless sensor networks and a smartphone offer an alternative to telemetry devices and significantly improve the monitoring and detection of arrhythmia and other measurable healthcare conditions. The three main components in a wearable computing system are monitoring, detection, and transmission. The following sections describe the energy requirements (see Figure 30):

- For the process of signal sensing
- For Bluetooth signal transmitting from the sensor to the GSM (Global System for Mobile communication) smartphone
- For the GSM smartphone receiving the signal from the Bluetooth sensor
- For smartphone conditioning and classifying the received data, and
- For smartphone transmitting the telemetry data and the detection results

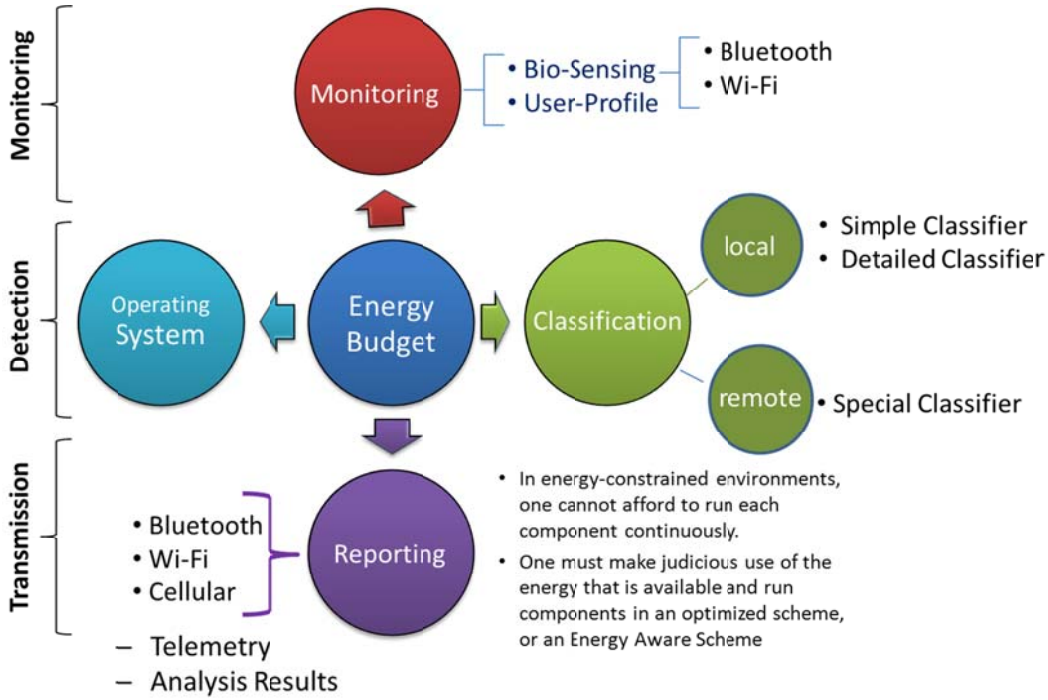

Figure 30: Wearable computing system requirements

6.1.1 Energy requirements of signal sensing

The sensing task receives its reading input from EKG sensors, and performs data collection and data aggregation. The sensed signals may be compressed to improve the system's performance further. Compressed EKG data reduces memory footprint and improves network traffic efficiency during transmission. User-profile and patient medical

history, usually a one-time input during initial set-up, are collected to improve the detection of arrhythmia.

Today, mobile devices use Bluetooth network to collect data wirelessly, whereas standalone systems (usually AC-wired) might use Wi-Fi or wired network where the energy is adequately abundant. Energy consumption might be reduced in a wearable healthcare device if one adapts a periodic monitoring sequence and a monitoring frequency.

In this dissertation, a portable, low-power wireless two-lead EKG system integrated with the University of California (UC) Berkley's MICA2 mote promises a potential solution to the challenges of monitoring and detection in a wearable healthcare computing device. The MICA2 mote is a wireless measurement system developed by UC Berkley and manufactured by Crossbow Technology, Inc. [69].

The design of our proposed energy-aware model uses measurements and characteristics from the aforementioned portable, low-power, wireless two-lead EKG system [70]. The device uses a two-lead connection and continuously monitors electrocardiogram activity and therefore arrhythmia. The device compares favorably with today's 12-lead EKG device which records only a snapshot of the heart's electrical activity, a short sample of no more than thirty seconds [71]. Today, each pair of electrodes in the standard EKG provides detailed information of the cardiac rhythm in a snapshot from different angles of the heart. A cardiologist will interpret the tracings engendered on paper or on a screen to diagnose the presence or absence of arrhythmia. However, sporadic or intermittent arrhythmia may not be easily identifiable since the cardiac abnormal conditions may have been missed because they were present only temporarily. Few healthcare centers

overcome these shortcomings by prescribing continuous EKG telemetry either by admitting the patient to an intensive care unit or by having the patient wear a portable heart monitoring device such as a Holter monitor or event monitor for a period of time. The data from these cardiac monitoring devices is transmitted to a healthcare center for analysis and detection indicating the presence or absence of arrhythmia. The EKG machines that are found in medical offices are AC powered and experience no energy constraints; however, the patient has to be coincidently present while he is experiencing arrhythmia. On the other hand, battery-operated portable monitoring devices such as Holter monitors and Event monitors exhibit many shortcomings including energy constraints, short sampling, and no local analysis or detection of arrhythmia.

6.1.2 Description of the sensing system

The MICA2 Mote is a third generation mote, or tiny wireless smart sensors system, developed by UC Berkley and manufactured by Crossbow Technologies Inc. to enable low-power, wireless, sensor networks. MICA2 wireless platform is used as a foundation for various wireless sensor network applications and research groups. One such application is the low power wireless 2-lead EKG circuit developed by the Division of Engineering and Applied Sciences at Harvard University, which plugs into the MICA2 platform through an expansion port. The MICA2 measures a compact 2.25 by 1.25 by 2.2 inches. It includes an embedded microcontroller, a multi-channel radio transceiver operating in the ISM band at 433MHz or 916MHz with an extended range between 20-30 meters and a data rate of 76,800 bps. It runs on a specialized event-driven TinyOS (TOS) [72] and supports a wide range of sensor boards and data acquisition add-on boards. TinyOS 1.0 is a small, open source, energy efficient, software operating system

developed by UC Berkeley which supports large scale, self-configuring sensor networks. The processor is based on the Atmel low power microcontroller ATmega 128L, which runs TOS from its internal flash memory. The MICA2 sports a 51-pin expansion connector and supports a wide variety of external peripherals through its Analog Inputs, Digital I/O, I2C, SPI, and UART interfaces. The MICA2 and the piggybacked low power wireless 2-lead EKG circuit make the monitoring and transmission of continuous electrocardiographic data possible. Performance evaluation of the device was assessed by medical expertise and pronounced indeed comparable to that of a commercial EKG [73]. The circuit reads from two electrodes and delivers the resulting trace to the MICA2 built-in ADC converter via the 51-pin expansion connector. The transmitted data is ultimately received by smartphones and computers equipped with receiver cards.

The device consumes 60mW of power when monitoring continuously in active mode and 30 microwatts in standby mode where monitoring is disabled. The EKG information is read at 120Hz sampling rate with four transmissions per second of 30 samples each.

6.1.3 Energy requirements of transmitting and receiving data using Bluetooth

We consider using Bluetooth wireless technology when transmitting data from an EKG data acquisition module (i.e. a portable, low power, wireless two-lead EKG system) to a smartphone and receiving the EKG information into the smartphone. Bluetooth transmits and receives data at rates up to 2Mbps in the 2.45GHz band. Radio communications expend 10^{-7} J/bit for transmission using Bluetooth [74] [105]. The Bluetooth Core Specification and Health Device Profile offer further low power features to help maintain and extend minimum battery life. Though this dissertation uses Bluetooth only for transferring data between devices, it is worthwhile to mention the power-saving modes

that are inherent in Bluetooth such as Sniff mode and Sniff Subtrate mode. The Sniff mode prolongs battery life by allowing two devices to only exchange data periodically and still stay connected between data transfers and frees the transmission bandwidth. Sniff Subrating mode reduces power consumption by allowing devices to increase the time between listening for data packets therefore reducing the number of packets exchanged. The normal mode in Bluetooth stays active at all times even when there is no data for transfer.

6.1.4 Energy requirements of reporting and transmitting using GSM/EDGE

The reporting task transmits data that may be compressed and encrypted, as well as detection results. We consider transmitting data using GSM/EDGE network to report arrhythmia results and telemetry information to a remote server. GSM (Global System for Mobile communication) is a digital mobile telephony system that operates in the 900 MHz band in Europe and Asia and in the 1.9 GHz band in the United States. EDGE is an enhanced GSM. It provides data at rates up to 384 Kbps. Radio communications expend $4*10^{-5}$ J/bit using GSM smartphone [74] [105].

6.1.5 Energy requirements to detect A-Fib

Data mining, a process of extracting patterns from a dataset, is increasingly used in bioinformatics for medical discovery. Classification in data mining is used to build models that can correctly predict the class of instances in a dataset. Classification algorithms shall be selected using machine learning algorithms [62] and adapted to detect the presence or absence of cardiac arrhythmia. The classifier is adaptive to different health profiles and different needs, which may require changing parameters. Patient's condition (data containing mostly outliers) sometimes varies, necessitating different

algorithm and analysis. The scheme may seamlessly adopt newly derived learning algorithms sent from remote application servers [75]. A-Fib detection typically executes in few mathematical operations (such as exponentiation, multiplication and addition/subtraction). The energy required to detect A-Fib is typical negligible compared to the energy to receive or transmit EKG signals.

6.1.6 Energy concerns

Holter monitoring, a battery operated portable continuous EKG monitoring and recording device, is used for 24/48 hours to capture any episodes of A-Fib and arrhythmias. Holter monitoring data is collected and saved together with patient's activities for later analysis and correlation by a physician. If the episodes are too infrequent to detect by Holter monitoring then Event monitoring is prescribed for a longer period such as a month. The recorder is activated by the patient when symptoms of arrhythmia occur. A memory loop enables EKG information to be stored for seconds before and after activation. The patient transmits the collected data to a physician via telephone. The continuous monitoring and reporting by these devices drains batteries very quickly. Batteries are the Achilles' heel of these portable devices. Batteries have to be changed periodically, sometimes as often as once a day such as in the Cardionet sensor [24].

6.1.7 Energy in a battery used in a wearable computing device

An electrical battery is a combination of one or more electrochemical cells that convert stored chemical energy into electrical energy. Batteries are simple devices used as a source of direct current in portable electric and electronic equipment. There are two types of batteries: disposable batteries, and rechargeable batteries. Disposable batteries are designed to be used once and discarded, while rechargeable batteries are designed to

be recharged and used multiple times. The capacity in a battery cell is expressed in ampere-hours. The energy (E) is expressed in Joules and watt-hours. The Joule is the international standard unit of energy defined as one watt-second. 3600 Joules are contained in one watt-hour.

$$E = P.T = V.I.T$$

Where E = Energy (watt-hour), P = Power (watts), T= Time (hours), I = DC Current (amperes), V = Electromotive force (volts).

Device battery lifetime varies depending on device power consumption, usage time, usage mode, and battery quality. The Duracell Copper Top MN 1500 – AA alkaline [76] battery has a nominal voltage of 1.5 volts, and comes with a rated capacity of 2.850 ampere-hours or (2.85 Ah) (1.5 V) (3600 s/h) =15,390 Joules. The fully rechargeable 3.7 V, 550 mAh Li-ion battery of type Casio NP20 or PowerSmart delivers an energy of 7326 Joules, (3.7 V) (550 mAh) (0.001 A/mA) (3600 s/h). In this analysis, we consider the BlackBerry Torch 9800 [77] which has a capacity of 1270 mAh or (1.270 Ah) (3.7 V) (3600 s/h) = 16,916.4 Joules. The Torch's battery life lasts 5.5 hours in GSM/EDGE Talk Time.

Figure 31 depicts an example of smartphone battery in various modes: a standby mode, an idle mode with Bluetooth connection (to a Bluetooth device), a continuous active mode while receiving and transmitting via Bluetooth (i.e. continuously listening to music), and a continuous talk mode using EDGE. Figure 32 displays typical battery life in a smartphone.

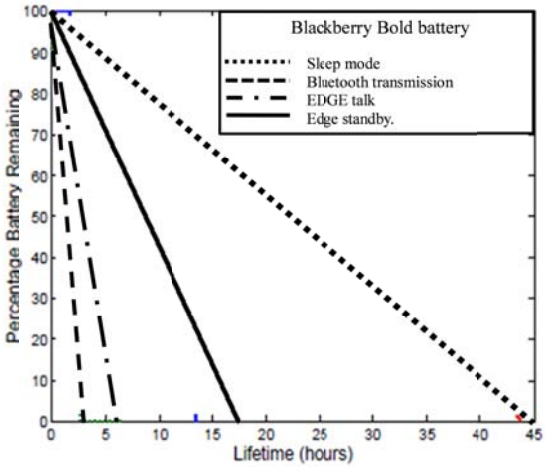

Figure 31: Lifetime of a Blackberry Bold battery

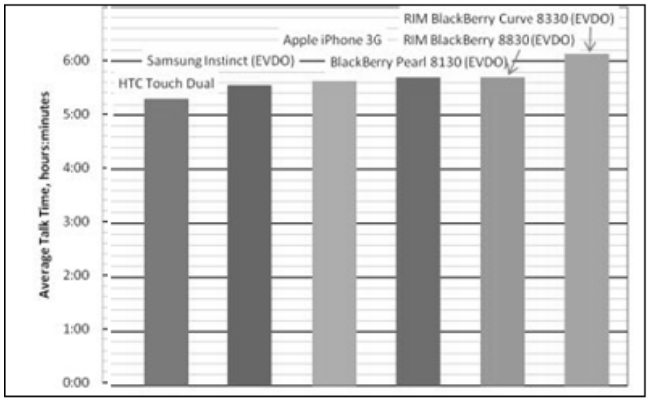

Figure 32: Typical battery life in a smartphone [102]

6.2 Energy models for the A-Fib detection schemes

There is an energy cost associated with each cycle of monitoring, classification and reporting. Decisions of when and what critical process needs to run must be made in order to deliver essential results where a critical battery capacity shortage exists. Today, telemetry and wearable computing devices are ubiquitous in healthcare monitoring. They are equipped with small batteries that have a limited life. They are used to monitor a patient heart's abnormal activity for periods ranging from days to weeks. Sensed or recorded EKG data is sent to a doctor or a care center for analysis and reporting (see Figure 33). Telemetry and wearable healthcare computing systems are concerned with

three main components: monitoring, detection, and transmission. In an energy-aware environment, the different components must run sensibly in order to extend battery life.

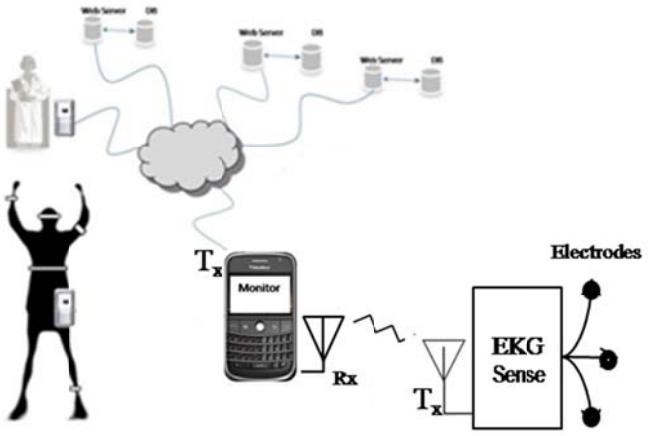

Figure 33: Overall view of a wearable computing system

6.3 Parameters affecting A-Fib detection and energy models

A-Fib monitoring and detection outcome accuracy and energy consumption levels depend on parameters such as the incidence rate of A-Fib, the distribution of the onset of A-Fib during a circadian rhythm, and the accuracy of a clinical diagnosis of the onset of A-Fib.

6.3.1 The incidence rate of A-Fib

The Manitoba follow-up study continuously observed 3,983 male aircrew recruits for 44 years and calculated the incidence of A-Fib based on 154,131 person-years of observation [50]. The study concluded that the incidence of A-Fib is 0.23 per 1,000 person-years at 95% confidence interval, 0.13 to 0.36 for people aged between 25 and 60 years, 5.7 per 1,000 person-years after age 60, and 9.7 per 1,000 person-years after age 70 (see Figure 34).

Similarly, the Framingham Heart study [6] [51] involving 2,325 men aged 25 to 65 years at enrollment reported the 22 year incidence of atrial fibrillation as 1.0 per 1,000 person

years, and later reported an incidence of 12 per l,000 person-years after age 70 [50]. The Ruigomez et al. study found that A-Fib incidence increases with advancing age [78], where the incidence rate of A-Fib varies between 0.4 and 0.7 per 1,000 person-years at

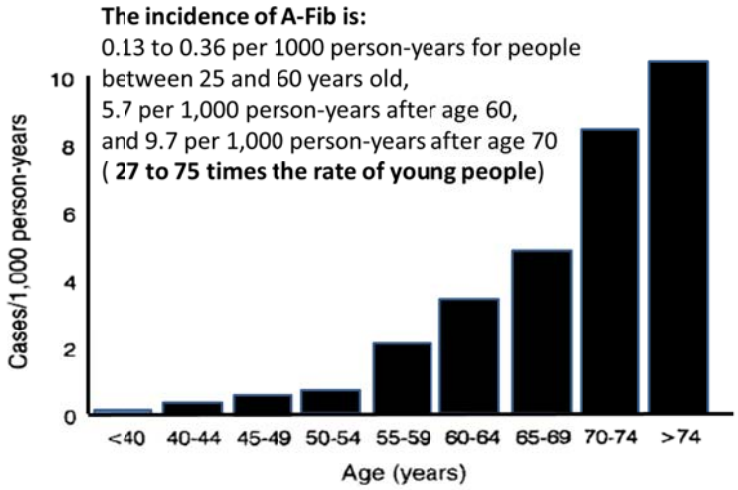

Figure 34: Incidence rate of A-Fib by age group [50]

age 50, and between 10 and 20 per 1,000 person-years at age 80. The incidence rate of chronic A-Fib was 1.7 per 1,000 person-years. In the Renfrew-Paisley project [79], the incidence of A-Fib was 0.54 cases per 1000 person years, and 0.3% for all cases of A-Fib in the Carroll and Majeed project [80]. All of the aforementioned studies draw attention to the significance of the higher frequency of A-Fib with advancing age. Early recognition of A-Fib is difficult because most people are not aware of this silent rhythm disturbance [81]. The first episode of A-Fib is diagnosed when heart palpitations last longer than 30 seconds. Frequent monitoring and screening of patients allow for early detection of arrhythmia. The latter might protect patients from the consequences of arrhythmia by introducing therapies early. It is worthwhile mentioning that at least one-third of the A-Fib episodes go undetected [50] because either people are not screened often or A-Fib diagnosis is missed by a general practitioner or a practice nurse.

The longer the heart remains out of normal sinus rhythm, the more difficult for the doctor to restore the normal sinus rhythm to the heart. The incidence of A-Fib is expected to more than double by the year 2050 [51] as the elderly population in America is expected to increase. The prevalence of A-FIB in persons younger than 55 years accounts for 0.1% and 3.8% in persons 60 years or older [48] [82] [83]. Incidence of A-Fib seems to be significantly higher in men than in women [78] (see Figure 35). The cost to treat A-Fib in the United States exceeds $6.4 billion per year [12]. People affected by A-Fib visit emergency rooms more often, and are four times more likely to be admitted into hospitals, than people who do not have A-Fib.

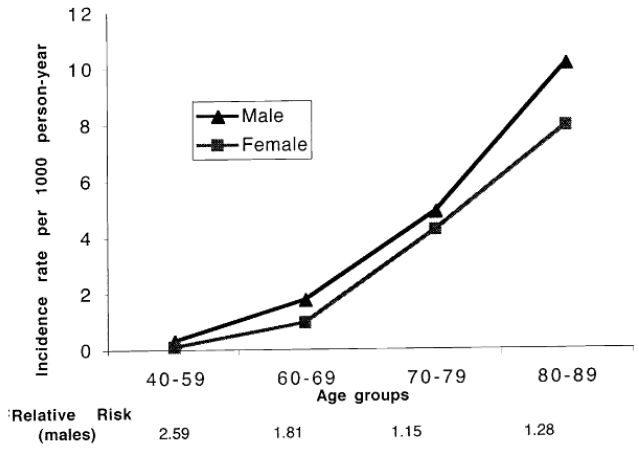

Figure 35: Incidence rates of chronic atrial fibrillation by sex [78].

6.3.2 The distribution of the onset of A-Fib during a circadian rhythm

The study by Georg Delle Karth et al. [84] assessed the diurnal distribution of ventricular tachycardia (VT) and A-Fib in critically ill patients during a circadian rhythm, the cyclical 24-hour period of human biological activity where a person usually sleeps approximately 8 hours and is awake 16. The study concluded that the onset of A-Fib

over a 24-hour period is non-uniformly distributed. A-Fib was prominent in the morning between 8:00 A.M. and 10:00 A.M. and around midnight (see Figure 36).

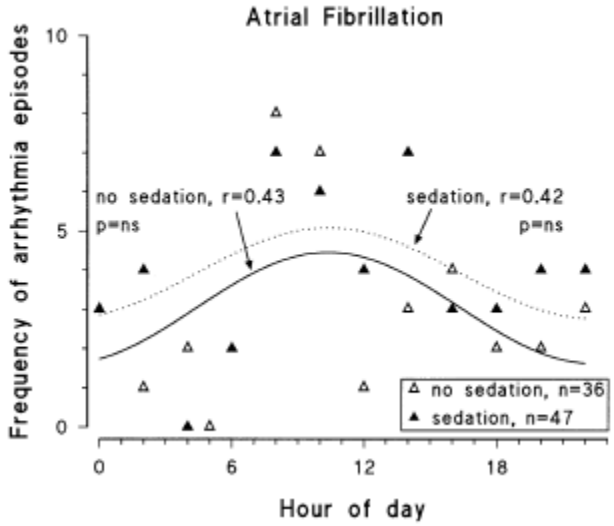

Figure 36: Circadian distribution of the onset of A-Fib episodes [84]

Another study by S. Viskin et al. [85] which used a large patient population (almost 10,000 episodes of A-Fib) suggests that the onset of paroxysmal A-Fib does not occur randomly, and that the circadian rhythm of paroxysmal A-Fib happens in clusters of events in the morning and (to a lesser degree) late in the evening. The findings are similar to those in the study by Georg Delle Karth et al. [84].

Among all arrhythmia, A-Fib is the most frequently diagnosed and affects 2.5 million people in the United States or close to 1% of the total population [12]. Its prevalence increases with a person's age, and it affects as many as 9% of the people older than 80 years [86]. Patients with A-Fib have a 1.5-2 fold increase in mortality rate when compared with the general population as suggested by Framingham Heart study data [6] [51].

6.3.3 The accuracy of a clinical diagnosis of the onset of A-Fib

Few studies have addressed the misdiagnosis of A-Fib from an electrocardiogram (EKG) and the potential risk of A-Fib misinterpretation errors. Knight et al. [54] concluded that A-Fib is more often misdiagnosed by internists than cardiology fellows and cardiologists. Mant et al. [55] discovered that general practitioners correctly detected A-Fib 80% (true positive) of the time when interpreting 12-lead EKG data and misinterpreted 8% (false positive) of sinus rhythm cases as A-Fib. Confusing A-Fib with atrial flutter is one of the most common misdiagnoses. Though both A-Fib and atrial flutter are clinically and electrocardiographically similar, the distinction between them is important since their treatment strategies may be different. Shiyovich et al. [56] concluded the misdiagnosis rate of electrocardiograms (EKG) consisting of 268 patients, interpreted as A-Fib by medical internists and corroborated by a cardiologist was 16%. The baseline diagnosis was correct in 212 of 246 (86%) for A-Fib, $p < 0.001$. Jonathan Mant et al. [55] discovered that general practitioners detected A-Fib on a 12 lead electrocardiogram with a sensitivity or True Positive rate of 80% at 95% confidence interval and misinterpreted cases of sinus rhythm as A-Fib with a specificity or True Negative rate of 92%. Similarly, practice nurses detected performed with a sensitivity of 77% and a specificity of 85%.

CHAPTER 7

7 THE BASELINE ENERGY MODEL

7.1 Defining the A-Fib telemetry energy components

Typically, a telemetry device may sense, store, and send the acquired EKG data to a remote server for analysis by a care center expert or a cardiologist. These on-body healthcare devices lack local detection, and are not energy-aware. The system transmits the EKG data wirelessly or through a phone line to a service center. The patient can also manually send the EKG data by pressing a button when experiencing a symptom. The results are not immediately known to the patient. The latter has to wait for analysis results to be available days later (see Figure 37).

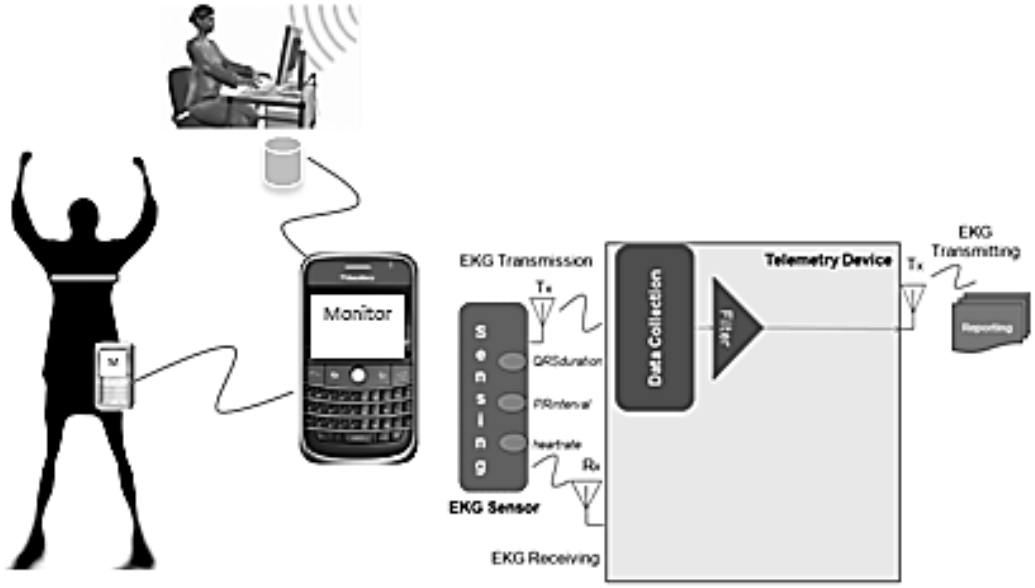

Figure 37: A telemetry monitoring device diagram

In our analysis, we adopt the MICA2 mote, a wireless EKG sensor developed by UC Berkley and manufactured by Crossbow Technology, Inc., and a smartphone. Figure 38 and Table 20 describe the energy components of a telemetry energy model capable of monitoring and transmitting EKG data.

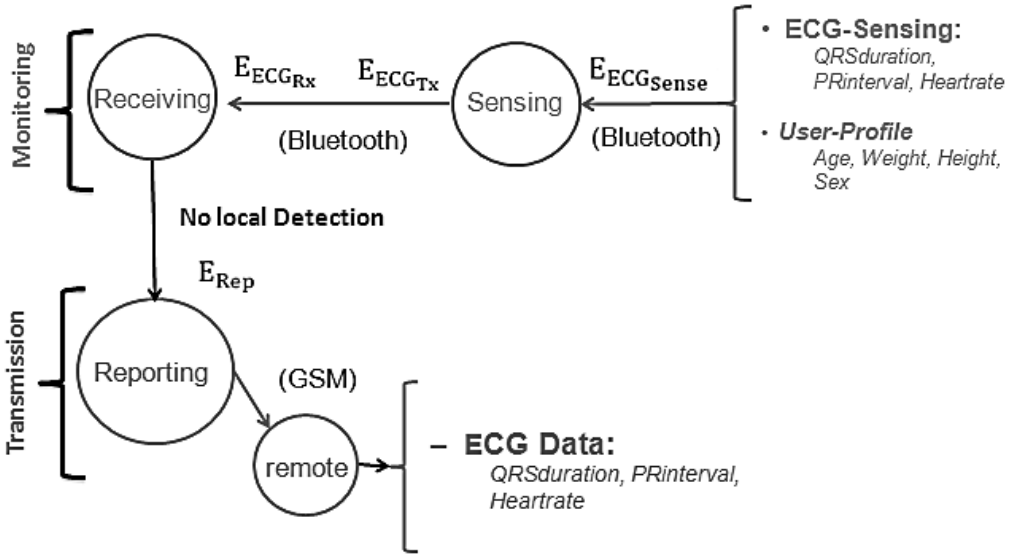

Figure 38: A-Fib telemetry energy distribution

The following calculations are estimates of the energy required in order to continuously transmit EKG records for a 24 hour period	
Battery capacity of 1270mAh or (1.270 Ah) x (3.7V) x (3600 s/h) = 16,916.4 Joules	The rechargeable smartphone battery such as the 3.7-volt Li-Polymer F-S1 battery [77]
$E_{telemetry}$	The total energy required by A-Fib telemetry model to continuously sense and transmit EKG records for a 24-hour period
$E_{TEtelemetry}$	The total energy required by event-triggered telemetry model to continuously sense and transmit EKG records for a 24-hour period
$T_{Sense} = 3600 \frac{\text{sec}}{\text{h}} * 24\ \text{h} = 86400\ \text{s}$	The 24 hour period in seconds of sensing EKG signals
$P_{Sense} = 60 * 10^{-3}$ Watts	The power consumed by a EKG sensing device (MICA2) sensing EKG signals
$E_{EKG_{Sense}} = P_{Sense} T_{Sense}$	The energy consumed by a EKG sensing device (MICA2) when continuously reading

$= 60 * 10^{-3} W * 86400 \text{ sec}$ $= 5184 \text{ Joules}$	EKG signals for a 24 hour period
Sampling rate $= 120$ Hz $= 120 \frac{\text{samples}}{\text{sec}}$ One sample size in bits $= 120 \frac{\text{samples}}{\text{sec}} * 8 \frac{\text{bits}}{\text{sample}} = 960 \frac{\text{bits}}{\text{sec}}$	MICA2 EKG Sampling rate where 1 sample = 1 byte = 8 bits
$n_{TxSense} = 960 \frac{\text{bits}}{\text{sec}} * 3600 \frac{\text{sec}}{\text{hr}} *$ 24 hr $=$ 82,944,000 bits = 10.368 Mbytes	The number of sensed EKG bits transmitted by the MICA2 EKG sensing device to the GSM/EDGE smartphone for a 24-hour period
$w_{Tx} = 10^{-7} \frac{\text{Joules}}{\text{bit}}$	Bluetooth transmits and receives data at rates up to 2Mbps in the 2.45GHz band. Radio communications expend 10^{-7} J/bit for transmission using Bluetooth. [74]
$E_{EKG_{Tx}} = n_{TxSense} w_{Tx}$ $= 82{,}944{,}000 \text{ bits} * 10^{-7} \frac{\text{Joules}}{\text{bit}}$ $= 8.3 \text{ Joules}$	The energy consumed by an EKG sensing device (Mica2) when continuously transmitting sensed EKG information via Bluetooth for a 24-hour period
$n_{RxSense} = n_{TxSense}$	The number of EKG bits received by smartphone for a 24-hour period
$w_{Rx} = 10^{-7} \frac{\text{Joules}}{\text{bit}}$	Bluetooth transmits and receives data at rates up to 2Mbps in the 2.45GHz band. Radio communications expend 10^{-7} J/bit for transmission using Bluetooth. [74]
$E_{EKG_{Rx}} = n_{RxSense} w_{Rx}$ $= 82{,}944{,}000 \text{ bits} * 10^{-7} \frac{\text{Joules}}{\text{bit}}$ $= 8.3 \text{ Joules}$	The energy consumed by a smartphone when continuously reading EKG information via Bluetooth for a 24-hour period
$n_{Rep} = n_{RxSense}$ + positive results in bits Slightly above 82,944,000 bits	The number of sensed EKG and positive results in bits transmitted via GSM/EDGE for a 24-hour period
$w_{Rep} = 4 * 10^{-5}$ Joules/bit	GSM (Global System for Mobile) communication expends $4*10^{-5}$ J/bit [74]
$E_{Rep} = n_{Rep} w_{Rep} =$ $82{,}944{,}000 \text{ bits} * 4 * 10^{-5} \frac{\text{Joules}}{\text{bit}} =$ 3318 Joules.	The energy consumed by the phone when continuously transmitting all EKG information (in case of telemetry) plus reporting all positive results (in case of detection model) via GSM/EDGE during a 24-hour period

Table 20: Energy requirements for a wearable computing device

7.2 Using telemetry as a baseline energy model

Healthcare physicians prescribe telemetry in one of two modes: continuous monitoring or user triggered monitoring. In the subsequent sections, A-Fib detection energy models will be compared to the continuous telemetry energy model.

7.2.1 Energy model of telemetry with continuous monitoring

Ambulatory Monitors such as Holter Monitors, Event Monitors, and telemetry fall short of providing adaptive, scalable, energy-aware real-time monitoring and analysis. Continuous monitoring, detecting and reporting of cardiac arrhythmia drain the battery quickly. Batteries in current devices last as a little as one day such as in Cardionet telemetry. Energy shortcomings may happen at the most unfortunate time and the onset of A-Fib goes undetected because the battery in the device is dead. Today, telemetry systems continuously sense EKG information for a period of time and transmit it to a healthcare center for further diagnostics and analysis by a doctor or a healthcare specialist. The system transmits all the monitored data including positive results as well as negative results.

$E_{EKG_{Sense}}$ is the energy consumed by an EKG sensing device (MICA2) when continuously reading EKG signals for a 24-hour period.
$E_{EKG_{Tx}}$ is the energy consumed by an EKG sensing device (MICA2) when continuously transmitting sensed EKG information via Bluetooth for a 24 hour period.
$E_{EKG_{Rx}}$ is the energy consumed by a smartphone when continuously reading EKG information via Bluetooth for a 24-hour period.
E_{Rep} is the energy consumed by the phone when continuously transmitting all EKG information via GSM/EDGE during a 24-hour period.

Table 21: Telemetry energy requirements

Today, when prescribed by a physician, telemetry is applied continuously for a few days in the hope of capturing episodes of A-Fib. However, the procedure is burdened by the need to replace drained batteries daily [23]. The telemetry energy model continuously senses EKG signals, transmits EKG data, receives EKG records, and reports.

$$E_{telemetry} = E_{monitor} + E_{transmission}$$

Where:

$$E_{monitor} = E_{EKG_{Sense}} + E_{EKG_{Tx}} + E_{EKG_{Rx}} = 5184 + 8.3 + 8.3 = 5200.6 \text{ Joules}$$

$$E_{transmission} = E_{Rep} = 3318 \text{ Joules}$$

$$E_{telemetry} = 8519 \text{ Joules}$$

The telemetry report includes all positive and negative results, depicted by the rate r_p and rate r_n respectively.

$$\text{Positive rate} = r_p = (TP + FP)/(TP + FP + TN + FN)$$

$$\text{Negative rate} = r_n = (TN + FN)/(TP + FP + TN + FN)$$

$$E_{telemetry} = E_{EKG_{Sense}} + E_{EKG_{Tx}} + E_{EKG_{Rx}} + (r_p + r_n) E_{Rep}$$

This mode of operation causes quick battery drainage and necessitates frequent battery replacement.

The total energy consumed is approximately 8519 Joules, i.e. the sum of the energies that are required for sensing EKG signals, transmitting to the smartphone via Bluetooth, receiving EKG record, and reporting EKG record for a period of 24 hours.

In a 24-hour period, such a telemetry system would use approximately 50% of the capacity of the 3.7-volt Li-Polymer F-S1 battery. Continuous telemetry does not discriminate between positive and negative results, in fact telemetry reports all the results to a remote healthcare center where physicians perform the detection of positive results. If we assume that telemetry EKG interpretations are conducted by a cardiologist or a cardio-physiologist who are trained experts at EKG readings, then all judgments of what constitutes A-Fib is going to be assumed to be as accurate as possible. Unfortunately, not every physician is a cardiologist, so general practitioners are often the first to interpret EKG readings during a general screening evaluation. General practitioners introduce human errors when interpreting EKG readings leading to a false positive rate of 8% and a false negative of 20%.

7.2.2 Energy model of telemetry with user-triggered event

The patient may trigger the detection of the first episode of A-Fib as soon as he or she feels symptoms of A-Fib such as heart palpitations. The telemetry system starts consuming energy as soon the user triggers the event. Similar to the continuous telemetry model, the user-triggered event energy model continually senses EKG signals, transmits EKG data, receives EKG records, and reports all data to a remote healthcare center.

$$\mathrm{E}_{\mathrm{TEtelemetry}} = \mathrm{E}_{\mathrm{monitor}} + \mathrm{E}_{\mathrm{transmission}} = 8519\ \mathrm{Joules}$$

The total energy consumed is approximately 8519 joules, i.e. the sum of the energies that are required for sensing EKG signals, transmitting to the smartphone via Bluetooth, receiving EKG records, and reporting EKG records for a period of 24 hours. Using triggered events to start an A-Fib telemetry-monitoring device saves energy early in

standby mode but runs the risk of missing the first 30 seconds of A-Fib. Moreover, triggering events might not be possible if the user is incapacitated.

In a 24-hour period, the user-triggered event energy model would use approximately 50% of the capacity of the 3.7-volt Li-Polymer F-S1 battery.

CHAPTER 8

8 A-FIB DETECTION ENERGY MODELS

8.1 Detection energy model of A-Fib

Typically, the detection A-Fib model discovers the first episode of A-Fib, by sensing EKG signals using the low-power, wireless two-lead EKG system [69] [87], transmitting EKG data to a smartphone via Bluetooth, receiving EKG records into a smartphone via Bluetooth, detecting A-Fib using the smartphone, and transmitting data via GSM/EDGE to a care center. The device senses, stores and processes the acquired data on the local, on-body network, or on a remote server to provide feedback of a patients' physiological and vital signals. Figure 39 describes schematically, the typical features of a wearable healthcare computing system capable of monitoring, detecting, and transmitting A-Fib EKG data and results.

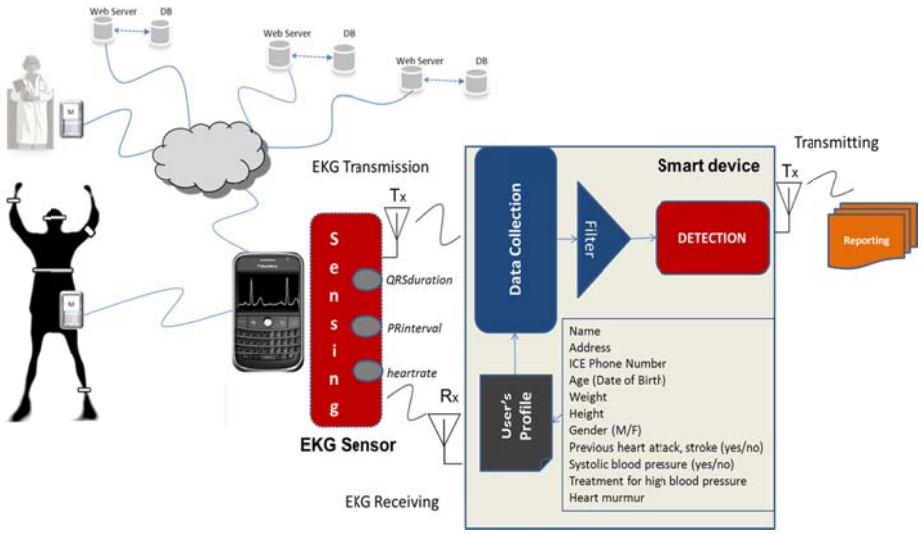

Figure 39: Typical wearable computing diagram

The energy model of a wearable healthcare device is typically comprised of the energy components described in Figure 40 and defined in Table 22.

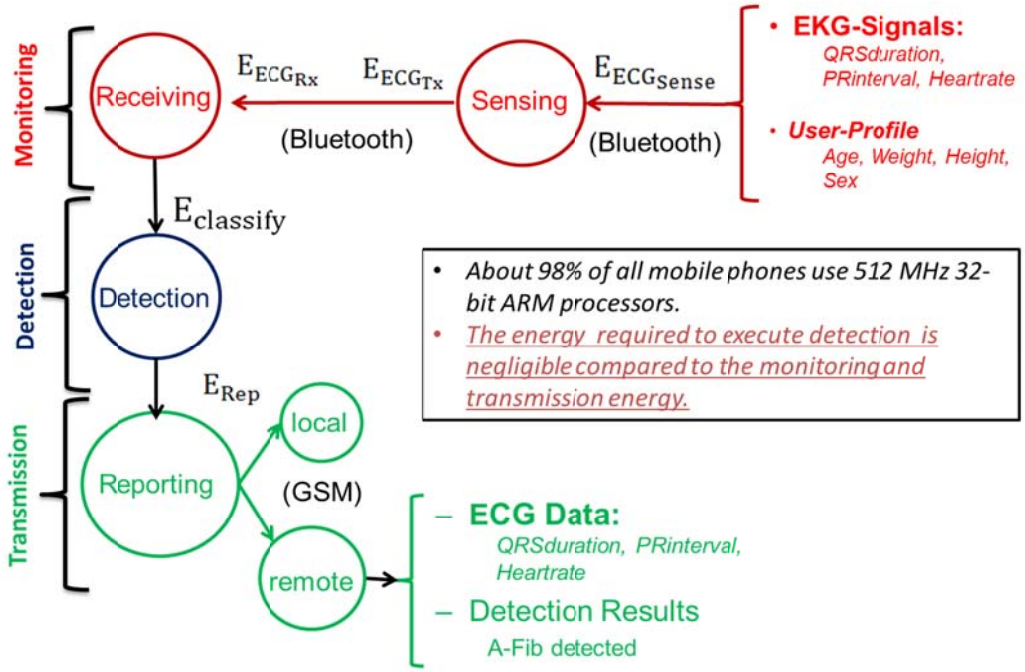

Figure 40: A-Fib monitoring and detection energy distribution

The following calculations are estimates of the energy required in order to continuously transmit EKG records for a 24 hour period	
TP = True Positive	**Sensitivity,** or TP rate (a.k.a. recall rate in data mining) measures the proportion of actual positives (people having arrhythmia) which are correctly identified
FP = False Positive	Type I error, a.k.a. α error or false positive is when a model classifies a patient as having arrhythmia when in fact the patient does not have arrhythmia
TN = True Negative	**Specificity,** or TN rate, measures the proportion of negatives that are correctly identified (i.e. the percentage of arrhythmia free people who are correctly identified as not having arrhythmia)
FN = False Negative	Type II error, a.k.a. β error or false negative, is when a model classifies a patient as not having arrhythmia when the patient has arrhythmia
Positive rate $= r_p = TP + FP$	The proportion of subjects with positive test

	results who are correctly or incorrectly diagnosed
$\text{Negative rate} = r_n = TN + FN$	The proportion of subjects with negative test results who are correctly or incorrectly diagnosed.
$r_p + r_n = 1$	Inclusive of all test results possibilities
Battery capacity = 16,916.4 Joules	3.7-volt Li-Polymer F-S1 battery
E_{active}	Required energy to keep the system in active or working mode
$E_{standby}$ A battery would last approximately 168 hours on standby.	Nominal energy to keep the system in standby or sleep mode, equal 30 micro-watts for MICA2
$E_{telemetry}$	The total energy required by A-Fib telemetry to continuously sense and transmit EKG records for a 24-hour period
$E_{TEtelemetry}$	The total energy required by event-triggered telemetry to continuously sense and transmit EKG records for a 24-hour period
$E_{TotalAFib}$	The total energy required to continuously sense, detect and transmit EKG records for a 24-hour period
MICA2 is a portable, low power, wireless two-lead EKG system integrated with the UC Berkley's MICA2 mote developed by UC Berkley and manufactured by Crossbow Technology, Inc. [69].	The device consumes 60mW of power when monitoring continuously (active mode) and 30 microwatts in standby mode where monitoring is disabled. The EKG information is read at 120Hz sampling rate with four transmissions per second of 30 samples each
$T_{Sense} = 3600 \frac{\text{sec}}{\text{hr}} * 24 \text{ hr} = 86400 \text{ sec}$	The 24 hour period in seconds of sensing EKG signals
$P_{Sense} = 60 * 10^{-3}\ Watts$	The power consumed by a EKG sensing device (MICA2) sensing EKG signals
$E_{EKG_{Sense}} = P_{Sense} T_{Sense} = 60 * 10^{-3} W * 86400 \text{ sec} = 5184 \text{ Joules}$	The energy consumed by a EKG sensing device (MICA2) when continuously reading EKG signals for a 24 hour period
$\text{Sampling rate} = 120 \text{ Hz} = 120 \frac{\text{samples}}{\text{sec}}$	MICA2 EKG Sampling rate where 1 sample = 1 byte = 8 bits

One sample size in bits $= 120\frac{\text{samples}}{\text{sec}} * 8\frac{\text{bits}}{\text{sample}} = 960\frac{\text{bits}}{\text{sec}}$	
$n_{TxSense} = 960\frac{\text{bits}}{\text{sec}} * 3600\frac{\text{sec}}{\text{hr}} * 24\text{ hr} = 82{,}944{,}000$ bits = 10.368 Mbytes	The number of sensed EKG bits transmitted by the MICA2 EKG sensing device to the GSM/EDGE smartphone for a 24-hour period
$w_{Tx} = 10^{-7}\frac{\text{Joules}}{\text{bit}}$	Bluetooth transmits and receives data at rates up to 2Mbps in the 2.45GHz band. Radio communications expend 10^{-7} J/bit for transmission using Bluetooth. [74]
$E_{EKG_{Tx}} = n_{TxSense}w_{Tx} = 82{,}944{,}000\text{ bits} * 10^{-7}\frac{\text{Joules}}{\text{bit}} = 8.3$ Joules	The energy consumed by an EKG sensing device (MICA2) when continuously transmitting sensed EKG information via Bluetooth for a 24-hour period
$n_{RxSense} = n_{TxSense}$	The number of sensed EKG bits received by GSM/EDGE smartphone for a 24-hour period
$w_{Rx} = 10^{-7}\frac{\text{Joules}}{\text{bit}}$	Bluetooth transmits and receives data at rates up to 2Mbps in the 2.45GHz band. Radio communications expend 10^{-7} J/bit for transmission using Bluetooth. [74]
$E_{EKG_{Rx}} = n_{RxSense}w_{Rx} = 82{,}944{,}000\text{ bits} * 10^{-7}\frac{\text{Joules}}{\text{bit}} = 8.3$ Joules	The energy consumed by a smartphone when continuously reading EKG information via Bluetooth for a 24-hour period
$n_{Rep} = n_{RxSense}$ + positive results in bits Slightly above 82,944,000 bits	The number of sensed EKG and positive results in bits transmitted via GSM/EDGE for a 24-hour period
$w_{Rep} = 4 * 10^{-5}$ Joules/bit	GSM (Global System for Mobile) communication expends $4*10^{-5}$ J/bit [74].
$E_{Rep} = n_{Rep}w_{Rep} = 82{,}944{,}000\text{ bits} * 4 * 10^{-5}\frac{\text{Joules}}{\text{bit}} =$ 3318 Joules.	The energy consumed by the phone when continuously transmitting all EKG information (in case of telemetry) plus reporting all positive results (in case of detection model) via GSM/EDGE during a 24-hour period

$E_{EKG_{Sense}}$ is the energy consumed by an EKG sensing device (MICA2) when continuously reading EKG signals for a 24-hour period
$E_{EKG_{Tx}}$ is the energy consumed by an EKG sensing device (MICA2) when continuously transmitting sensed EKG information via Bluetooth for a 24-hour period
$E_{EKG_{Rx}}$ is the energy consumed by a smartphone when continuously reading EKG information via Bluetooth for a 24-hour period
E_{active} is the energy required to keep the system in monitoring, detecting and transmission mode
$E_{standby}$ is the energy required to keep the system in standby or sleep mode., A battery would last approximately 168 hours on standby
$E_{detectingAFib}$ is the energy required by A-Fib detection algorithm to detect A-Fib
$E_{TotalAFib}$ is the total energy required to detect A-Fib during a 24-hour period
E_{Rep} is the energy consumed by the phone when continuously transmitting all EKG information plus reporting all positive results via GSM/EDGE during a 24-hour period
Positive rate $= r_p =$ True Positive + False Positive

Table 22: Energy requirements for a general detection model

An A-Fib detection energy model and an A-Fib telemetry energy model are different models. Both energy models are capable of sensing EKG signals, transmitting EKG data, receiving EKG records, and reporting results; however, an A-Fib detection energy model has the capability of detecting A-Fib locally and transmitting the results when an episode of A-Fib is detected.

The telemetry energy model:

$$E_{telemetry} = E_{monitor} + E_{transmission}$$

$$E_{telemetry} = E_{EKG_{Sense}} + E_{EKG_{Tx}} + E_{EKG_{Rx}} + E_{Rep}$$

For the detection energy model of A-Fib, we propose a basic general energy model, starting with telemetry energy model as reference platform to which we add features such as an A-Fib risk factor, an incidence rate, a prevalent window, and/or a user-triggered event in order to create primary and hybrid energy models.

Figure 41 shows the design progression of our energy models starting with a telemetry model as a reference. We add an A-Fib detection algorithm in order to get a general detection model. We inject an incidence rate to the general detection model to get an incidence based detection energy model. We finally include an A-Fib prevalence window in order to achieve the Adaptive Energy-aware Real-time Detection Models for Cardiac Atrial Fibrillation.

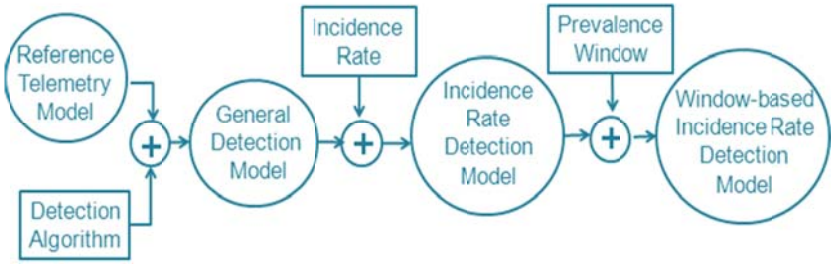

Figure 41: telemetry to detection energy-aware models design progression

The general A-Fib detection energy model:

Case 1: If one assumes there is plenty of energy then one could use a telemetry model with a detection algorithm where monitoring, detection and reporting are on continuously.

$$E_{TotalAFib} = E_{monitor} + E_{detectingAFib} + E_{transmission}$$

$$E_{monitor} = E_{EKG_{Sense}} + E_{EKG_{Tx}} + E_{EKG_{Rx}} = 5184 + 8.3 + 8.3 = 5200.6 \text{ Joules}$$

$$E_{transmission} = E_{Rep} = 3318 \text{ Joules}$$

$$E_{TotalAFib} = 8519 + E_{detectingAFib}$$

Case 2: Today, energy is scarce and needs to be optimized in order to extend battery life in wearable computing healthcare devices. The general detection energy model below will be modified in order to achieve energy consumption optimization. The model would transmit the positive results of the classifier and the corresponding data at the positive rate r_p .

$$E_{TotalAFib} = E_{monitor} + E_{detectingAFib} + r_p E_{transmission}$$

$$E_{TotalAFib} = E_{EKG_{Sense}} + E_{EKG_{Tx}} + E_{EKG_{Rx}} + E_{detectingAFib} + r_p E_{Rep}$$

$$E_{monitor} = E_{EKG_{Sense}} + E_{EKG_{Tx}} + E_{EKG_{Rx}} = 5200.6 \text{ Joules}$$

$$E_{transmission} = E_{Rep} = 3318 \text{ Joules}$$

$$E_{TotalAFib} = 5200.6 + E_{detectingAFib} + r_p\, 3318$$

A-Fib is predicted present, with an accuracy of 98.67%, a false positive of 3.1% and a false negative of 1.3% (see Section 5.2.6), if probability p (A-Fib is Present | Age, Age^2, Gender, BMI, QRSduration, $PR_{interval}$, Heartrate) > 0.5

Otherwise, A-Fib is absent

$$\text{logit}(p) = -41.175 + 0.820\,\text{Age} - 0.006\,\text{Age}^2 + 4.737\,\text{Gender} - 0.047\,\text{BMI} + 0.098\,\text{QRSduration} - 0.178\,\text{PR}_{\text{interval}} + 0.066\,\text{Heartrate}$$

And

$$p = 1 / (1 + e^{-\text{logit}(p)})$$

8.2 Detection energy model based on a risk factor, an incidence rate, a prevalence window, and/or a user-triggered event

Since A-Fib is not a common occurrence [94] and, in order to judiciously optimize energy consumption in wearable healthcare monitoring and detection devices, monitoring should occur during a window in time when A-Fib is more prevalent, or should a patient feel heart palpitations. The implementation of a risk and incidence based A-Fib detection within a prevalence window in such devices helps extends the monitoring device battery life. A-Fib risk factors k may be classified in categories made up of risk ranges such as $k < 0.05$, $0.05 < k < 0.15$, $k > 0.15$. Knowing the A-Fib risk factor of a patient allows one to prescribe an A-Fib monitoring and detection schedule (see Figure 42). A high A-Fib risk factor may suggest more frequent monitoring compared to a low A-Fib risk factor.

In the following sections, we explore the design of an A-Fib detection energy model by adopting an A-Fib risk factor assessment algorithm from [89], an A-Fib incidence rate, an A-Fib detection algorithm, and an A-Fib prevalence window. We consider an incidence rate equal to 0.02 for illustrative purposes.

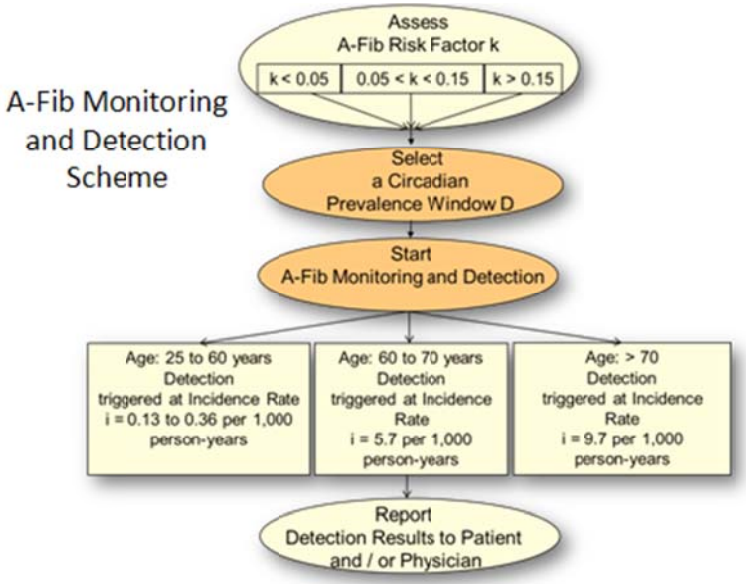

Figure 42: Overview of an efficient wearable computing device

8.2.1 Detection energy model based on a A-Fib group incidence rate i

We design an incidence rate based A-Fib detection energy model by integrating the incidence rate into the general energy model for A-Fib [88]. In this dissertation, we consider an incidence rate i equal to 2% for illustration purposes. If the detection algorithm is as accurate as the cardiologist's interpretation of EKG readings, then having a detection positive rate equal to the clinical incidence rate gives our energy-aware model the best energy performance. Because A-Fib is not a common occurrence [56], energy consumption can be reduced and therefore device battery life extended if A-Fib is reported only when there is an actual occurrence of A-Fib. The incidence rate based A-Fib energy model detects the first episode of A-Fib by continually sensing EKG signals, transmitting EKG data, receiving EKG records, classifying, and reporting when the classifier detects the first 30 seconds of A-Fib. The report includes all positive results, that is all True Positive and False Positive outcomes and the corresponding data.

A-Fib is predicted present, with an accuracy of 98.67%, a false positive of 3.1% and a false negative of 1.3% (see Section 5.2.6), if probability p (A-Fib is Present | Age, Age^2, Gender, BMI, QRSduration, $PR_{interval}$, Heartrate) > 0.5

Otherwise, A-Fib is absent.

The covariates coefficients are extracted from the logistic regression results in Section 5.2.6:

$$\text{logit}(p) = -41.175 + 0.820\ \text{Age} - 0.006\ \text{Age}^2 + 4.737\ \text{Gender} - 0.047\ \text{BMI} + 0.098\ \text{QRSduration} - 0.178\ \text{PR}_{\text{interval}} + 0.066\ \text{Heartrate}$$

$$p = 1 / (1 + e^{-\text{logit}(p)})$$

The A-Fib detection model executes in twenty arithmetic operations (ten multiplication operations and ten additions/subtractions). About 98% of all mobile phones use at least one ARM-designed core on their motherboards [89]. ARM processors account for approximately 90% of all embedded 32-bit RISC processors. Using a 32 bit 512 MHz processor [90], the energy $E_{detectingAFib}$ required when executing 20 arithmetic operations is negligible compared to the energy E_{Rep} expended when transmitting reports.

$$E_{TotalAFib} = E_{monitor} + E_{detectingAFib} + r_p E_{transmission}$$

$$E_{monitor} = E_{EKG_{Sense}} + E_{EKG_{Tx}} + E_{EKG_{Rx}} = 5200.6\, Joules$$

$$E_{transmission} = E_{Rep} = 3318\, Joules$$

$$E_{TotalAFib} = 5200.6 + E_{detectingAFib} + r_p\, 3318$$

The ideal general detection energy model for predicting A-Fib is when $r_p = i = 0.02$

$$E_{TotalAFib} = 5200.6 + E_{detectingAFib} + i\, 3318$$

$E_{TotalAFib} = 5267$ Joules if $r_p = i = 0.02$ and $E_{detectingAFib}$ is negligible

Figure 43 illustrates the energy consumption as the positive detection rate varies with respect to the clinical incidence rate.

r_p	Energy Consumed
0.02	5267
0.1	5532
0.2	5864
0.3	6196
0.4	6528
0.5	6860
0.6	7191
0.7	7523
0.8	7855
0.9	8187
1	8519

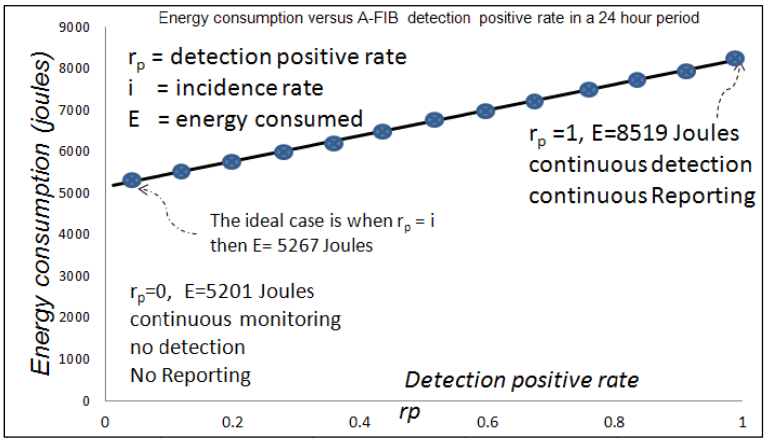

Figure 43: Energy required depends on A-Fib positive rate

Figure 44 suggests that the ideal detection case is when the logistic regression positive rate r_p is equal to cardiologist referenced A-Fib incidence rate i. The worst case is when the positive rate equals 1, that is, the telemetry energy model.

rp	(i-rp)/i	Corresponding EdetectingA-Fib	Percent Energy Change
0.02	0	5267	0.0%
0.1	400	5532.4	5.0%
0.2	900	5864.2	11.3%
0.3	1400	6196	17.6%
0.4	1900	6527.8	23.9%
0.5	2400	6859.6	30.2%
0.6	2900	7191.4	36.5%
0.7	3400	7523.2	42.8%
0.8	3900	7855	49.1%
0.9	4400	8186.8	55.4%
1	4900	8518.6	61.7%

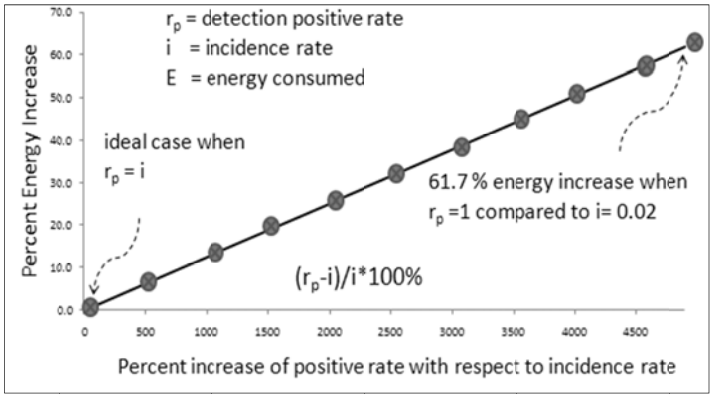

Figure 44: Energy required as positive rate varies with respect to incidence rate

Ideally, when there are no A-Fib episodes (r_p is equal to 0), the model spends its time in a monitoring state. On the other hand, when the model continuously monitors, and continuously transmits, r_p is equal 1. False positive outcomes result in wasted energy that is needlessly spent transmitting inaccurate information. The total energy consumed is approximately 5267 Joules, i.e. when $r_p = i = 0.02$ and $E_{detectingAFib}$ is negligible, the

sum of the energies that are required for sensing EKG signals, transmitting to the smartphone via Bluetooth, receiving EKG records, detecting and reporting EKG records and positive results during a 24-hour period. In a 24-hour period, such a detection system would necessitate 31% of the capacity of the 3.7-volt Li-Polymer F-S1 battery.

8.2.2 Detection energy model based on prevalence window D

We design a prevalence window-based A-Fib detection energy model by incorporating the prevalence window into the general energy model for A-Fib [91] [92]. Prevalence window D is defined as the fraction of the period the device is in one of two states. A state could be defined as ON (monitoring) and OFF (not monitoring or sleeping). We apply the model for a short time during the morning and evening and turn it off the rest of the day because when A-Fib exists it is prominent in the morning between 8 AM and 10 AM and also around 10 PM and 12 AM [85][86] (see Figure 45). The energy model in this case runs continuously two hours in the morning and two hours in the evening with the anticipation that A-Fib occurs predominantly during these prescribed windows of time. In a 24-hour period, the energy model is on during the two 2-hour windows and off during twenty hours.

Essentially this scheme senses EKG signals, transmits EKG data, receives EKG records, classifies and reports positive results depicted by the rate r_p and the corresponding data during a prevalence window $D = \frac{T_{on}}{24} = \frac{4}{24} = 1/6 = 16.67\%$ of the 24-hour period. The prevalence windows widths, when A-Fib monitoring occurs, are described by $t1_{on}$ and $t2_{on}$.

$$\text{Prevalence window} = D = \frac{t1_{on} + t2_{on}}{24} = \frac{T_{on}}{24}$$

$$E_{TotalAFib} = E_{active}D + E_{standby}(1 - D)$$

Where:

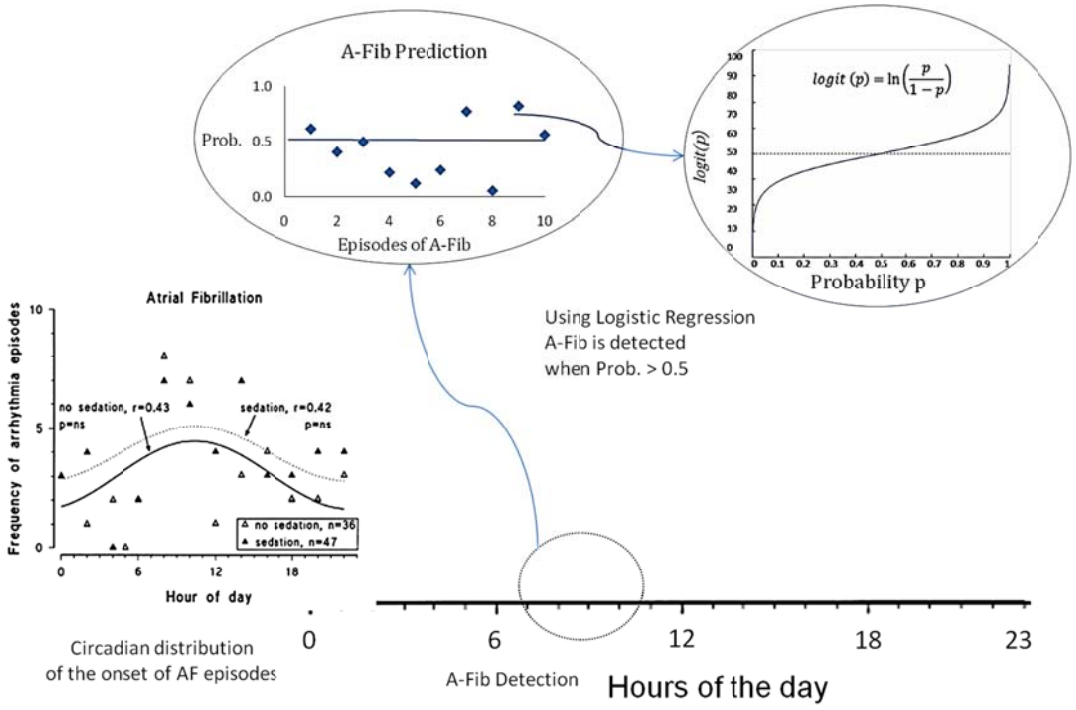

Figure 45: First diagnosed episode of A-Fib using prevalence window

$$E_{active} = \left(E_{monitor} + E_{detectingAFib} + r_p \; E_{transmission} \right)$$

$$E_{standby} = \text{energy to keep the system in standby or sleep mode}$$

$E_{detectingAFib}$ is assumed to be negligible compared to the other energies.

$E_{TotalAFib} =$

$$\left(E_{monitor} + E_{detectingAFib} + r_p \; E_{transmission}\right)D + E_{standby}(1 - D)$$

Special case 1: The energy model monitoring and transmitting continuously inside a prevalence window D = 4 hours

We run the proposed prevalence window-based energy model during window $D = \frac{4}{24} =$

$1/6 = 16.67\%$ of the 24-hour period. This scheme senses EKG signals, transmits EKG

data, receives EKG records, detects A-Fib locally and reports all data to a remote care center, a remote server, or cardiologist.

$$E_{TotalAFib} = \left(E_{monitor} + E_{detectingAFib} + r_p E_{transmission}\right)\left(\frac{1}{6}\right) + E_{standby}\left(\frac{5}{6}\right)$$

For $r_p = 1$

$$= 8518 * \frac{1}{6} + 16919 * \frac{24}{168} * \frac{5}{6} = 3334 \text{ Joules}$$

The prevalence window-based A-Fib detection energy model uses 3334 Joules or 19.7% of the battery capacity as compared to the full time telemetry; it represents 39.1% of the energy consumed by telemetry.

Special case 2: The energy model monitoring continuously inside a prevalence window D = 4 hours but transmits with incidence rate = 0.02

This model runs continuously two hours in the morning and two hours in the evening with the anticipation that A-Fib occurs predominantly during these prescribed windows of time at the incidence rate r_p. This scheme is overridden by a user-triggered event as soon as the patient feels heart palpitations. In this case, the model senses EKG signals, transmits EKG data, receives EKG records, classifies A-Fib locally and reports detection positive results to a care center or cardiologist at the incidence rate $r_p = 0.02$ during prevalence window $D = 4$ hours or $1/6$ of the 24-hour period.

$$E_{TotalAFib} = \left(E_{monitor} + E_{detectingAFib} + r_p E_{transmission}\right)\left(\frac{1}{6}\right) + E_{standby}\left(\frac{5}{6}\right)$$

For incidence rate = 0.02

$$E_{TotalAFib} = \left(E_{monitor} + E_{detectingAFib} + 0.02\, E_{transmission}\right)\left(\frac{1}{6}\right) + E_{standby}\left(\frac{5}{6}\right)$$

$$= (5200.6 + 0.02 * 3318) * \frac{1}{6} + 16919 * \frac{24}{168} * \frac{5}{6} = 2892 \text{ Joules}$$

The prevalence window-based A-Fib detection energy model uses 2892 Joules or 17 % of the battery capacity; it represents 33.9 % of the energy consumed by telemetry.

8.2.3 A user-triggered event energy model of A-Fib detection

The patient may trigger the detection of the first episode of A-Fib as soon as he or she feels symptoms of A-Fib, such as heart palpitations. The energy model then continually senses EKG signals, transmits EKG data, receives EKG records, classifies, and reports all the EKG data and detection results. The report includes all results, i.e., positive and negative results.

$$E_{TotalAFib} = E_{monitor} + E_{detectingAFib} + r_p E_{transmission}$$

For incidence rate = 1, the model approaches a telemetry model

$$E_{TotalAFib} = 8518.6 \text{ Joules}$$

For incidence rate = 0.02,

$$E_{TotalAFib} = 5267 \text{ Joules}$$

The total energy consumed is approximately 5267 Joules, i.e. once the device is activated, the sum of the energies that are required for sensing EKG signals, transmitting to the smartphone via Bluetooth, receiving EKG records, classifying and reporting EKG records for a period of 24 hours.

In a 24-hour period, such a detection system would use approximately 31% of the capacity of the 3.7-volt Li-Polymer F-S1 battery or 61.8 % as compared to telemetry.

A user-triggered monitoring device saves energy because the device is in standby mode, but runs the risk of missing the first 30 seconds of A-Fib especially if the user is incapacitated.

8.3 Summary of A-Fib energy models

Figures 46 and 47 show the design progression using energy equations for a telemetry energy model, a general detection energy model, an incidence based energy model, and a prevalence-window energy model.

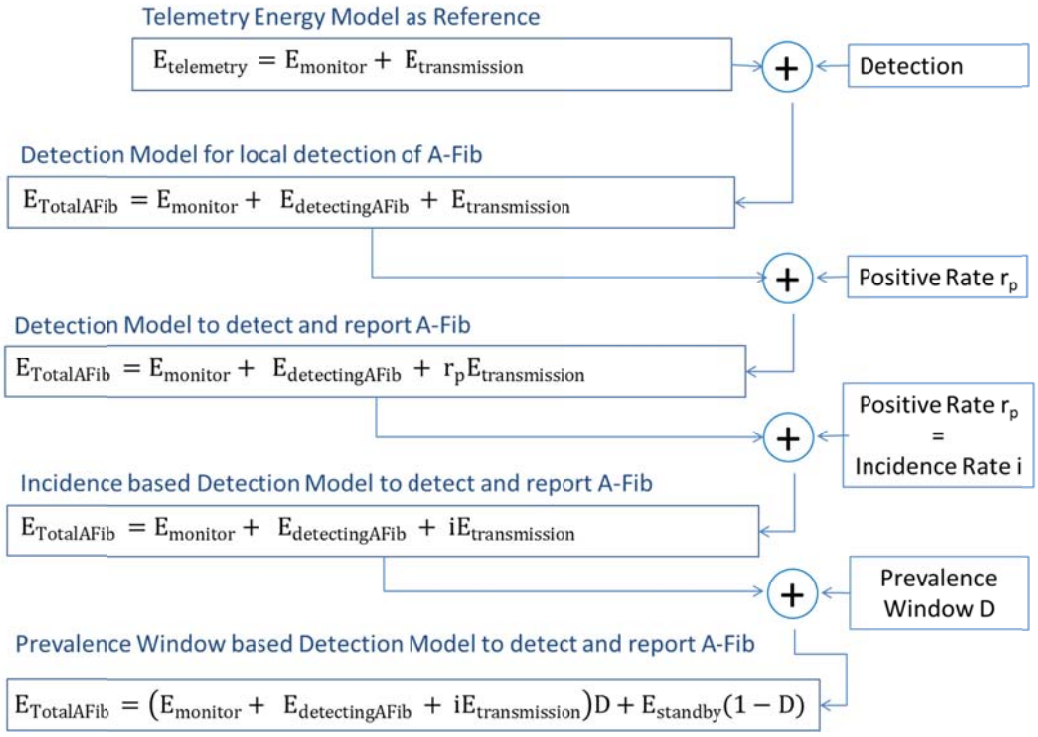

Figure 46: General description of A-Fib energy models

8.4 Comparing A-Fib detection and telemetry energy models

Telemetry is widely accepted in healthcare for remotely collecting and sending vital data to a monitoring station for analysis and interpretation. However telemetry drains the battery quickly which forces the patient to replace the battery as often as every day. Wearable computing in healthcare offers the benefits of telemetry when needed, provides detection results when available, and saves energy when compared to telemetry. Table 23 and Figure 48 summarize the energy consumption from the various models.

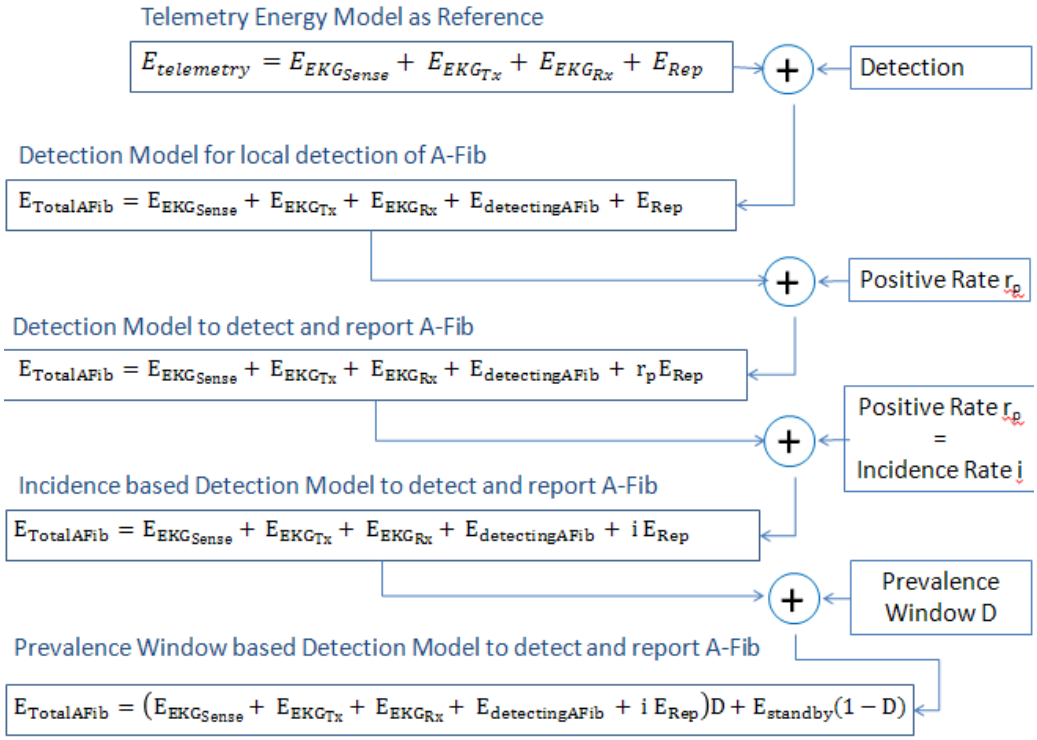

Figure 47: A-Fib energy-aware models

	Percentage	Joules
Battery : 3.7-volt Li-Polymer F-S1	100%	16,916
Energy consumption during a 24-hour period		
Telemetry Device:		
• **Telemetry (continuous monitoring and transmission)**	50.4%	8,519
Wearable Computing Device:		
• **Incidence rate = 1, prevalence window = 4 hours**		
o **Detection + incidence rate**	50.4%	8,519
o **Detection + incidence rate + prevalence window**	19.7%	3,334
• **incidence rate = 0.02, prevalence window = 4 hours**		
o **Detection + incidence rate**	31.1%	5,267
o **Detection + incidence rate + prevalence window**	17.0%	2,892

Table 23: Energy consumption of energy models in a 24-hour period

The largest energy consumed during a 24-hour period is by continuous telemetry; (about 50.4% of battery capacity), compared to the energy consumed by the detection energy model using an incidence rate of 0.02 and a 4-hour circadian prevalence window (17% of battery capacity).

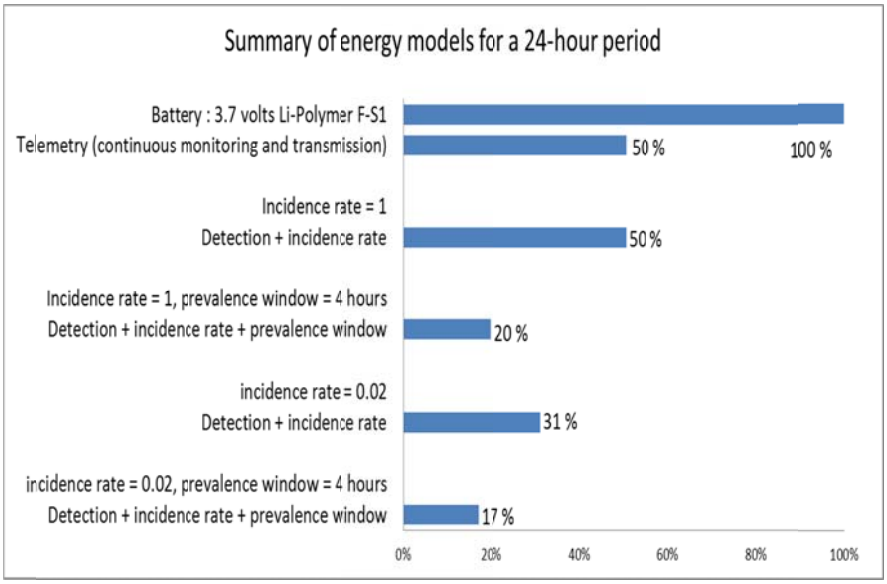

Figure 48: Ranking of 24-hour energy consumption percentage by model type

Adapting any one of the detection energy schemes above is an improvement over telemetry. The 24-hour general detection energy model for the detection of A-Fib includes an incidence rate i or positive rate r_p and operating windows with a period D such as the AM/PM windows. It expends less energy than telemetry but unfortunately introduces Type I, False Positive and Type II, False Negative errors.

Type I and Type II errors of detection may be costly and dangerous; one may want to transmit all the EKG raw data just as telemetry would, plus the results to a remote care center where cardiologists can expertly determine the presence or absence of A-Fib. This approach would favor the hybrid energy model that combines an incidence rate, a prevalence window-based energy model, and user-triggered event model.

$$E_{TotalAFib} =$$

$$(E_{monitor} + E_{detectingAFib} + iE_{transmission})D + E_{standby}(1 - D)$$

$$E_{TotalAFib} = (E_{monitor} + E_{detectingAFib} + iE_{transmission})\left(\frac{1}{6}\right) + E_{standby}\left(\frac{5}{6}\right)$$

This decision also offers the benefit of having all the telemetry data remotely available and the ability to retrain and update the A-Fib detection algorithm in order to achieve better detection accuracy and confidence. Table 24 and Figure 49 compare the energy models to the telemetry model.

	Percentage	Joules
Energy consumption during a 24 hour period		
Telemetry Device:		
• **Telemetry (continuous monitoring and transmission)**	100%	8,519
Wearable Computing Device:		
• **Incidence rate = 1**		
o **General Detection + incidence rate**	100%	8,519
• **Incidence rate = 1, prevalence window = 4 hours**		
o **Detection + incidence rate + prevalence window**	39.1%	3,334
• **Incidence rate = 0.02, prevalence window = 4 hours**		
o **General Detection + incidence rate**	61.8%	5,267
• **Incidence rate = 0.02, prevalence window = 4 hours**		
o **Detection + incidence rate + prevalence window**	33.9%	2,892

Table 24: Energy models compared to telemetry

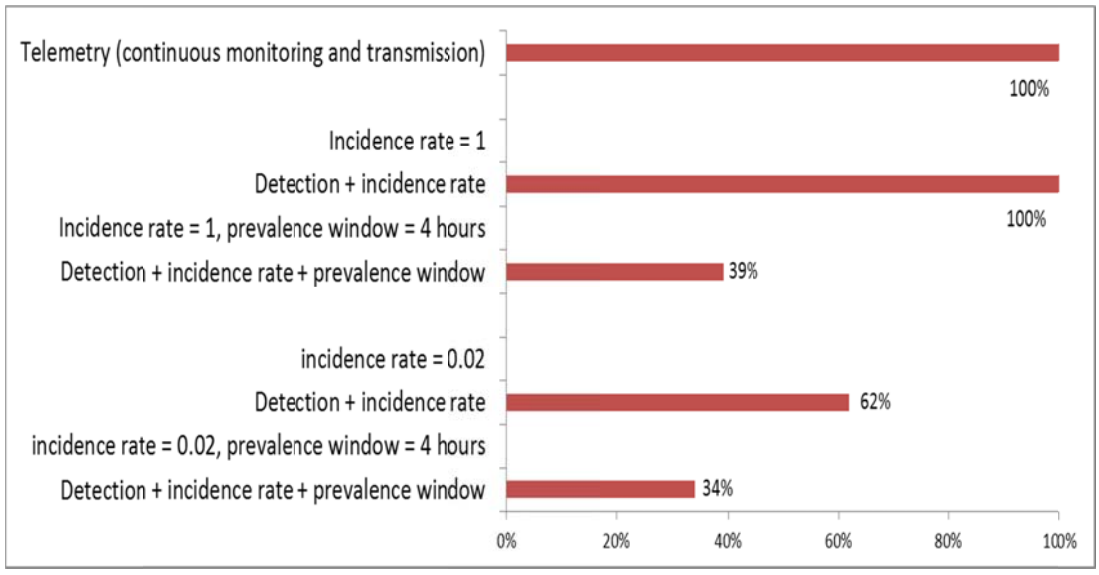

Figure 49: Comparing the proposed energy models to telemetry energy model

8.4.1 Special cases of A-Fib detection energy model

In the following section, we determine the amount of energy that would be saved when replacing the telemetry with a detection model under different special cases of incidence rate and prevalence window.

Telemetry energy equation:

$$E_{telemetry} = E_{EKG_{Sense}} + E_{EKG_{Tx}} + E_{EKG_{Rx}} + E_{Rep}$$

The general detection energy equation:

$$E_{TotalAFib} = \left(E_{EKG_{Sense}} + E_{EKG_{Tx}} + E_{EKG_{Rx}} + E_{detectingAFib} + r_p E_{Rep}\right)D + E_{standby}(1 - D)$$

$$E_{telemetry} - E_{TotalAFib} = E_{EKG_{Sense}} + E_{EKG_{Tx}} + E_{EKG_{Rx}} + E_{Rep} - \left(E_{EKG_{Sense}} + E_{EKG_{Tx}} + E_{EKG_{Rx}} + E_{detectingAFib} + r_p E_{Rep}\right)D - E_{standby}(1 - D)$$

Where: $0 \leq D \leq 1\,, \quad 0 \leq r_p \leq 1$

The difference in energy is dependent on the positive rate r_p and the prevalence window D.

If $E_{telemetry} - E_{TotalAFib} = 0$ implies that there is no energy consumption difference between telemetry and a detection model.

If $E_{telemetry} - E_{TotalAFib} < 0$ implies that the energy consumption caused by detection exceeds the one caused by telemetry.

If $E_{telemetry} - E_{TotalAFib} > 0$ implies that there is a gain in switching monitoring from a telemetry model to a detection model.

Assuming $(E_{detectingAFib})D$ to be negligible compared to E_{active}, we explore some special cases.

Case 1: $D = 0$, $r_p = 0$ or $i = 1$

The detection model never runs because the prevalence window is 0. The difference is all telemetry assuming $E_{standby}$ is negligible.

$$E_{telemetry} - E_{TotalAFib} = E_{EKG_{Sense}} + E_{EKG_{Tx}} + E_{EKG_{Rx}} + E_{Rep}$$

Case 2: $D = 1$, $r_p = 0$

The detection model never runs because the incidence rate is set to 0.

$$E_{telemetry} - E_{TotalAFib} = 0$$

Case 3: $D = 1$, $r_p = 1$

The detection model runs continuously during the 24-hour period because the incidence rate i is set to 1 and the prevalence window is 100%, and continuously reports. The difference is $\mathbf{E_{Rep}}$ assuming $E_{detectingAFib}$ is negligible when comparing it to $\mathbf{E_{Rep}}$

$$E_{telemetry} - E_{TotalAFib} = E_{Rep}$$

Experimental cases:

$$E_{telemetry} - E_{TotalAFib}$$
$$= E_{EKG_{Sense}} + E_{EKG_{Tx}} + E_{EKG_{Rx}} + E_{Rep}$$
$$- (E_{EKG_{Sense}} + E_{EKG_{Tx}} + E_{EKG_{Rx}} + E_{detectingAFib} + r_p E_{Rep})D$$
$$- E_{standby}(1 - D)$$

$E_{telemetry} = 8519$ Joules

$$\mathrm{E_{telemetry}} - \mathrm{E_{TotalAFib}}$$

$$= 8519 - \left(5184 + 8.3 + 8.3 + \mathrm{E_{detectingAFib}} + 3{,}318\,\mathrm{r_p}\right)\mathrm{D}$$

$$- \mathrm{E_{standby}}(1 - \mathrm{D})$$

Using a 32-bit 512 MHz processor [90], the energy $\mathrm{E_{classify}}$ required when executing 20 arithmetic operations is negligible compared to the energy $\mathrm{E_{Rep}}$ expended when transmitting reports.

$$\mathrm{E_{standby}} = 16919 * \frac{24}{168} * (1 - \mathrm{D}) = 2417 * (1 - D)$$

$$\mathrm{E_{telemetry}} - \mathrm{E_{TotalAFib}} = 8519 - \left(5200.6 + 3{,}318\ \mathrm{r_p}\right)\mathrm{D} - 2417 * (1 - D)$$

$$\text{Energy Reduction} = \mathrm{R} = \frac{\mathrm{E_{telemetry}} - \mathrm{E_{TotalAFib}}}{\mathrm{E_{telemetry}}} * 100\%$$

$$\mathrm{R} = \frac{8519 - (5200.6 + 3{,}318 * \mathrm{r_p})\mathrm{D} - 2417 * (1 - \mathrm{D})}{8519}\,100\%$$

Where: $0 \le \mathrm{D} \le 1\,, \quad 0 \le \mathrm{r_p} \le 1$

In the following section, we examine the range of values of different D and $\mathrm{r_p}$ for which the energy reduction between telemetry and detection scheme is significant.

What would be the energy reduction when switching from telemetry to detection scheme?

Fixing $\mathrm{D} = 1\,, \ \mathrm{r_p} = 1 \qquad R = 0\%$

Fixing $\mathrm{D} = 1\,, \quad \mathrm{r_p} = .02$

$$R = \frac{8519 - (5200.6 + 3{,}318 * 0.02) - 2417 * (1 - D)}{8519}\ 100\% = 14.5\%$$

Fixing $\mathrm{D} = 1\,, \quad \mathrm{r_p} = 0$

$$R = \frac{8519 - (5200.6) - 2417 * (1 - D)}{8519}\ 100\% = 15.3\%$$

Fixing $D = .167$, $r_p = 1$,

$$R = \frac{8519 - (5200.6 + 3{,}318)0.167 - 2417 * (1 - D)}{8519} \ 100\% = 59.7\%$$

Fixing $D = .167$, $r_p = .02$,

$$R = \frac{8519 - (5200.6 + 3{,}318 * 0.02)0.167 - 2014}{8519} \ 100\% = 66.0\%$$

Fixing $D = .167$, $r_p = 0$,

$$R = \frac{8519 - (5200.6)0.167 - 2014}{8519} \ 100\% = 66.2\%$$

Table 25 and Figure 50 summarize the energy reduction when switching from telemetry to a detection model while applying a different prevalence window and positive rate:

D	$\mathbf{r_p}$	Energy Reduction	$\boldsymbol{R = \frac{8519 - (5200.6 + 3{,}318 * r_p)D - 2417(1 - D)}{8519} 100\%}$
1	**1**	**0%**	Running and reporting continuously for the 24-hour period.
1	**.02**	**38.2%**	Running continuously for the 24-hour period and reporting 2% of the time. Incidence rate is enabled.
1	**0**	**39 %**	Only local storage is allowed. Running continuously for the 24-hour period, but no reporting.
.167	**1**	**59.7%**	Running and reporting continuously for 16.7% of the 24-hour period.
.167	**.02**	**66%**	Running continuously for 16.7% of the 24-hour period and reporting 2% of the time.
.167	**0**	**66.2%**	Only local storage is allowed. Running and reporting continuously for 16.7% of the 24-hour period but no reporting.

Table 25: Varying positive rate r_p, and prevalence window D affects energy reduction

Figure 50 shows the energy consumption with respect to prevalence window D given an A-Fib incidence rate of 0.02.

$$E_{TotalAFib} =$$

$$(E_{EKG_{Sense}} + E_{EKG_{Tx}} + E_{EKG_{Rx}} + E_{detectingAFib} + r_p E_{Rep})D + E_{standby}(1 - D)$$

$$= \left(5200.6 + 3{,}318\ \mathrm{r_p}\right)\mathrm{D} + 2417 * (1 - D)$$

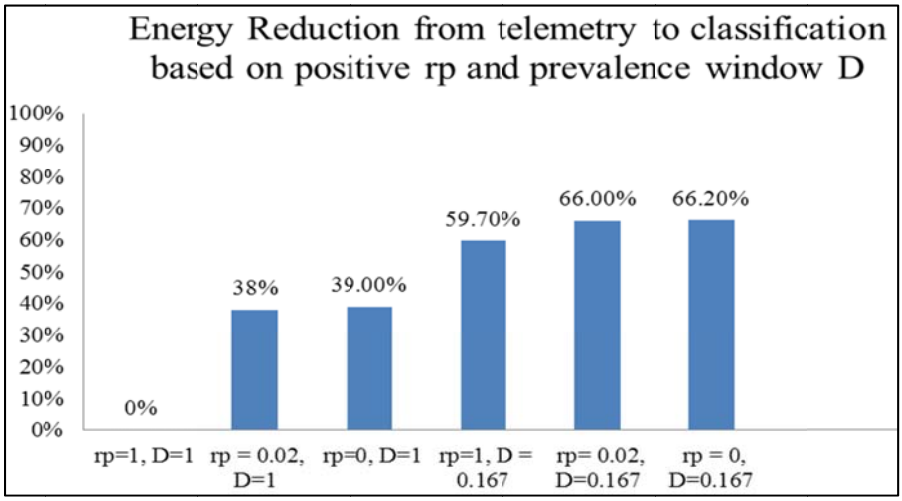

Figure 50: Energy reduction when varying incidence rate r_p and prevalence window D

Prevalence	r_p = 0.02
Window D	$E_{TotalAFib}$
0.167	2892
0.200	2987
0.250	3129
0.300	3272
0.400	3557
0.500	3842
0.600	4127
0.700	4412
0.800	4697
0.900	4982
1.000	5267

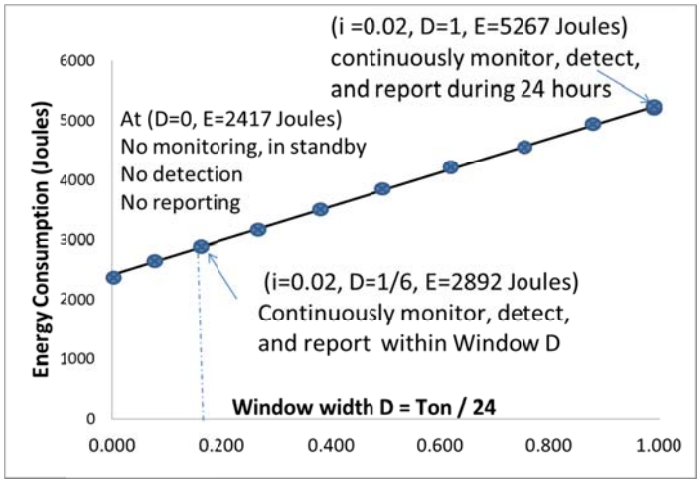

Figure 51: Energy consumption versus prevalence window D

8.5 Scalability of the energy models based on risk factors

The various combinations of the proposed energy models save more energy than telemetry models in practically every case. A recommendation would be to use the proposed models based on a scalability risk factor. The implementation helps extend the

battery life of a monitoring device. For instance, A-Fib risk factors may be classified in three categories made up of risk ranges such as $k < 0.05$, $0.05 < k < 0.15$, $k > 0.15$. Knowing the A-Fib risk factor of a patient allows one to prescribe an A-Fib monitoring and detection scheme (see Figures 52 and 53) and schedule (see Table 26). A high A-Fib risk factor may suggest more frequent monitoring compared to a low A-Fib risk factor.

Select Energy Model based on Risk Factor	**Risk Factor**	**Use Energy Model**	**Compared to Telemetry Energy**
Risk factor category 1 would be for a user who is healthy, athletic; this is similar to wearing a sports watch.	$k < 0.05$	Incidence and prevalence window	33.9%
Risk factor category 2 would be for a user who wants to monitor A-Fib daily during an AM/PM windows.	$0.05 \leq k < 0.15$	Incidence	39.1%
Risk factor category 3 is for the chronic case where a user monitors continuously with the data and detection results transmitted to a care center.	$k \geq 0.15$	Telemetry	100.0%

Table 26: Risk factors and energy models

For example, a user who is healthy, and athletic, having an A-Fib risk factor category 1, $k < 0.05$, would require occasional A-Fib monitoring as depicted by Figure 52. The proposed scheme would select a schedule requiring an assessed A-Fib risk factors k, a circadian prevalence window D, and an age dependent incidence rate. However, a user with a risk factor category 2, $0.05 \leq k < 0.15$, or category 3, $k \geq 0.15$ would be interested in monitoring A-Fib daily as depicted by Figure 53. In this case, the proposed scheme would select a schedule requiring an assessed A-Fib risk factors k, and an age dependent incidence rate, requiring continuous monitoring and detection.

Figure 52 proposes a schedule for an A-Fib risk with $K < 0.05$ that would casually monitor A-Fib episodes. This is the case for a rare A-Fib condition requiring less frequent

monitoring. The schedule depends on an assessed A-Fib risk factor, a prevalence window and an age dependent incidence rate.

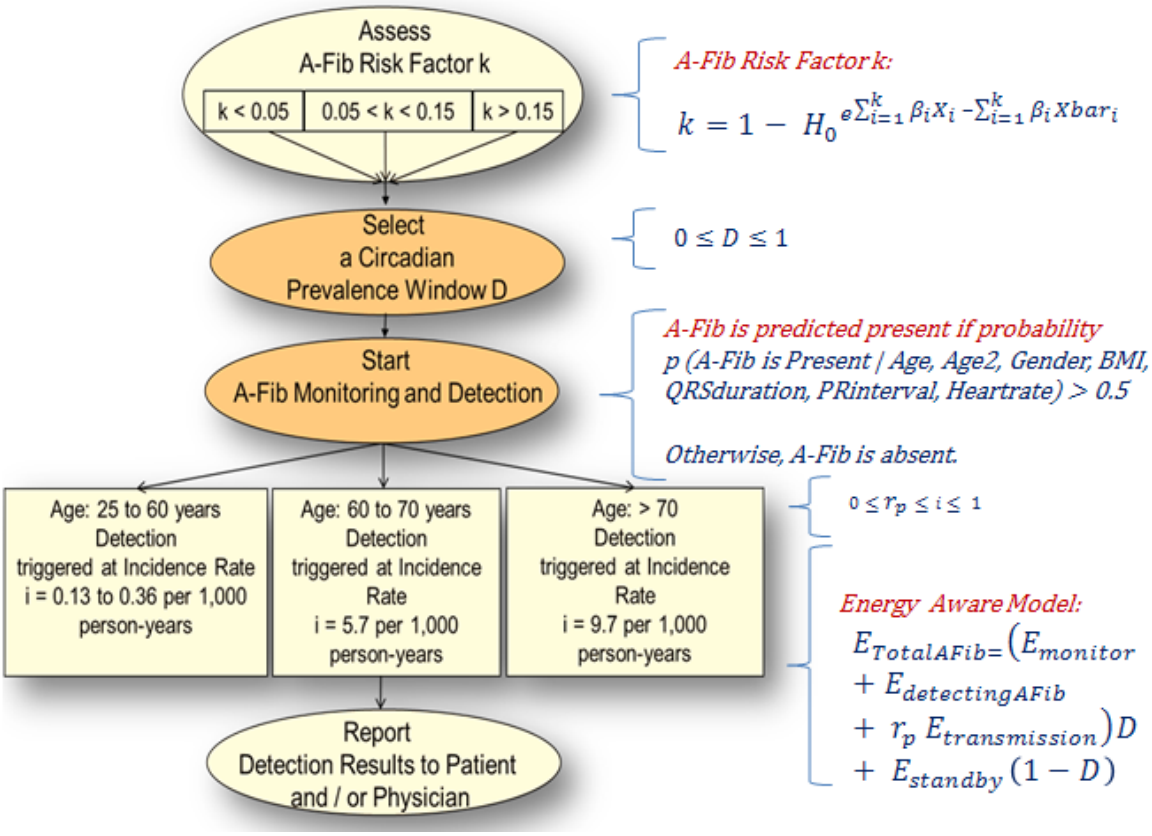

Figure 52: Efficient wearable monitoring and detection scheme based on A-Fib Risk Factor k, Incidence Rate r_p and Circadian Prevalence Window D

Figure 53 proposes a schedule for a high A-Fib risk factor with K ≥ 0.15 that would continuously monitor A-Fib episodes and transmit detection results to a care center. This is the case for a chronic A-Fib condition requiring frequent monitoring. The aggressive schedule does not depend on the prevalence window and only requires an assessed A-Fib risk factor K, and an age dependent incidence rate.

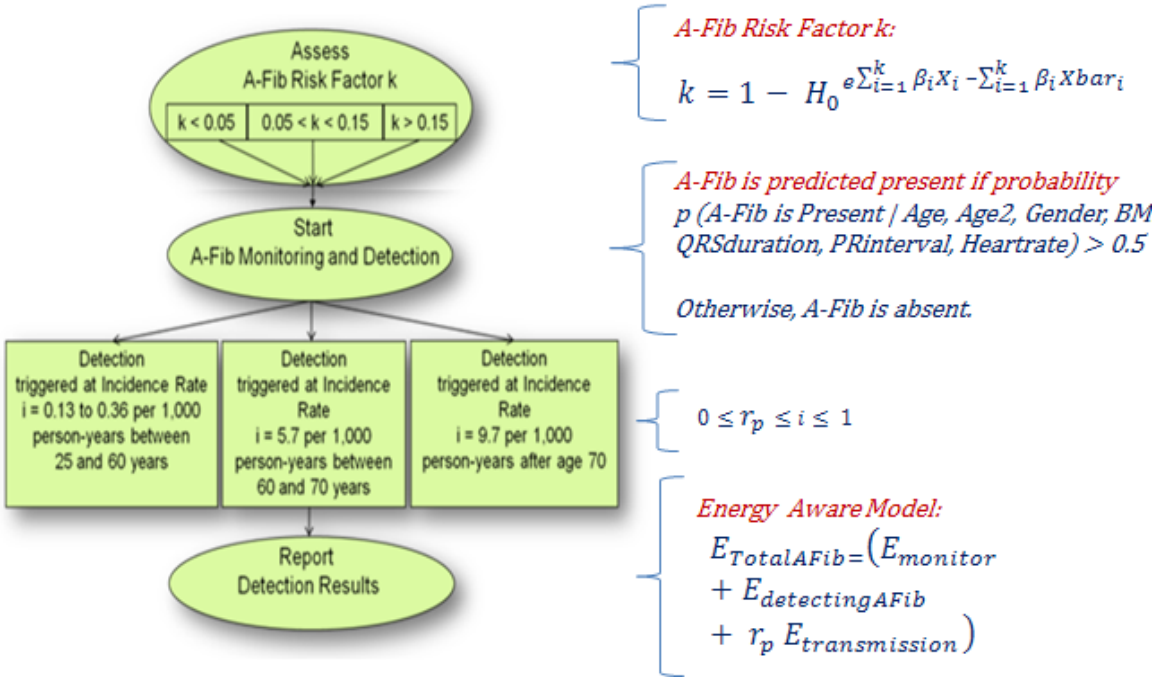

Figure 53: Efficient wearable monitoring and detection scheme based on A-Fib Risk Factor k and A-Fib Incidence Rate r_p

CHAPTER 9

9 ADAPTING THE ENERGY-AWARE MODELS TO THE PAROXYSMAL A-FIB PHASE

In order to optimize the execution of an energy-constrained healthcare application such as A-Fib, one must make sensible use of the energy that is available. One must make judicious decision as to when to run different components and dynamically switch on and off monitoring and detection. Three parameters identified as incidence rate, prevalence window, and positive rate, have a decisive impact on energy consumption. They must be sensibly selected to reduce energy consumption, extend battery life and ultimately expand A-Fib monitoring and detection. We design a hierarchical scheme to detect A-Fib from its onset to its final stage. The total energy model would be a combination of a first episode of A-Fib energy model, a paroxysmal energy model, and if necessary a persistent/permanent energy model (see Figure 54). First, we diagnose the first episode of A-Fib by applying a classifier that would detect heart palpitations that last longer than 30 seconds in the received data packet. If the result is positive, we check for the next stage of A-Fib known as paroxysmal A-Fib. A strong indicator of A-Fib presence is the absence of P waves on the EKG plot and an erratic noise-like activity in their place, combined with irregular R-R intervals [20]. Sometimes when the heart rate is too fast, irregular R-R intervals may be difficult to determine [93]. In addition, wide QRS complexes may be present with rapid ventricular response.

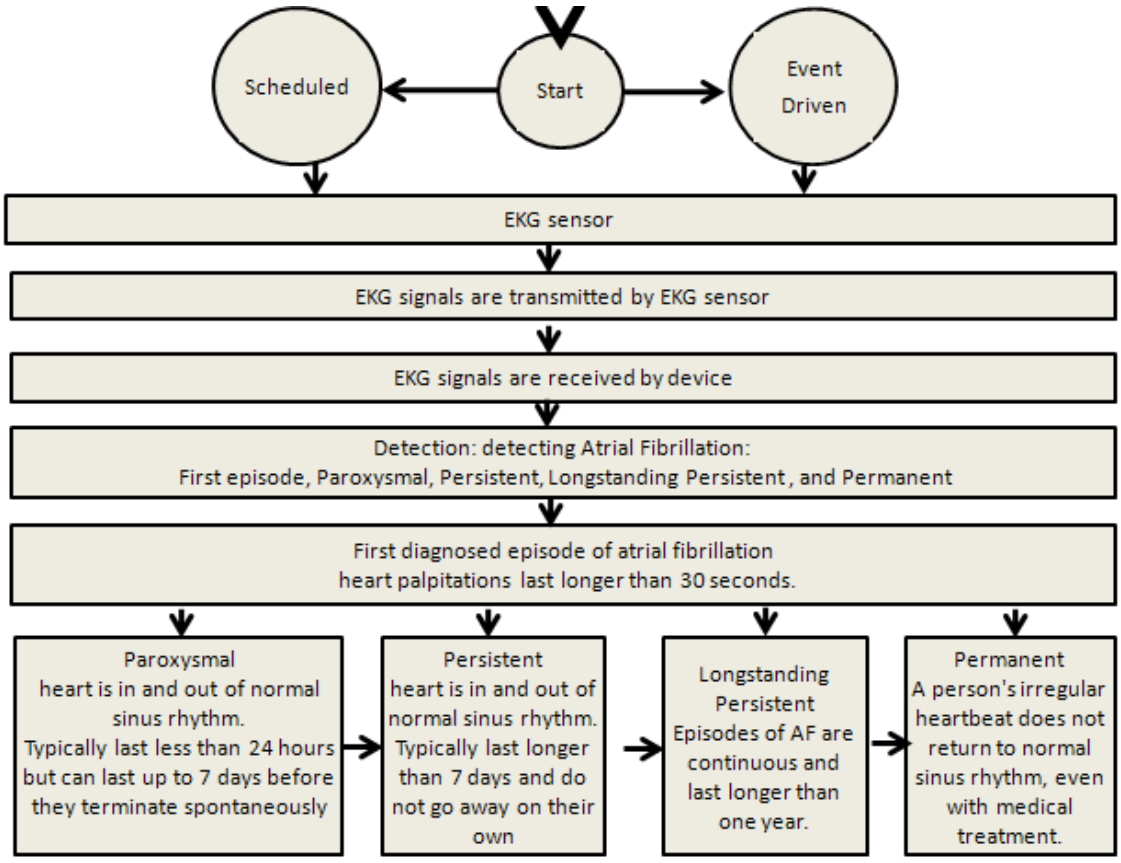

Figure 54: Flow diagram of A-Fib

9.1 Detecting paroxysmal A-Fib

After the first episode of A-Fib has been detected, it becomes critically important to diagnose the next level of A-Fib, paroxysmal A-Fib. In paroxysmal A-Fib, the heart is in and out of normal sinus rhythm. Episodes of A-Fib come and go on their own. They typically last less than 24 hours but can last up to seven days before they terminate spontaneously [94] [95]. Figure 55 reveals how prevalent paroxysmal A-Fib is during a 24-hour period while examining 100 patients [96].

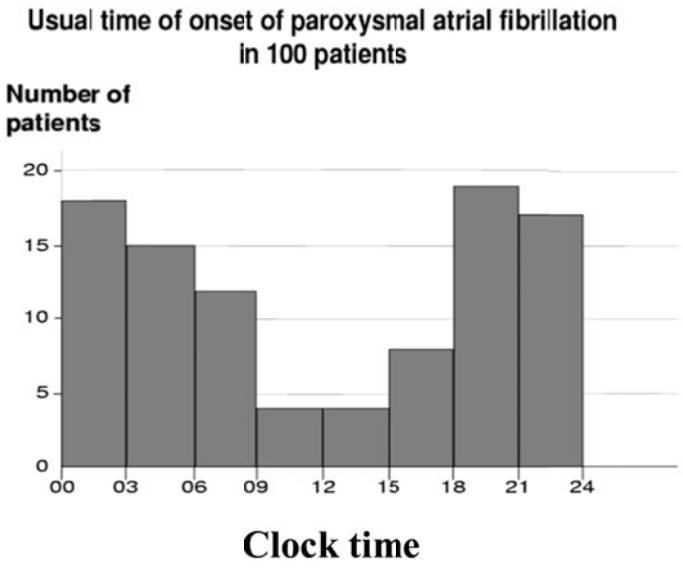

Figure 55: Most palpitations typically start in the morning or at night

The corresponding energy model in Figure 56 would run continuously until it detects the suggestive paroxysmal A-Fib within each 24-hour period for seven days straight. That would require a minimum sustainable energy lasting seven days. Considering a 2% incidence rate and a four hour circadian prevalence window, the energy model for detecting paroxysmal A-Fib is

$$E_{\text{detectingAFib}} =$$

$$\left(E_{EKG_{Sense}} + E_{EKG_{Tx}} + E_{EKG_{Rx}} + E_{\text{detectingAFib}} + i\,E_{Rep}\right)D + E_{\text{standby}}(1 - D)$$

$$E_{\text{TotalAFib}} =$$

$$\left(E_{EKG_{Sense}} + E_{EKG_{Tx}} + E_{EKG_{Rx}} + E_{\text{detectingAFib}} + .02\,E_{Rep}\right)\left(\frac{1}{6}\right) + E_{\text{standby}}\left(\frac{5}{6}\right)$$

The smallest energy consumption (2892 Joules, 17% of battery capacity) occurs when A-Fib is detected as early as possible, that is at the 30-second marker. Next in the progression of A-Fib development is the paroxysmal, which typically lasts less than 24 hours but can last up to seven days before palpitations terminate spontaneously. The

corresponding energy that would be spent in seven days is approximately 7 days * 2892 Joules / day = 20244 Joules or about 120% battery capacity (compared to telemetry where the progression from the first episode of A-Fib to paroxysmal phase would require 8519 Joules / day * 7 days = 59633 Joules representing 353% battery capacity, see Figure 57). Once we confirm the presence of paroxysmal A-Fib, we start checking for persistent A-Fib in the next stage.

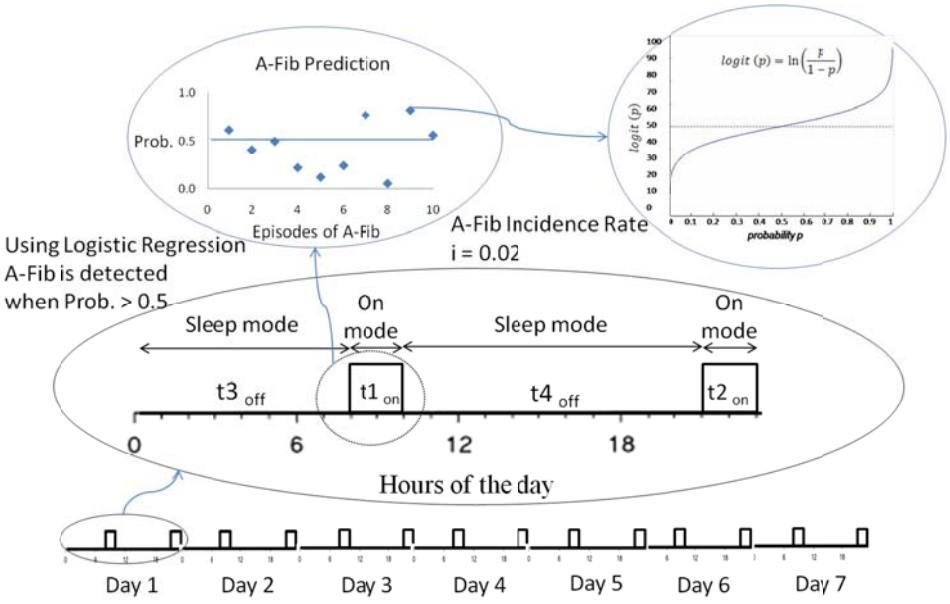

Figure 56: Detection of A-Fib progression from onset to paroxysmal phase

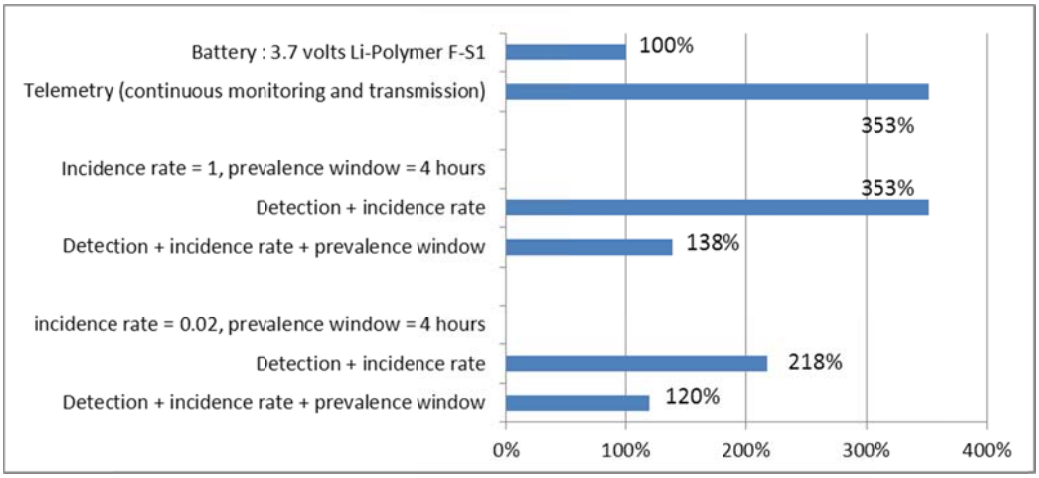

Figure 57: A 7-day energy consumption from first episode to paroxysmal A-Fib

9.2 Detecting persistent A-Fib

In persistent A-Fib, episodes last longer than seven days and do not go away on their own. Medical treatment is necessary to restore normal sinus rhythm. The next stage is longstanding persistent where episodes of A-Fib are continuous and last longer than one year leading to a permanent A-Fib where a person's irregular heartbeat does not return to normal sinus rhythm, even with medical treatment.

9.3 Detecting permanent A-Fib

In permanent A-Fib, a person's irregular heartbeat does not return to normal sinus rhythm, even with medical treatment [55] [56].

CHAPTER 10

10 VALIDATING A-FIB ENERGY-AWARE DETECTION MODELS

The following sub-sections validate our A-Fib energy-aware detection models by first summarizing the energy consumption results of our study and then validating them by testing a few cases. Figure 58 summarizes the energy distribution for a wearable computing system.

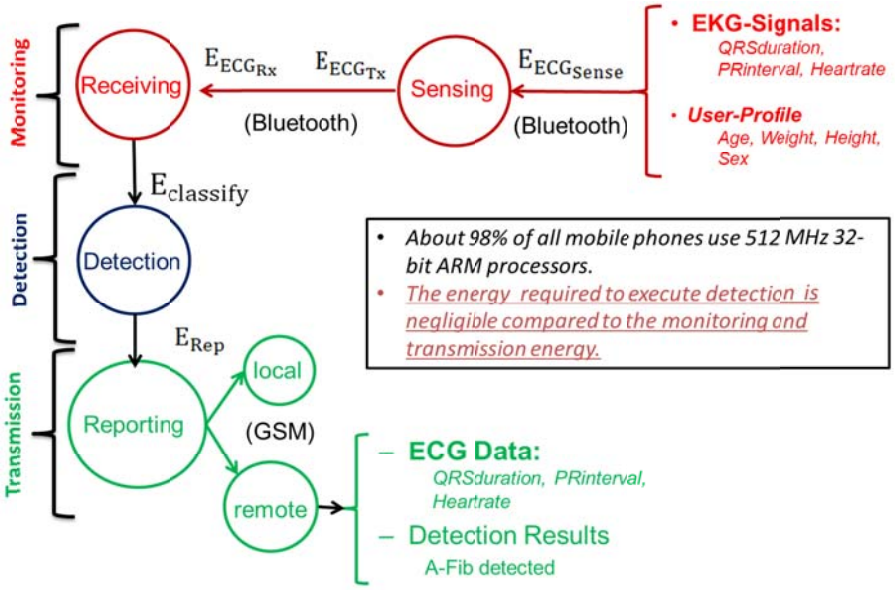

Figure 58: Wearable computing system requirements

10.1 Study results summarized

The results in our study show that the energy-aware detection models perform better, i.e. consume less energy than the telemetry energy model. We used a theoretical model

borrowing specification from the MICA2, a portable, low power, wireless two-lead EKG system integrated with the UC Berkley's MICA2 mote developed by UC Berkley and manufactured by Crossbow Technology, Inc. [69], and a GSM/EDGE smartphone.

Telemetry is widely accepted in healthcare for remotely collecting and sending vital data to a monitoring station for analysis and interpretation. However telemetry drains the battery quickly which forces the patient to replace the battery often, as often as every day.

Telemetry energy equation:

$$E_{Telemetry} = E_{monitor} + E_{transmission} = 8519 \text{ Joules}$$

Our energy-aware detection models use an efficient wearable computing scheme that outperforms telemetry energy models. They include an A-Fib incidence rate i or a detection positive rate r_p and A-Fib prevalence window D. The prevalence window D is defined as the fraction of the period the device is ON monitoring (T_{on}) during a 24-hour period. The energy model is active (E_{active}) during two hours in the morning t_{1on} and two hours in the evening t_{2on} with the anticipation that A-Fib occurs predominantly during these windows of time; otherwise it is on standby ($E_{standby}$).

$$\text{Window} = D = \frac{T_{on}}{T_{on} + T_{off}} = \frac{t1_{on} + t2_{on}}{24}$$

$$E_{TotalAFib} = E_{active} D + E_{standby}(1 - D)$$

The general energy-aware detection model equation:

$$E_{TotalAFib} = (E_{monitor} + E_{detectingAFib} + r_p E_{transmission})D + E_{standby}(1 - D)$$

$$(E_{EKG_{Sense}} + E_{EKG_{Tx}} + E_{EKG_{Rx}} + E_{detectingAFib} + r_p E_{Rep})D + E_{standby}(1 - D)$$

$$0 \le D \le 1, \quad 0 \le r_p \le 1$$

We use a detection positive rate i = 0.02 and a prevalence window $D = 1/6$ representing monitoring two hours in the morning and two hours in the evening.

$$E_{TotalAFib} = 2892 \text{ Joules}$$

Our study suggests that the largest energy consumed is by continuous telemetry, compared to the energy consumed by the energy-aware detection model using an incidence rate r_p of 0.02 and a 4-hour circadian prevalence window D (see Table 27)

$$34\% \text{ of telemetry energy model} < \text{Proposed Models} < 100\% \text{ of telemetry energy model}$$

	Percentage	Joules
Energy consumption during a 24-hour period		
Telemetry Device:		
• **Telemetry (continuous monitoring and transmission)**	100%	8,519
• **incidence rate = 1, prevalence window = 4 hours**		
o **detection + incidence rate + prevalence window**	39%	3,334
• **incidence rate = 0.02, prevalence window = 4 hours**		
o **detection + incidence rate + prevalence window**	34%	2,892

Table 27: Energy models compared to telemetry

10.2 Validating the Results

In this section, we validate our study results summarized in Section 10.1 using a two-lead EKG Heart Monitor A102D7 device from Alive Technologies wirelessly [88] connected to an Apple MacBook computer via Bluetooth. Although our validation uses a different wearable healthcare device depicted in Figure 59, our goal is to confirm comparable results to our study findings where the proposed energy-aware models consumption varies as follows:

$$34\% \text{ of telemetry energy model} < \text{Proposed Models} < 100\% \text{ of telemetry energy model}$$

The following sub-sections describe the validation set-up, the testing methodology, and the different testing scenarios such as establishing the battery lifetime when the device is in standby.

10.2.1 Describing the validation set-up

In this validation, we connect the Heart Monitor device A102D7 to an Apple MacBook laptop via Bluetooth and use the AliveECG software for Windows to display the captured EKG recordings.

The Alive Heart Monitor is a data acquisition, wireless EKG transmitter and recording device. The captured EKG recordings are displayed with a title bar, a serial number of the connected device, and a status area. The status area displays information including the connected symbol, the battery level of the heart monitor, the recording duration, and current heart rate.

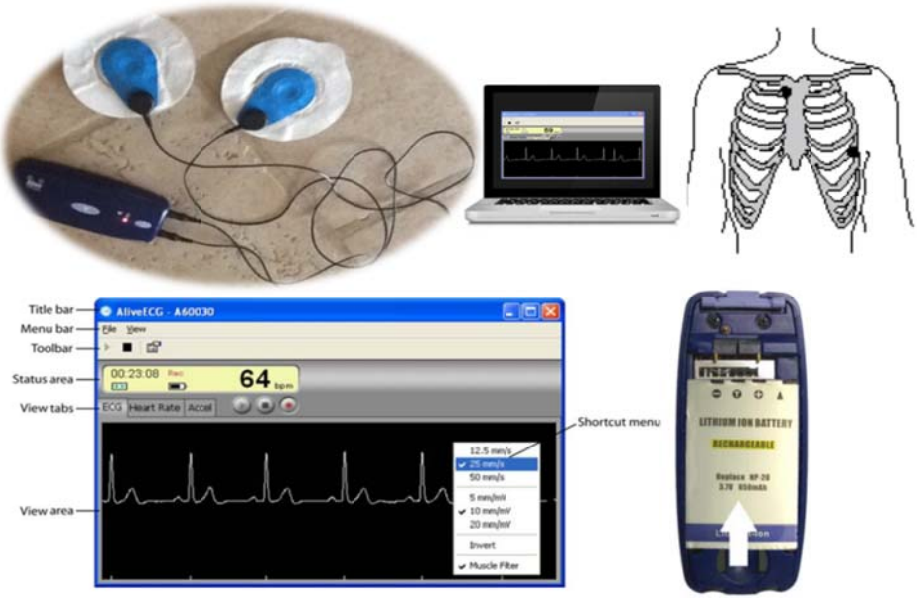

Figure 59: Monitoring and transmitting EKG signals via Bluetooth using a two-lead Heart Monitor A102D7 from Alive Technologies and an Apple MacBook

10.2.2 Methodology

We use a standard two lead configuration to connect the Alive Heart Monitor to the human body as shown in Figure 60. In all cases, we initiate the test by pushing the record button and capture different views displaying the heart rate, the elapsed time, and the percentage of battery capacity remaining. All tests start with the battery at 100% capacity and stop when the battery capacity reaches 0%.

The Alive Heart Monitor is powered by a rechargeable 3.7V, 650mAh Li-ion battery of type Casio NP20 or PowerSmart. The energy delivered by a full battery is 8658 Joules, (650mAh * 0.001* 3.7V * 3600 seconds). Table 28 describes the estimated battery life of the Alive Heart Monitor from Alive Technologies.

Mode	Estimated Battery Life
Recording to SD card	5 days
Continuous wireless transmission	2.5 days
Both recording to SD card and wireless transmission	2 days
Standby	7 days

Table 28: Alive Technologies Heart Monitor energy profile

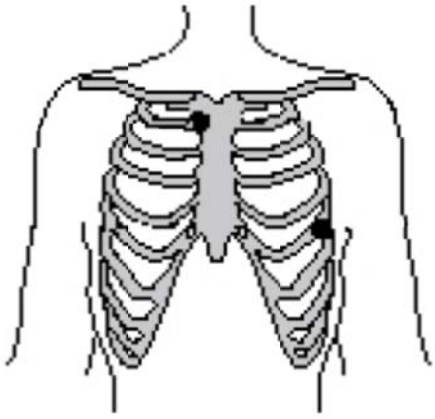

Figure 60: Heart Monitor A102D7 electrodes placement

10.2.2.1 Test cases

Typically, batteries discharge nonlinearly with respect to time. In the following test cases, we focus on battery lifetime and average rate of energy consumption. The following steps enumerate the various test cases:

a. Establishing the battery lifetime and the average rate of energy consumption for when the device is in standby.

b. Establishing the baseline battery lifetime and the average rate of energy consumption for when the device is monitoring and transmitting continuously.

c. Measuring the battery lifetime and the average rate of energy consumption required for a risk, incidence and window-based model:

- Case one: Using an incidence rate of 1 to represent a worst-case scenario, (i.e. monitoring continuously and transmitting continuously inside two 2-hour windows to simulate A-Fib prevalence circadian windows between 8 AM – 10 AM and 10 PM- 12 AM).
- Case two: Repeating case 1 except we use an incidence rate of 0.02 to represent an optimum case scenario when the detection algorithm is as accurate as possible, and the positive rate is equal to the incidence rate.

d. Summarizing the validation results: we compare the energy consumption of the detection models from steps c and d to the energy consumption of the telemetry model in step b.

10.2.2.1.1 Establishing the battery lifetime and the average consumption for when the device is in standby mode

In the standby mode, we turn off both the monitoring and the transmission. Using the two-lead Heart Monitor A102D7 device from Alive Technologies wirelessly connected to an Apple MacBook laptop via Bluetooth, we run the device in standby starting with the battery (rechargeable Li-ion battery of type Casio NP-20 3.7V 670mAh) at full capacity (100%) and let it run until the battery is fully discharged (0%). Table 29 and Figure 61 display the cumulative Joules consumed versus the corresponding elapsed time. In standby mode, the estimated battery lifetime, for the two-lead Heart Monitoring device A102D7 from Alive Technologies is 168 hours. The estimated cumulative consumed energy is 8658 Joules; that is, 51.54 joules per hour.

Standby				
Elapsed Time	**Decimal Hours Value**	**Percent of Battery Capacity Remaining**	**Current Joules Consumed**	**Cumulative Joules Consumed**
0 0 0	0.0	100	0	0
0 54 29	3.4	98	173.2	173.2
2 34 47	10.1	94	346.3	519.5
5 02 38	20.2	88	519.5	1039.0
8 04 01	28.6	83	432.9	1471.9
11 06 11	42.0	75	692.6	2164.5
13 44 11	50.4	70	432.9	2597.4
15 21 58	57.1	66	346.3	2943.7
18 26 09	67.2	60	519.5	3463.2
21 25 24	80.6	52	692.6	4155.8
23 32 11	87.4	48	346.3	4502.2
24 59 06	95.8	43	432.9	4935.1
26 39 54	100.8	40	259.7	5194.8
28 00 50	105.8	37	259.7	5454.5
29 03 18	112.6	33	346.3	5800.9
32 19 14	122.6	27	519.5	6320.3

34 58 55	134.4	20	606.1	6926.4
37 00 15	142.8	15	432.9	7359.3
39 02 48	147.8	12	259.7	7619.0
40 03 41	151.2	10	173.2	7792.2
41 02 38	154.6	8	173.2	7965.4
42 05 54	157.9	6	173.2	8138.5
43 04 23	161.3	4	173.2	8311.7
44 00 13	164.6	2	173.2	8484.8
45 05 28	166.3	1	86.6	8571.4
46 04 35	168.0	0	86.6	8658.0

Table 29: Alive Technologies Heart Monitoring Device A102D7 in standby

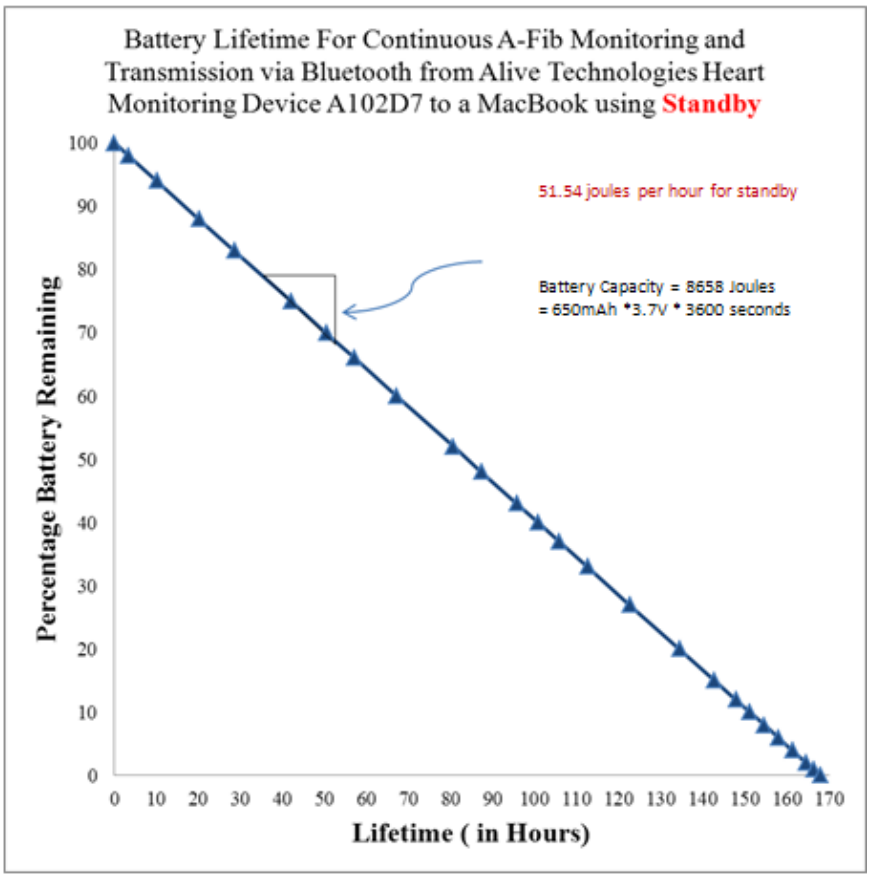

Figure 61: Alive Technologies Heart Monitoring Device A102D7 in standby

10.2.2.1.2 Establishing the baseline battery lifetime and the average consumption rate for when the device is in telemetry mode

In telemetry mode (incidence rate =1), we turn on both the monitoring and the transmission on the Alive Heart Monitor. The two-lead Heart Monitor A102D7 device from Alive Technologies is wirelessly connected to an Apple MacBook laptop via Bluetooth. We run the device in telemetry mode, starting with the battery (rechargeable Li-ion battery of type Casio NP-20 3.7V 670mAh) at full capacity (100%) and let it run until the battery is fully discharged (0%). Figure 62 displays the monitored and transmitted EKG recordings and their remaining battery capacity.

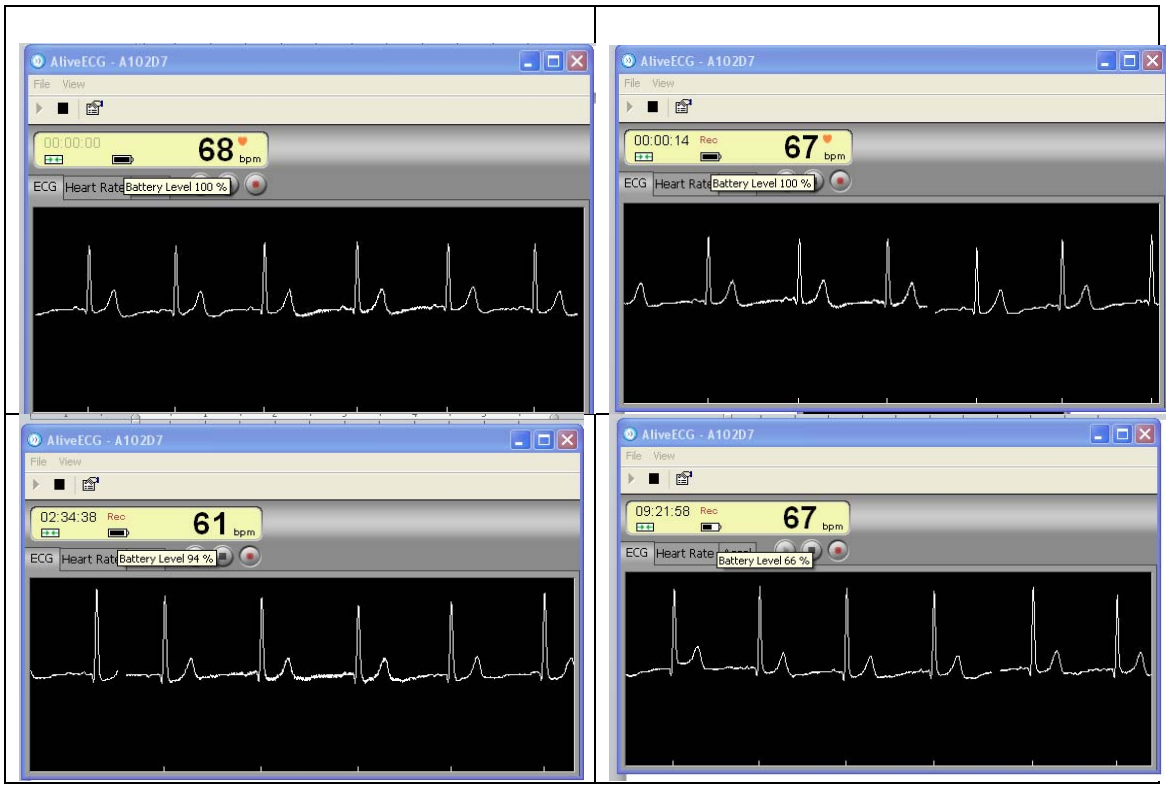

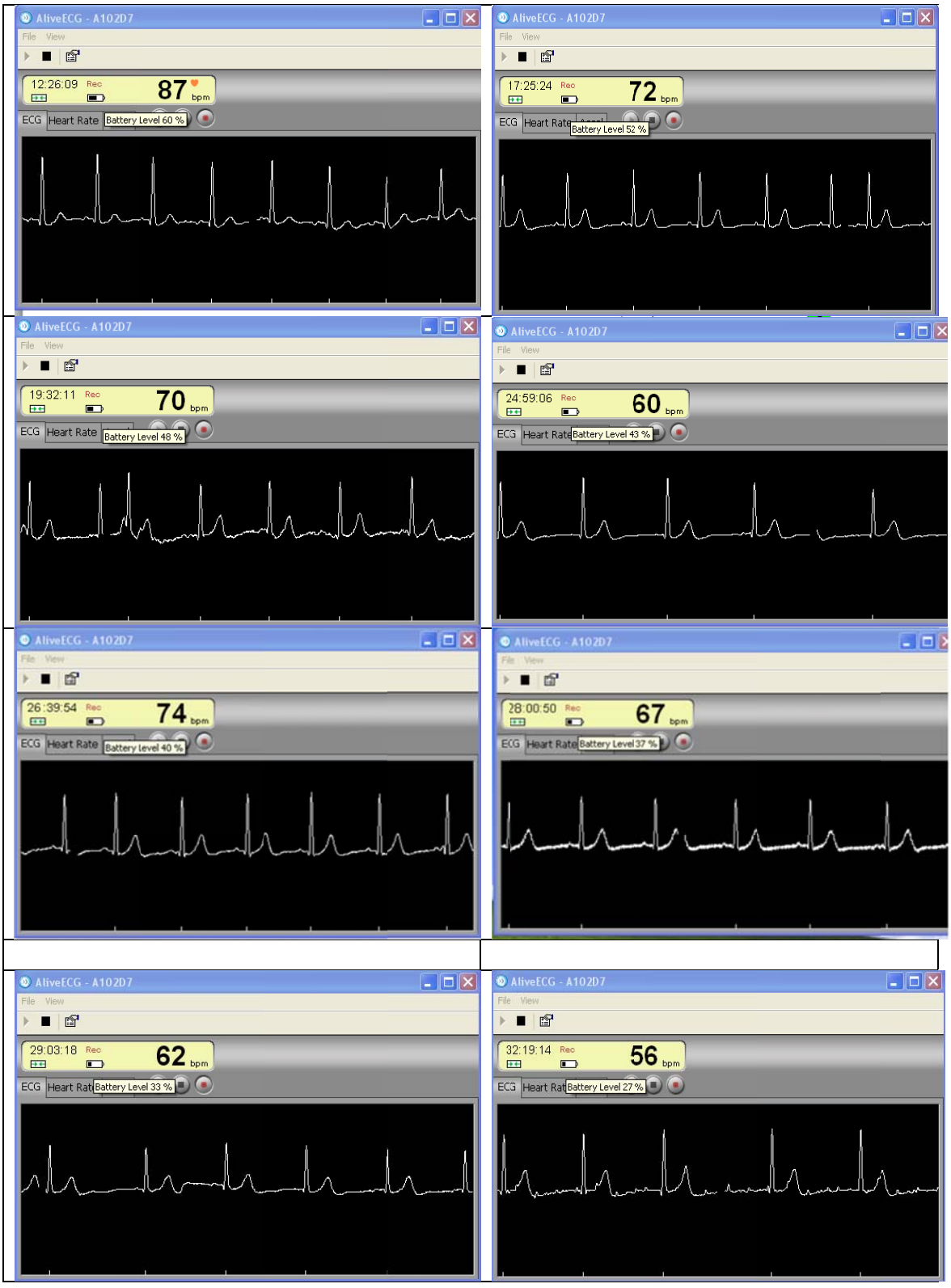
AliveECG - A102D7
File View
12:26:09 Rec
87 bpm
ECG Heart Rate Battery Level 60 %
AliveECG - A102D7
File View
17:25:24 Rec
72 bpm
ECG Heart Rate Battery Level 52 %
AliveECG - A102D7
File View
19:32:11 Rec
70 bpm
ECG Heart Rate Battery Level 48 %
AliveECG - A102D7
File View
24:59:06 Rec
60 bpm
ECG Heart Rate Battery Level 43 %
AliveECG - A102D7
File View
26:39:54 Rec
74 bpm
ECG Heart Rate Battery Level 40 %
AliveECG - A102D7
File View
28:00:50 Rec
67 bpm
ECG Heart Rate Battery Level 37 %
AliveECG - A102D7
File View
29:03:18 Rec
62 bpm
ECG Heart Rate Battery Level 33 %
AliveECG - A102D7
File View
32:19:14 Rec
56 bpm
ECG Heart Rate Battery Level 27 %

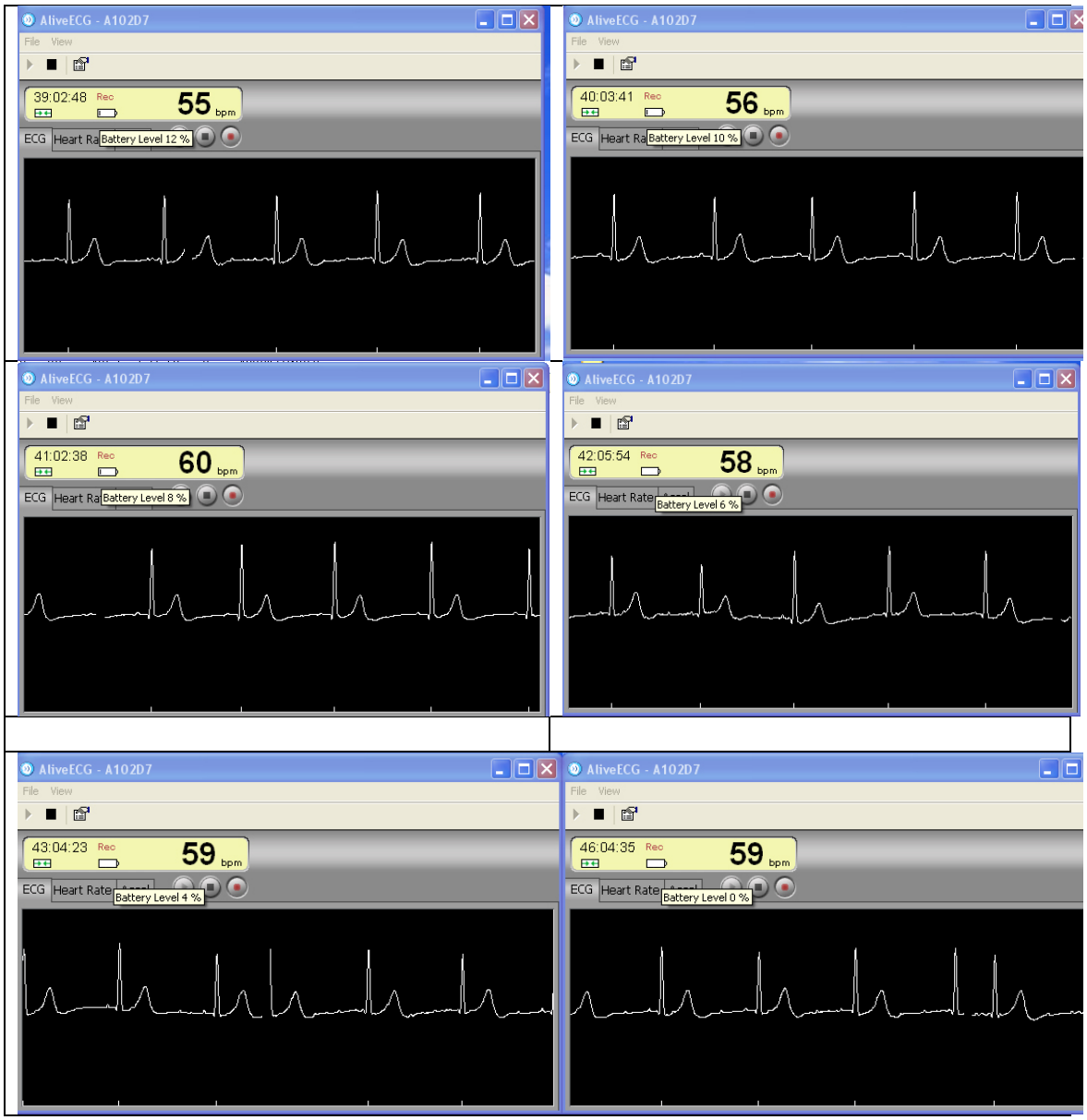

Figure 62: Timed EKG recordings and remaining battery capacity for monitoring and transmitting EKG signals via Bluetooth using a two-lead Heart Monitor A102D7 from Alive Technologies and an Apple MacBook

Table 30 and Figure 63 display the cumulative consumed Joules and the corresponding elapsed time. In telemetry mode, the estimated battery lifetime, for the two-lead Heart Monitoring device A102D7 from Alive Technologies, is 46 Hours, 4 Minutes and 35

Seconds. The estimated cumulative consumed energy is 8658 Joules; that is, 187.81 joules per hour.

Telemetry: continuous monitoring and transmission with Incidence rate = 1					
Detection Mode	**Elapsed Time hr min sec**	**Decimal (hours)**	**Percent Battery Capacity Remaining**	**Current Joules Consumed**	**Cumulative Joules Consumed**
Continuous Transmission	0 0 0	0	100	0	0
Continuous Transmission	0 54 29	0.9	98	169.0	169.0
Continuous Transmission	2 34 47	2.6	94	319.3	488.3
Continuous Transmission	5 02 38	5.0	89	450.7	939.0
Continuous Transmission	8 04 01	8.1	82	582.2	1521.3
Continuous Transmission	11 06 11	11.1	76	563.4	2084.7
Continuous Transmission	13 44 11	13.7	70	488.3	2573.0
Continuous Transmission	15 21 58	15.4	67	319.3	2892.3
Continuous Transmission	18 26 09	18.4	60	563.4	3455.7
Continuous Transmission	21 25 24	21.4	54	563.4	4019.1
Continuous Transmission	23 32 11	23.5	49	394.4	4413.5
Continuous Transmission	24 59 06	25.0	46	281.7	4695.2
Continuous Transmission	26 39 54	26.7	42	319.3	5014.5
Continuous Transmission	28 00 50	28.0	39	244.2	5258.7
Continuous Transmission	29 03 18	29.1	37	206.6	5465.2
Continuous Transmission	32 19 14	32.3	30	601.0	6066.2
Continuous Transmission	34 58 55	35.0	24	507.1	6573.3
Continuous Transmission	37 00 15	37.0	20	375.6	6948.9
Continuous Transmission	39 02 48	39.0	15	375.6	7324.6
Continuous Transmission	40 03 41	40.1	13	206.6	7531.1
Continuous Transmission	41 02 38	41.0	11	169.0	7700.2
Continuous Transmission	42 05 54	42.1	9	206.6	7906.8
Continuous Transmission	43 04 23	43.1	7	187.8	8094.6
Continuous Transmission	44 00 13	44.0	5	169.0	8263.6
Continuous Transmission	45 05 28	45.1	2	206.6	8470.2
Continuous Transmission	46 04 35	46.1	0	187.8	8658.0

Table 30: Baseline percent battery capacity remaining versus elapsed time (Telemetry mode)

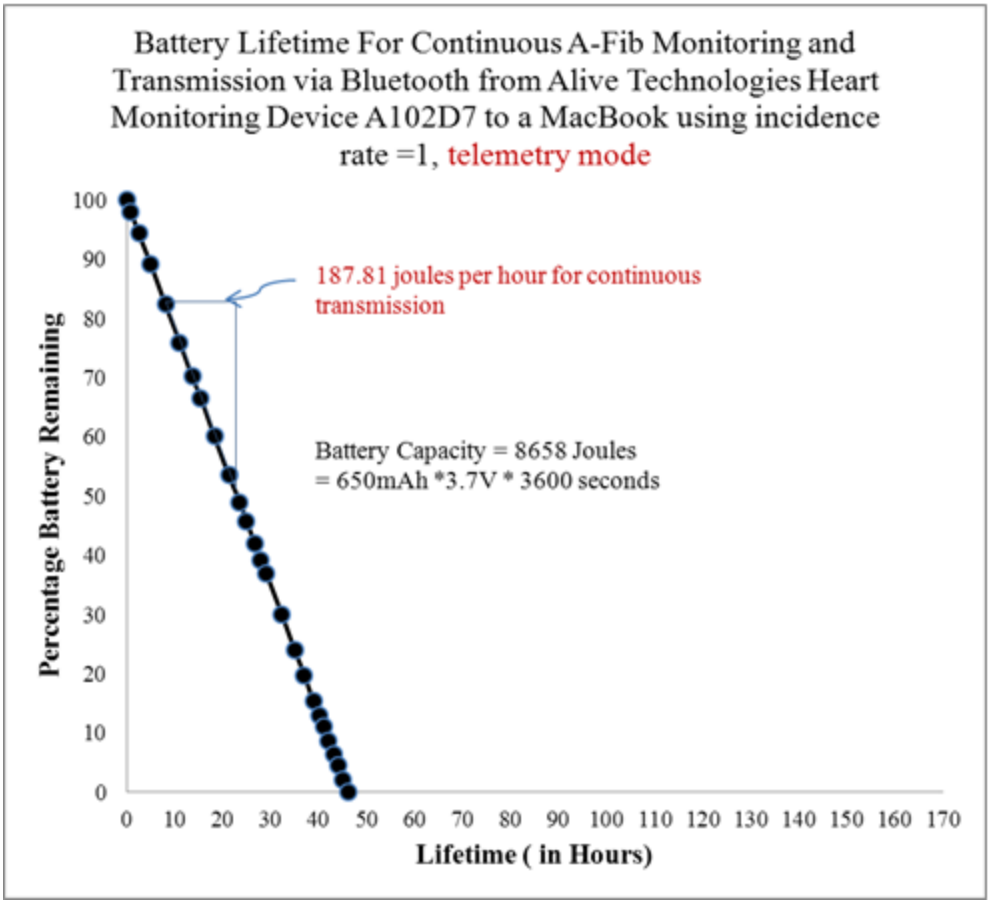

Figure 63: Battery lifetime for A-Fib continuously monitoring and transmission via Bluetooth using Alive Technologies Heart Monitor A102D7 and an Apple MacBook

10.2.2.1.3 Measuring the battery lifetime and the energy consumption rate required for a risk-based, incidence and window-based A-Fib detection model

The implementation of a risk and incidence-based A-Fib detection helps extend the battery life of the Alive Technologies Heart Monitor A102D7 device. Knowing the A-Fib risk factor of a patient allows one to prescribe an A-Fib monitoring and detection scheme (see Figure 64) and schedule (see Table 31). A high A-Fib risk factor may suggest more frequent monitoring compared to a low A-Fib risk factor. A-Fib risk factors may be classified in three categories made up of risk ranges such as low risk with $k < 0.05$, medium risk with $0.05 < k < 0.15$, and high risk with $k > 0.15$. A low risk A-Fib factor or

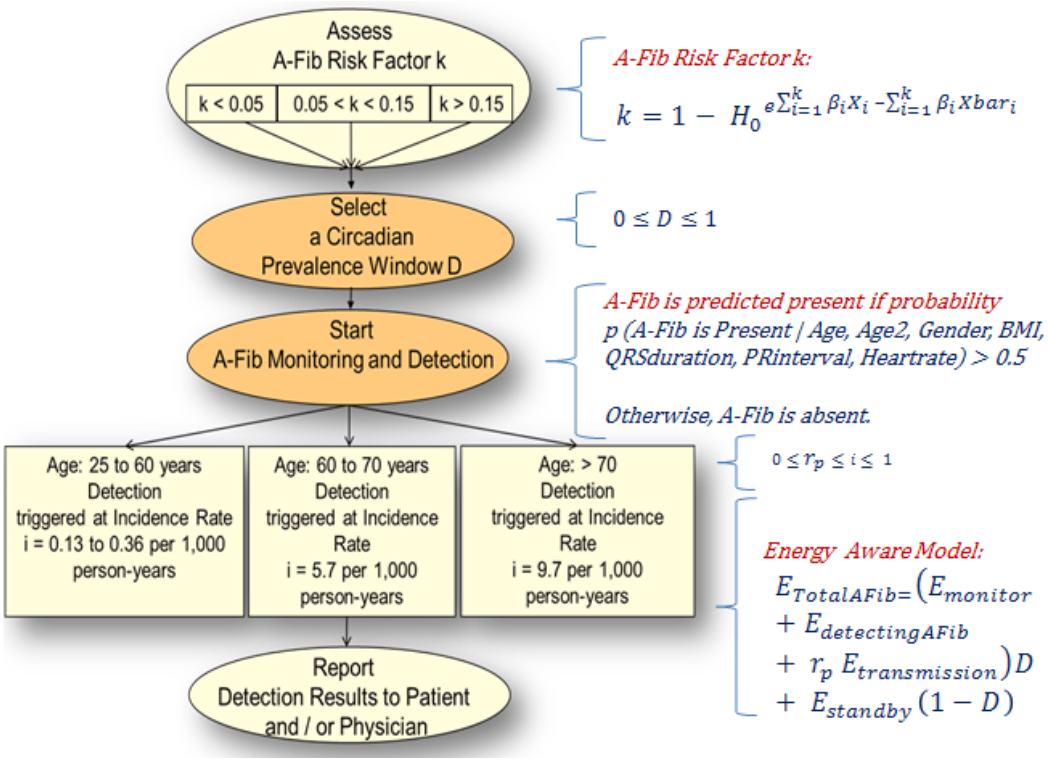

Figure 64: Efficient wearable monitoring and detection scheme based on A-Fib Risk Factor k, Incidence Rate r_p and circadian prevalence window D

category 1, may require an energy-aware detection model that would best fit a user who is healthy and athletic where monitoring is triggered occasionally during exercises. A medium risk A-Fib factor or category 2 may require an energy-aware model that would best fit a user who needs monitoring during AM and PM prevalence windows. A high-risk A-Fib factor may require a telemetry model that is fit for a user who needs to monitor A-Fib continuously because he may have a chronic case of A-Fib.

Select Energy Model based on Risk Factor	**Risk Factor**	**Use Energy Model**	**Compared to Telemetry Energy**
Risk factor category 1 is for a user who is healthy; similar to wearing a sports watch.	K < 0.05	Based on incidence and prevalence window	33.9%
Risk factor category 2 is for a user	0.05≤ K <	Based on incidence	39.1%

who wants to monitor A-Fib daily during AM/PM windows.	0.15		
Risk factor category 3 is for the chronic case. The user monitors continuously. Results are transmitted to a care center.	$K \geq 0.15$	Use Telemetry	100.0%

Table 31: Energy-aware detection model selection based on risk factor category

The A-Fib detection algorithm outputs a positive result when the probability of A-Fib being present is greater than 0.5. We utilize an asymmetric prevalence window D = 1/6 within a 24 hour period and an incidence rate i=0.02 in the energy model (see Figure 65). The EKG signals are sensed and transmitted to an Apple MacBook laptop during windows of time where A-Fib is assumed prevalent.

A-Fib is predicted present if probability p (A-Fib is Present | Age, Age^2, Gender, BMI, QRSduration, $PR_{interval}$, Heartrate) > 0.5

Otherwise, A-Fib is absent.

Where:

$$\text{logit}(p) = -41.175 + 0.820\ \text{Age} - 0.006\ \text{Age}^2 + 4.737\ \text{Gender} - 0.047\ \text{BMI} + 0.098\ \text{QRSduration} - 0.178\ \text{PR}_{\text{interval}} + 0.066\ \text{Heartrate}$$

And

$$p = 1 / (1 + e^{-\text{logit}(p)})$$

Prevalence window D is defined as the fraction of the period the device is ON monitoring (T_{on}) during a 24-hour period. The energy model E_{active} runs during two hours in the morning t_{1on} and two hours in the evening t_{2on} with the anticipation that A-Fib occurs predominantly during these windows of time; otherwise it is on standby $E_{standby}$.

$$\text{Window} = D = \frac{T_{on}}{T_{on} + T_{off}} = \frac{t1_{on} + t2_{on}}{24} = \frac{1}{6}$$

$$E_{TotalAFib} = E_{active}D + E_{standby}(1 - D)$$

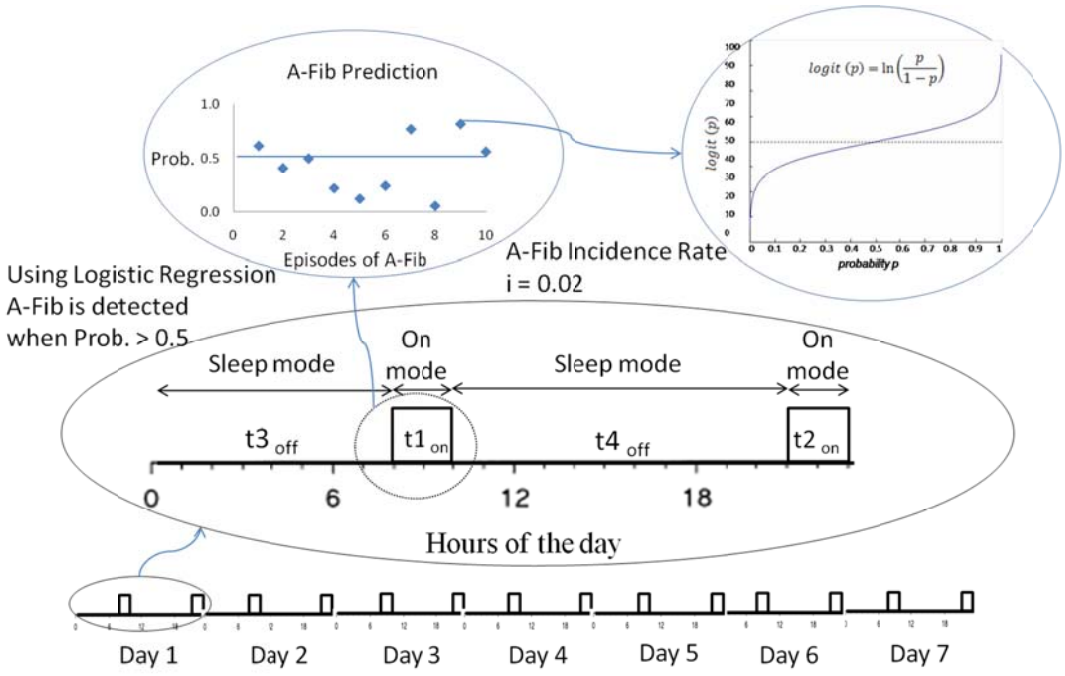

Figure 65: Episodes of A-Fib inside a prevalence window

- ***Case one: Using an incidence rate of 1 to represent a worst-case scenario, (i.e. monitoring continuously and transmitting continuously inside a four-hour window)***

In case one, while in active mode, we monitor and transmit inside two 2-hour prevalent windows between 8 AM - 10 AM and 10 PM - 12 AM with incidence rate = 1, and stay in standby mode the remainder of the 24-hour period. An incidence rate equal to 1 means that we are continuously monitoring and continuously transmitting inside the two windows. The 2-hour circadian windows require 187.81 joules per hour while the standby requires 51.54 joules per hour. Table 32 and Figure 66 display the percentage of battery capacity remaining versus the elapsed time. When applying our energy-aware model, with monitoring and transmitting inside two 2-hour prevalent windows between 8 AM - 10 AM and 10 PM - 12 AM and an A-Fib incidence rate = 1, the estimated battery

lifetime, for the two-lead Heart Monitoring device A102D7 from Alive Technologies is approximately 128 hours. The estimated cumulative consumed energy is 8658 Joules; that is, an average of 68 joules per hour.

Continuous monitoring and transmission with two 2-hour circadian windows with incidence rate = 1				
Detection Mode	**Elapsed Time (hours)**	**Percent Battery Capacity Remaining**	**Current Joules Consumed**	**Cumulative Joules Consumed**
Standby	0	100	0.0	0.0
Standby	8	95	412.3	412.3
2 hour window	10	91	375.6	787.9
Standby	22	84	618.4	1406.3
2 hour window	24	79	375.6	1782.0
Standby	32	75	412.3	2194.2
2 hour window	34	70	375.6	2569.9
Standby	46	63	618.4	3188.3
2 hour window	48	59	375.6	3563.9
Standby	56	54	412.3	3976.2
2 hour window	58	50	375.6	4351.8
Standby	70	43	618.4	4970.2
2 hour window	72	38	375.6	5345.9
Standby	80	33	412.3	5758.1
2 hour window	82	29	375.6	6133.8
Standby	94	22	618.4	6752.2
2 hour window	96	18	375.6	7127.8
Standby	104	13	412.3	7540.1
2 hour window	106	9	375.6	7915.7
Standby	128	0	618.4	8534.1

Table 32: Percent of battery capacity discharge versus time inside two 2-hour windows with incidence rate = 1 and in standby otherwise

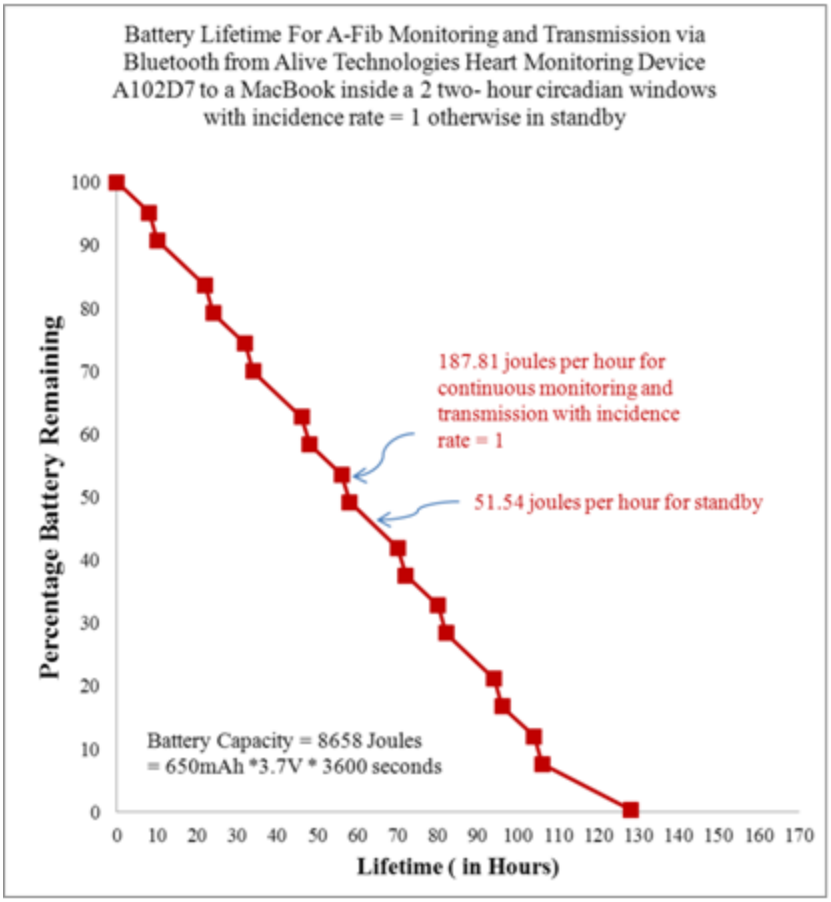

Figure 66: Percent of battery capacity discharge versus elapsed time inside two 2-hour windows with incidence rate = 1 and in standby otherwise

- ***Case two: Using an incidence rate of 0.02 to represent an optimum case scenario when the detection algorithm is as accurate as possible, and the positive rate is equal to the incidence rate***

In case two, while in active mode, we monitor and transmit inside two 2-hour prevalent windows between 8 AM - 10 AM and 10 PM - 12 AM at the incidence rate of 0.02, and in standby mode the remainder of the 24-hour period. The 2-hour circadian windows require 0.98*51.54 + 0.02*187.81= 54.25 Joules per hour. Table 33 and Figure 67 display the percentage of battery capacity remaining versus elapsed time during two 2-hour prevalent windows with incidence rate = 0.02, and during a standby the remainder of the 24-hour period. When applying our energy-aware model, with monitoring and

transmitting inside two 2-hour prevalent windows between 8 AM - 10 AM and 10 PM - 12 AM and an A-Fib incidence rate = 0.02, the estimated battery lifetime, for the two-lead Heart Monitoring device A102D7 from Alive Technologies is approximately 166 hours. The estimated cumulative consumed energy is 8658 Joules; that is, an average of 52 joules per hour.

Continuous monitoring and transmission, two 2-hour windows with incidence rate = 0.02				
Detection Mode	**Elapsed Time (hours)**	**Percent Battery Capacity Remaining**	**Current Joules Consumed**	**Cumulative Joules Consumed**
Standby	0	100	0	0.0
Standby	8	95	412.3	412.3
2 hour window	10	94	108.5	520.8
Standby	22	87	618.4	1139.2
2 hour window	24	86	108.5	1247.8
Standby	32	81	412.3	1660.0
2 hour window	34	80	108.5	1768.6
Standby	46	72	618.4	2387.0
2 hour window	48	71	108.5	2495.5
Standby	56	66	412.3	2907.8
2 hour window	58	65	108.5	3016.3
Standby	70	58	618.4	3634.8
2 hour window	72	57	108.5	3743.3
Standby	80	52	412.3	4155.6
2 hour window	82	51	108.5	4264.1
Standby	94	43	618.4	4882.5
2 hour window	96	42	108.5	4991.0
Standby	104	37	412.3	5403.3
2 hour window	106	36	108.5	5511.8
Standby	118	29	618.4	6130.3
2 hour window	120	28	108.5	6238.8
Standby	128	23	412.3	6651.1
2 hour window	130	22	108.5	6759.6
Standby	142	15	618.4	7378.0
2 hour window	144	13	108.5	7486.6
Standby	152	8	412.3	7898.8
2 hour window	154	7	108.5	8007.4
Standby	166	0	618.4	8625.8

Table 33: Percent of battery capacity discharge versus time inside two 2-hour windows with incidence rate = 0.02 and in standby otherwise

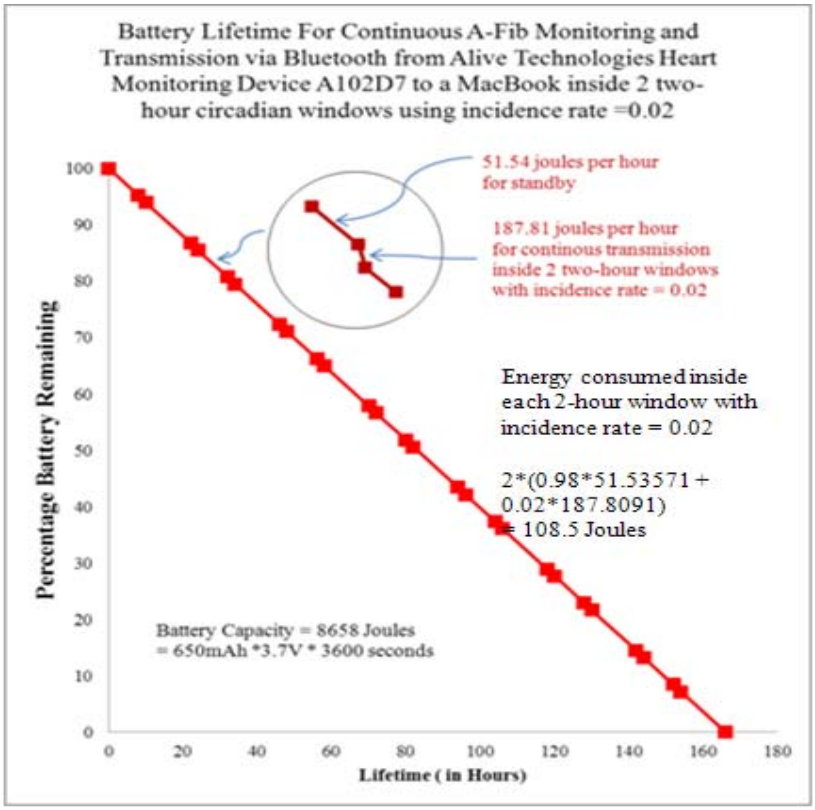

Figure 67: Percent of battery capacity discharge versus elapsed time inside two 2-hour windows with incidence rate = 0.02 and otherwise in standby

10.2.2.1.4 Summarizing the validation results

- In standby mode, the estimated battery lifetime, for the two-lead Heart Monitoring device A102D7 from Alive Technologies, is 168 hours. The estimated cumulative consumed energy is 8658 Joules; that is, 51.54 joules per hour.
- In telemetry mode, the estimated battery lifetime, for the two-lead Heart Monitoring device A102D7 from Alive Technologies, is 46 Hours, 4 Minutes and 35 Seconds (46.08 hours). The estimated cumulative consumed energy is 8658 Joules; that is, 187.81 joules per hour.
- Energy-aware detection model with i=1, D=0.167. When applying our energy-aware model, with monitoring and transmitting inside two 2-hour prevalent

windows between 8 AM - 10 AM and 10 PM - 12 AM and an A-Fib incidence rate = 1, the estimated battery lifetime, for the two-lead Heart Monitoring device A102D7 from Alive Technologies is approximately 128 hours. The estimated cumulative consumed energy is 8658 Joules; that is, an average of 68 joules per hour.

- Energy-aware detection model with i=0.02, D=0.167. When applying our energy-aware model, with monitoring and transmitting inside two 2-hour prevalent windows between 8 AM - 10 AM and 10 PM - 12 AM and an A-Fib incidence rate = 0.02, the estimated battery lifetime, for the two-lead Heart Monitoring device A102D7 from Alive Technologies is approximately 166 hours. The estimated cumulative consumed energy is 8658 Joules; that is, an average of 52 joules per hour.

Figure 68 summarizes the energy consumption ranging from when the device is in telemetry to when the device is in standby mode. Depending on the values assigned to the incidence rate and circadian A-Fib prevalence windows parameters our energy models consume as much as telemetry at the lower bound and as little as a standby in the upper bound.

$$\text{Telemetry Energy} \leq \text{Proposed Models Energy} \leq \text{Standby Energy}$$

$$46.1 \text{ hours} \leq \text{Proposed Models Battery lifetime} \leq 168 \text{ hours}$$

$$51.54 \frac{\text{Joules}}{\text{hour}} \leq \text{E}_{\text{TotalAFib}} \leq 187.81 \frac{\text{Joules}}{\text{hour}}$$

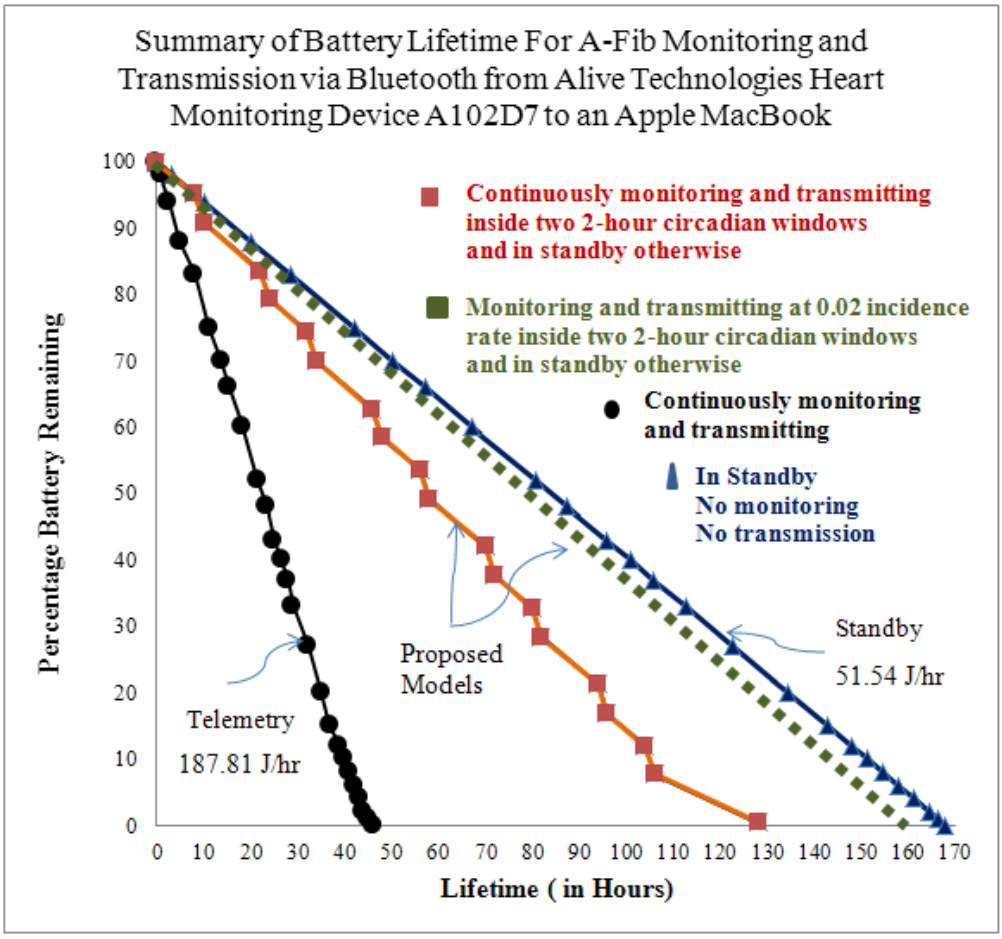

Figure 68: Validation results from the energy-aware models and telemetry

Table 34 compares validation results percentages between our energy-aware models and telemetry for the two-lead Heart Monitoring device A102D7 from Alive Technologies.

$$28\ \%\ \text{of telemetry} < E_{TotalAFib} < 100\%\ \text{telemetry}$$

Mode Type	Validation
Telemetry (continuous monitoring and transmission)	100%
detection + incidence rate + prevalence window	28%
incidence rate = 0.02, prevalence window = 4 hours	
detection + incidence rate + prevalence window	36%
incidence rate = 1, prevalence window = 4 hours	

Table 34: Validation results summary

10.3 Comparing validation results to study results

As anticipated, our goal is to confirm that our validation results are comparable to our study findings. Table 35 displays both validation results and study results. Our validation confirms our study results; that our proposed energy-aware detection models perform better than telemetry energy model.

From our study results, we claim:

$$34\% \text{ of telemetry energy } \leq \text{Proposed Models energy} \leq 100\% \text{ of telemetry energy}$$

From our validation, we verify that depending on the values assigned to the incidence rate and circadian A-Fib prevalence windows parameters our energy models consume as much as 28% of telemetry at the lower bound and as much as 100% of telemetry energy.

$$28\ \% \text{ telemetry energy} \leq \text{Proposed Models energy } \leq 100\% \text{ telemetry energy}$$

For example, Table 35 and Figure 69 show that the energy-aware model that uses an incidence rate i=1 and a prevalence window D=0.167 consumes 39% of the energy consumed by telemetry according to our study as compared to 36% in validation. The differences in the results may be explained by the fact that our study and our validation use different monitoring and transmission devices. Both devices use different chip technology and different firmware. We expect power efficiency in both hardware and software technologies to contribute to the difference between the results.

Mode Type	Validation	Study
Telemetry (continuous monitoring and transmission)	100%	100%
Detection + incidence rate + prevalence window		
incidence rate = 0.02, prevalence window = 4 hours	28%	34%
Incidence rate = 1, prevalence window = 4 hours	36%	39%

Table 35: Comparing validation results and study results

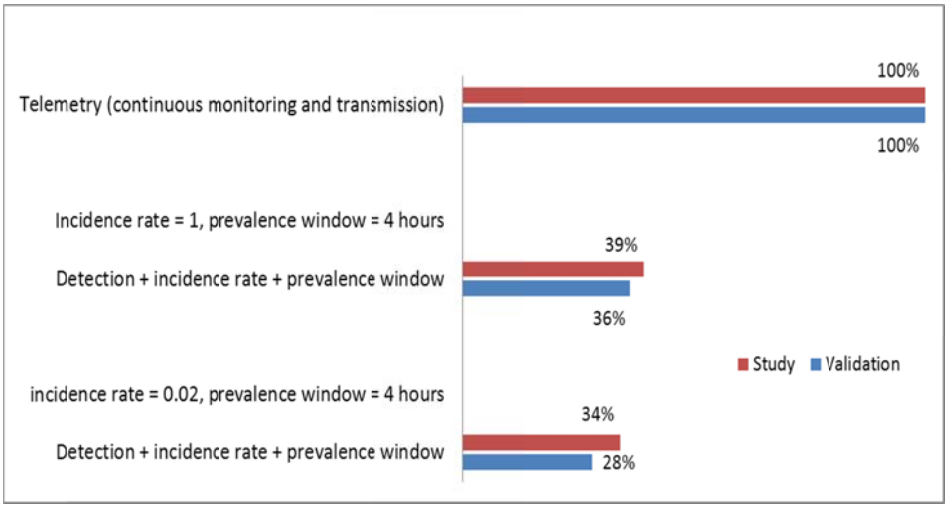

Figure 69: Comparing validation results and study results

10.4 Validating detection algorithm

In the next sub-sections, we will summarize the detection algorithm results from our study and validate the detection algorithm accuracy

10.4.1 Study detection algorithm results summarized

Our study concludes that A-Fib is predicted present if probability p (A-Fib is Present | Age, Age^2, gender, BMI, QRSduration, $PR_{interval}$, Heartrate) > 0.5

Otherwise, A-Fib is absent.

Where:

$$\text{logit}(p) = -41.175 + 0.820\ \text{Age} - 0.006\ \text{Age}^2 + 4.737\ \text{Gender} - 0.047\ \text{BMI} + 0.098\ \text{QRSduration} - 0.178\ PR_{interval} + 0.066\ \text{Heartrate}$$

And

$$p = 1 / (1 + e^{-\text{logit}(p)})$$

The derived logistic regression algorithm identifies the instances with the A-Fib disease with 98.8% sensitivity, and identifies those without the disease with 96.9% specificity. A specificity of 96.9% leads to a false positive result of 3.1%. A sensitivity of 98.8% means

that the classifier does not recognize all actual positives. A sensitivity of 100% implies that the test extracted all actual positives whereas in a high specificity test, negative results are used to rule out the disease. Our algorithm exhibits better sensitivity and specificity when compared to clinical measurements diagnosing A-Fib are performed by internists and general practitioners instead of cardiologists. Studies [59] suggest sensitivity (True Positive rate) of 80% and specificity (True Negative rate) of 92%. Our detection algorithm has an overall detection accuracy of 97.37%.

10.4.2 Validating detection algorithm accuracy

We validate the accuracy of our detection algorithm using a test data in logistic regression model.

In our validation, we use a Hold Out method and a cross-validation method. In the Hold Out, we randomly partition the data into two disjoint set, one with 2/3 of dataset for training and 1/3 of the dataset for testing. In the k-Fold Cross-Validation method, we randomly partition data into 10 disjoint sets, equal in size, then sequentially choose one set for testing and nine for training. The testing/training process is conducted ten times. We compare the outcome of our detection algorithm with the actual clinical values.

Table 36 displays the actual versus predicted values of A-Fib logistic regression algorithm results from a Hold Out method inputting a randomly generated test dataset made up of 1/3 of the original dataset. The overall detection accuracy is:

$$\text{Overall Accuracy } = \frac{100}{103} * 100\% = 97.09\%$$

Table 37 displays the actual versus predicted values of A-Fib logistic regression algorithm results from a 10-Fold Cross-Validation method. The overall detection accuracy is:

$$\text{Overall Accuracy } = \frac{296}{304} * 100\% = 97.36\%$$

Both methods offer similar accuracies of 97.09% and 97.36% respectively, and validate the accuracy from our study at 97.37%.

Actual versus prediction values of A-Fib using logistic regression model:

P is the probability of predicting correctly the presence or absence of A-Fib given an actual value

No.	actual	predicted	error	p
1	2:NOAF	2:NOAF		1
2	1:AF	1:AF		0.835
3	2:NOAF	2:NOAF		1
4	2:NOAF	2:NOAF		1
5	2:NOAF	2:NOAF		1
6	2:NOAF	2:NOAF		1
7	2:NOAF	2:NOAF		1
8	2:NOAF	2:NOAF		0.988
9	2:NOAF	2:NOAF		1
10	1:AF	1:AF		0.867
11	2:NOAF	2:NOAF		1
12	2:NOAF	2:NOAF		1
13	2:NOAF	2:NOAF		1
14	2:NOAF	2:NOAF		1
15	1:AF	1:AF		0.869
16	2:NOAF	2:NOAF		1
17	2:NOAF	2:NOAF		1
18	2:NOAF	2:NOAF		1
19	2:NOAF	2:NOAF		1
20	2:NOAF	2:NOAF		1
21	2:NOAF	1:AF	+	0.895
22	1:AF	1:AF		0.985
23	2:NOAF	2:NOAF		1
24	1:AF	1:AF		0.96
25	2:NOAF	2:NOAF		1
26	2:NOAF	2:NOAF		1
27	2:NOAF	2:NOAF		1
28	2:NOAF	2:NOAF		1
29	2:NOAF	2:NOAF		1
30	2:NOAF	2:NOAF		1
31	2:NOAF	2:NOAF		1
32	2:NOAF	2:NOAF		1
33	2:NOAF	2:NOAF		1
34	2:NOAF	2:NOAF		1
35	2:NOAF	2:NOAF		1
36	2:NOAF	2:NOAF		1
37	2:NOAF	2:NOAF		1
38	1:AF	1:AF		0.946
39	1:AF	1:AF		0.887
40	2:NOAF	2:NOAF		1
41	2:NOAF	1:AF	+	0.926
42	2:NOAF	2:NOAF		1
43	2:NOAF	2:NOAF		0.736
44	2:NOAF	2:NOAF		1
45	2:NOAF	2:NOAF		1
46	2:NOAF	2:NOAF		1
47	2:NOAF	2:NOAF		1
48	2:NOAF	2:NOAF		1

No.	actual	predicted	error	p
53	1:AF	1:AF		0.95
54	2:NOAF	2:NOAF		1
55	2:NOAF	2:NOAF		1
56	1:AF	1:AF		0.966
57	2:NOAF	2:NOAF		1
58	1:AF	1:AF		0.97
59	1:AF	1:AF		0.916
60	2:NOAF	2:NOAF		1
61	2:NOAF	2:NOAF		1
62	2:NOAF	2:NOAF		1
63	2:NOAF	1:AF	+	0.902
64	2:NOAF	2:NOAF		1
65	2:NOAF	2:NOAF		1
66	1:AF	1:AF		0.789
67	2:NOAF	2:NOAF		1
68	2:NOAF	2:NOAF		1
69	1:AF	1:AF		0.87
70	1:AF	1:AF		0.991
71	1:AF	1:AF		0.916
72	2:NOAF	2:NOAF		1
73	2:NOAF	2:NOAF		1
74	2:NOAF	2:NOAF		1
75	1:AF	1:AF		0.876
76	1:AF	1:AF		0.957
77	2:NOAF	2:NOAF		1
78	2:NOAF	2:NOAF		1
79	2:NOAF	2:NOAF		1
80	2:NOAF	2:NOAF		1
81	2:NOAF	2:NOAF		1
82	2:NOAF	2:NOAF		1
83	1:AF	1:AF		0.955
84	2:NOAF	2:NOAF		1
85	1:AF	1:AF		0.959
86	1:AF	1:AF		0.976
87	2:NOAF	2:NOAF		1
88	2:NOAF	2:NOAF		1
89	2:NOAF	2:NOAF		1
90	2:NOAF	2:NOAF		1
91	2:NOAF	2:NOAF		1
92	2:NOAF	2:NOAF		1
93	1:AF	1:AF		0.587
94	2:NOAF	2:NOAF		1
95	2:NOAF	2:NOAF		1
96	2:NOAF	2:NOAF		1
97	2:NOAF	2:NOAF		1
98	1:AF	1:AF		0.93
99	1:AF	1:AF		0.936
100	2:NOAF	2:NOAF		1

49	2:NOAF	2:NOAF		1
50	2:NOAF	2:NOAF		1
51	1:AF	1:AF		0.959
52	2:NOAF	2:NOAF		1

101	2:NOAF	2:NOAF		1
102	2:NOAF	2:NOAF		1
103	2:NOAF	2:NOAF		1

Table 36: Actual versus prediction values of A-Fib using logistic regression model using 1/3-2/3 Hold Out method

Actual versus prediction values of A-Fib using logistic regression model:

P is the probability of predicting correctly the presence or absence of A-Fib given an actual value

No.	actual	predicted	err	p
1	1:AF	1:AF		0.991
2	1:AF	1:AF		0.955
3	1:AF	1:AF		0.998
4	1:AF	1:AF		0.915
5	1:AF	1:AF		0.953
6	1:AF	1:AF		0.995
7	1:AF	1:AF		0.992
8	1:AF	1:AF		0.991
9	2:NOAF	2:NOAF		1
10	2:NOAF	2:NOAF		1
11	2:NOAF	2:NOAF		1
12	2:NOAF	1:AF	+	0.897
13	2:NOAF	2:NOAF		1
14	2:NOAF	2:NOAF		1
15	2:NOAF	2:NOAF		1
16	2:NOAF	2:NOAF		1
17	2:NOAF	2:NOAF		1
18	2:NOAF	2:NOAF		1
19	2:NOAF	1:AF	+	0.959
20	2:NOAF	2:NOAF		1
21	2:NOAF	2:NOAF		1
22	2:NOAF	2:NOAF		1
23	2:NOAF	2:NOAF		1
24	2:NOAF	2:NOAF		1
25	2:NOAF	2:NOAF		1
26	2:NOAF	2:NOAF		1
27	2:NOAF	2:NOAF		1
28	2:NOAF	2:NOAF		1
29	2:NOAF	2:NOAF		1
30	2:NOAF	2:NOAF		1
31	2:NOAF	2:NOAF		1
1	1:AF	1:AF		0.952
2	1:AF	1:AF		0.926
3	1:AF	1:AF		0.96
4	1:AF	1:AF		0.908
5	1:AF	1:AF		0.889
6	1:AF	1:AF		0.98
7	1:AF	1:AF		0.908
8	1:AF	1:AF		0.965
9	2:NOAF	2:NOAF		1
10	2:NOAF	2:NOAF		1
11	2:NOAF	2:NOAF		1
12	2:NOAF	2:NOAF		1
13	2:NOAF	2:NOAF		1
14	2:NOAF	2:NOAF		1
15	2:NOAF	2:NOAF		1

No.	actual	predicted	err	p
29	2:NOAF	2:NOAF		1
30	2:NOAF	2:NOAF		1
1	1:AF	1:AF		0.955
2	1:AF	1:AF		0.906
3	1:AF	1:AF		0.985
4	1:AF	1:AF		0.977
5	1:AF	1:AF		0.993
6	1:AF	1:AF		0.995
7	1:AF	1:AF		0.967
8	1:AF	1:AF		0.903
9	2:NOAF	2:NOAF		1
10	2:NOAF	2:NOAF		1
11	2:NOAF	2:NOAF		1
12	2:NOAF	2:NOAF		1
13	2:NOAF	2:NOAF		1
14	2:NOAF	2:NOAF		1
15	2:NOAF	2:NOAF		1
16	2:NOAF	2:NOAF		1
17	2:NOAF	2:NOAF		1
18	2:NOAF	2:NOAF		1
19	2:NOAF	2:NOAF		1
20	2:NOAF	2:NOAF		1
21	2:NOAF	2:NOAF		1
22	2:NOAF	2:NOAF		1
23	2:NOAF	2:NOAF		1
24	2:NOAF	2:NOAF		1
25	2:NOAF	2:NOAF		1
26	2:NOAF	2:NOAF		1
27	2:NOAF	2:NOAF		1
28	2:NOAF	2:NOAF		1
29	2:NOAF	2:NOAF		1
30	2:NOAF	2:NOAF		1
1	1:AF	1:AF		0.976
2	1:AF	1:AF		0.875
3	1:AF	1:AF		0.825
4	1:AF	1:AF		0.933
5	1:AF	1:AF		0.832
6	1:AF	1:AF		0.789
7	1:AF	1:AF		0.975
8	1:AF	1:AF		0.935
9	2:NOAF	2:NOAF		1
10	2:NOAF	2:NOAF		1
11	2:NOAF	2:NOAF		1
12	2:NOAF	2:NOAF		1
13	2:NOAF	2:NOAF		1
14	2:NOAF	2:NOAF		1

16	2:NOAF	2:NOAF		1
17	2:NOAF	2:NOAF		1
18	2:NOAF	2:NOAF		1
19	2:NOAF	2:NOAF		1
20	2:NOAF	2:NOAF		1
21	2:NOAF	2:NOAF		1
22	2:NOAF	2:NOAF		1
23	2:NOAF	1:AF	+	0.918
24	2:NOAF	2:NOAF		1
25	2:NOAF	1:AF	+	0.752
26	2:NOAF	2:NOAF		1
27	2:NOAF	2:NOAF		1
28	2:NOAF	2:NOAF		1
29	2:NOAF	2:NOAF		1
30	2:NOAF	2:NOAF		1
31	2:NOAF	2:NOAF		1
1	1:AF	1:AF		0.745
2	1:AF	1:AF		0.995
3	1:AF	1:AF		0.824
4	1:AF	1:AF		0.997
5	1:AF	1:AF		0.985
6	1:AF	1:AF		0.721
7	1:AF	1:AF		0.909
8	1:AF	1:AF		0.742
9	2:NOAF	2:NOAF		1
10	2:NOAF	2:NOAF		1
11	2:NOAF	2:NOAF		1
12	2:NOAF	2:NOAF		1
13	2:NOAF	2:NOAF		1
14	2:NOAF	2:NOAF		1
15	2:NOAF	2:NOAF		1
16	2:NOAF	2:NOAF		1
17	2:NOAF	2:NOAF		1
18	2:NOAF	2:NOAF		1
19	2:NOAF	2:NOAF		1
20	2:NOAF	2:NOAF		1
21	2:NOAF	1:AF	+	1
22	2:NOAF	2:NOAF		1
23	2:NOAF	2:NOAF		1
24	2:NOAF	2:NOAF		1
25	2:NOAF	2:NOAF		1
26	2:NOAF	2:NOAF		1
27	2:NOAF	2:NOAF		1
28	2:NOAF	2:NOAF		1
29	2:NOAF	2:NOAF		1
30	2:NOAF	2:NOAF		1
31	2:NOAF	2:NOAF		1
1	1:AF	1:AF		0.811
2	1:AF	1:AF		0.783
3	1:AF	1:AF		0.991
4	1:AF	1:AF		0.997
5	1:AF	1:AF		0.985
6	1:AF	1:AF		0.714
7	1:AF	1:AF		0.992
8	1:AF	1:AF		0.923
9	2:NOAF	2:NOAF		0.713
10	2:NOAF	2:NOAF		1
11	2:NOAF	2:NOAF		1
12	2:NOAF	2:NOAF		1
13	2:NOAF	2:NOAF		1
14	2:NOAF	2:NOAF		1
15	2:NOAF	2:NOAF		1

15	2:NOAF	2:NOAF		1
16	2:NOAF	2:NOAF		1
17	2:NOAF	2:NOAF		1
18	2:NOAF	2:NOAF		1
19	2:NOAF	2:NOAF		1
20	2:NOAF	2:NOAF		1
21	2:NOAF	2:NOAF		1
22	2:NOAF	2:NOAF		1
23	2:NOAF	2:NOAF		1
24	2:NOAF	2:NOAF		1
25	2:NOAF	2:NOAF		1
26	2:NOAF	2:NOAF		1
27	2:NOAF	2:NOAF		1
28	2:NOAF	2:NOAF		1
29	2:NOAF	2:NOAF		1
30	2:NOAF	2:NOAF		1
1	1:AF	1:AF		0.803
2	1:AF	1:AF		0.842
3	1:AF	1:AF		0.994
4	1:AF	1:AF		0.887
5	1:AF	1:AF		0.767
6	1:AF	1:AF		0.878
7	1:AF	1:AF		0.901
8	1:AF	2:NOAF	+	0.571
9	2:NOAF	2:NOAF		1
10	2:NOAF	2:NOAF		1
11	2:NOAF	2:NOAF		1
12	2:NOAF	2:NOAF		0.967
13	2:NOAF	2:NOAF		1
14	2:NOAF	2:NOAF		1
15	2:NOAF	2:NOAF		1
16	2:NOAF	2:NOAF		1
17	2:NOAF	2:NOAF		1
18	2:NOAF	2:NOAF		1
19	2:NOAF	2:NOAF		1
20	2:NOAF	2:NOAF		1
21	2:NOAF	2:NOAF		1
22	2:NOAF	2:NOAF		1
23	2:NOAF	2:NOAF		1
24	2:NOAF	2:NOAF		1
25	2:NOAF	2:NOAF		1
26	2:NOAF	2:NOAF		1
27	2:NOAF	2:NOAF		1
28	2:NOAF	2:NOAF		1
29	2:NOAF	2:NOAF		1
30	2:NOAF	2:NOAF		1
1	1:AF	1:AF		0.957
2	1:AF	1:AF		0.995
3	1:AF	1:AF		0.988
4	1:AF	1:AF		0.865
5	1:AF	1:AF		0.996
6	1:AF	1:AF		0.777
7	1:AF	1:AF		0.715
8	1:AF	1:AF		0.975
9	2:NOAF	2:NOAF		1
10	2:NOAF	2:NOAF		1
11	2:NOAF	2:NOAF		1
12	2:NOAF	2:NOAF		1
13	2:NOAF	2:NOAF		1
14	2:NOAF	2:NOAF		1
15	2:NOAF	2:NOAF		1
16	2:NOAF	2:NOAF		1

16	2:NOAF	1:AF	+	0.987
17	2:NOAF	2:NOAF		1
18	2:NOAF	2:NOAF		1
19	2:NOAF	2:NOAF		1
20	2:NOAF	2:NOAF		1
21	2:NOAF	2:NOAF		1
22	2:NOAF	2:NOAF		1
23	2:NOAF	2:NOAF		1
24	2:NOAF	2:NOAF		1
25	2:NOAF	2:NOAF		0.666
26	2:NOAF	2:NOAF		1
27	2:NOAF	1:AF	+	0.602
28	2:NOAF	2:NOAF		1
29	2:NOAF	2:NOAF		1
30	2:NOAF	2:NOAF		1
31	2:NOAF	2:NOAF		1
1	1:AF	1:AF		0.965
2	1:AF	1:AF		0.98
3	1:AF	1:AF		0.883
4	1:AF	1:AF		0.865
5	1:AF	1:AF		0.982
6	1:AF	1:AF		0.988
7	1:AF	1:AF		0.895
8	1:AF	1:AF		0.869
9	2:NOAF	2:NOAF		1
10	2:NOAF	2:NOAF		1
11	2:NOAF	2:NOAF		1
12	2:NOAF	2:NOAF		1
13	2:NOAF	2:NOAF		1
14	2:NOAF	2:NOAF		1
15	2:NOAF	2:NOAF		1
16	2:NOAF	2:NOAF		1
17	2:NOAF	2:NOAF		1
18	2:NOAF	2:NOAF		1
19	2:NOAF	2:NOAF		1
20	2:NOAF	2:NOAF		1
21	2:NOAF	2:NOAF		1
22	2:NOAF	2:NOAF		1
23	2:NOAF	2:NOAF		1
24	2:NOAF	2:NOAF		1
25	2:NOAF	2:NOAF		1
26	2:NOAF	2:NOAF		1
27	2:NOAF	2:NOAF		1
28	2:NOAF	2:NOAF		1

17	2:NOAF	2:NOAF		1
18	2:NOAF	2:NOAF		1
19	2:NOAF	2:NOAF		1
20	2:NOAF	2:NOAF		1
21	2:NOAF	2:NOAF		0.896
22	2:NOAF	2:NOAF		1
23	2:NOAF	2:NOAF		1
24	2:NOAF	2:NOAF		1
25	2:NOAF	2:NOAF		1
26	2:NOAF	2:NOAF		1
27	2:NOAF	2:NOAF		1
28	2:NOAF	2:NOAF		1
29	2:NOAF	2:NOAF		1
30	2:NOAF	2:NOAF		1
1	1:AF	1:AF		0.897
2	1:AF	1:AF		0.968
3	1:AF	1:AF		0.973
4	1:AF	1:AF		0.921
5	1:AF	1:AF		0.971
6	1:AF	1:AF		0.991
7	1:AF	1:AF		0.948
8	1:AF	1:AF		0.919
9	2:NOAF	2:NOAF		1
10	2:NOAF	2:NOAF		1
11	2:NOAF	2:NOAF		1
12	2:NOAF	2:NOAF		1
13	2:NOAF	2:NOAF		1
14	2:NOAF	2:NOAF		1
15	2:NOAF	2:NOAF		1
16	2:NOAF	2:NOAF		0.899
17	2:NOAF	2:NOAF		1
18	2:NOAF	2:NOAF		1
19	2:NOAF	2:NOAF		1
20	2:NOAF	2:NOAF		1
21	2:NOAF	2:NOAF		1
22	2:NOAF	2:NOAF		1
23	2:NOAF	2:NOAF		1
24	2:NOAF	2:NOAF		1
25	2:NOAF	2:NOAF		1
26	2:NOAF	2:NOAF		1
27	2:NOAF	2:NOAF		1
28	2:NOAF	2:NOAF		1
29	2:NOAF	2:NOAF		1
30	2:NOAF	2:NOAF		1

Table 37: Actual versus prediction values of A-Fib using logistic regression model using a 10-Fold Cross-Validation method

CHAPTER 11

11 CONCLUSION AND FUTURE WORK

11.1 Conclusion

A-Fib is a condition proven potentially dangerous and is prevalent in 2.2 million Americans. The likelihood of developing the condition increases with age. Serious arrhythmia is responsible for 500,000 deaths annually [13]. The cost to treat A-Fib in the United States exceeds $6.4 billion per year [12]. Early recognition of A-Fib is difficult because most people are not aware of this silent rhythm disturbance [50]. A-Fib is typically diagnosed or misdiagnosed during a routine screening visit or during a yearly scheduled check-up by a general practitioner or a referred cardiologist; it is possible that some patients have paroxysmal A-Fib that is not detected until it is too late. Current A-Fib telemetry devices do not deliver continuous real-time detection, require a long battery life, and necessitate patient interaction and device activation. They may become impractical when the patient is incapacitated during symptomatic periods. The focus of this dissertation is the design of a class of adaptive and efficient energy-aware models for real-time monitoring, early detection and reporting of progressive development of cardiac A-Fib. The design realizes the personalized energy-aware models by using a baseline energy model and incorporating a real-time detection algorithm for the onset of A-Fib, individual A-Fib risk factors, A-Fib incidence rates, and A-Fib prevalence circadian

windows. We recommend an A-Fib Risk factor assessment beforehand to determine a risk category and implement a monitoring and a detection schedule. Different combinations of values of incidence rate and prevalence window contribute to different energy reductions in the detection energy model. Our energy models may consume as much as telemetry when the model is continuously monitoring and transmitting EKG data, and almost as little as standby when the model operates inside two 2-hour circadian prevalence windows with an incidence rate equal to 0.02, resulting in an energy reduction by as much as 66% when compared to telemetry. We further extend the detection of A-Fib to the paroxysmal phase, and derive the total energy-aware model for the detection and reporting of A-Fib from its onset to its final stage. Studies [50] suggest if the detection algorithm is as accurate as the cardiologist's accuracy of interpreting EKG readings then having a detection positive rate equal to the incidence rate gives our energy-aware model the best energy performance. The detection positive rate plays an important role in the validity of the energy reduction scheme. The design promises to provide a greater positive public health impact from predicting A-Fib and a viable approach to meeting the energy needs of current and future real-time monitoring, detecting and reporting required in wearable computing healthcare applications that are constrained by scarce energy resources. Efficiently applying these energy models in wearable computing and monitoring devices will keep people out of overburdened hospitals and emergency rooms by continuously providing feedback of patients' physiological and vital signals to the local, on-body network, or remote server.

11.2 Future Work

This work has bridged the gap between health science and engineering by introducing energy-aware monitoring schemes and few atrial fibrillation detection algorithms. Although, this body of work concentrates on atrial fibrillation, our results suggest that future work may use machine learning and mathematical methods such as support vector machines, neural networks, and Fast Fourier to diagnose other maladies. It is hoped that further algorithm discoveries will aid the creation of open source repositories. Future work may embed a variety of healthcare monitoring and detection applications in current ubiquitous wearable devices such as smartphones, and use them as surrogate tools to provide patients and doctors with less expensive monitoring and detection alternatives. The constant progress in mobile hardware technology, wireless personal area networking, wireless security and bio-sensing technology makes the smartphone platform an ideal candidate for the areas of on-body healthcare monitoring and detection. However, further improvements to the smartphone platform are needed to balance innovative interfaces, energy management, network resources, and privacy concerns. The smartphone platform must be cost-effective to economically monitor a patient's health on a continuous basis and rival the more traditional, cumbersome and significantly more expensive, stationary monitoring system presently located in emergency rooms and hospitals. It must be able to monitor and collect biomedical data continuously over a long period and detect the health problem before the patient's condition deteriorates.

In our future work, we wish to develop accurate detection algorithms for other types of arrhythmias and extend our energy-aware models to optimize the energy consumption required to monitor and detect all arrhythmias. Early real time detection of dangerous

arrhythmias allows for earlier and less expensive medical intervention than what is provided with today's conventional clinical means.

APPENDIX

A-Fib is predicted present if probability p (A-Fib is Present | Age, Age2, Gender, BMI, QRSduration, PRinterval, Heartrate) > 0.5

Otherwise, A-Fib is absent.

Where:

logit (p) = - 41.175 + 0.820 Age – 0.006 Age2 + 4.737 Gender – 0.047 BMI +

0.098QRSduration - 0.178 PRinterval + 0.066 Heartrate

$p = 1 / (1 + e^{-\text{logit (p)}})$ for predicting the presence of A-Fib (AF)

and

$1-p = e^{-\text{logit (p)}} / (1 + e^{-\text{logit (p)}})$ for predicting the absence of A-Fib (NOAF)

Dataset used in our study:

No.	age (yrs)	ag^2 (yrs^2)	sex (M=0, F =1)	BMI (kg /m2)	QRS Dur. (ms)	PR Int. (ms)	Heart Rate (b/ min)	Actual Class (1:AF, 2:NOAF)	predicted (1:AF, 2:NOAF)	Logit(p)	prediction (AF: p, NOAF:1-p)	Err
1	25	625	1	19	97	133	93	2:NOAF	2:NOAF	-28.611	1	
2	25	625	1	30	77	141	73	2:NOAF	2:NOAF	-33.832	1	
3	26	676	1	25	71	150	70	2:NOAF	2:NOAF	-35.471	1	
4	26	676	0	15	92	0	73	2:NOAF	2:NOAF	-10.782	1	
5	27	729	1	20	82	168	70	2:NOAF	2:NOAF	-36.86	1	
6	29	841	1	22	83	164	71	2:NOAF	2:NOAF	-35.11	1	
7	29	841	0	23	81	143	78	2:NOAF	2:NOAF	-35.89	1	
8	30	900	0	25	91	180	56	2:NOAF	2:NOAF	-42.576	1	
9	30	900	0	28	87	164	68	2:NOAF	2:NOAF	-39.469	1	
10	31	961	1	21	95	161	67	2:NOAF	2:NOAF	-32.697	1	
11	31	961	1	28	82	195	76	2:NOAF	2:NOAF	-39.758	1	
12	32	1024	0	25	111	171	74	2:NOAF	2:NOAF	-36.93	1	
13	32	1024	1	24	100	145	72	2:NOAF	2:NOAF	-28.728	1	
14	32	1024	1	24	78	174	68	2:NOAF	2:NOAF	-36.31	1	
15	33	1089	1	31	80	149	87	2:NOAF	2:NOAF	-30.309	1	
16	33	1089	1	21	76	130	92	2:NOAF	2:NOAF	-26.519	1	
17	34	1156	0	25	94	186	83	2:NOAF	2:NOAF	-39.824	1	
18	34	1156	1	20	90	135	73	2:NOAF	2:NOAF	-26.826	1	
19	35	1225	1	35	82	133	55	2:NOAF	2:NOAF	-28.741	1	
20	35	1225	1	21	55	163	81	2:NOAF	2:NOAF	-34.353	1	

21	35	1225	1	26	87	142	62	2:NOAF	2:NOAF	-28.968	1	
22	36	1296	0	26	90	156	72	2:NOAF	2:NOAF	-34.849	1	
23	36	1296	0	28	96	159	85	2:NOAF	2:NOAF	-34.031	1	
24	37	1369	0	23	88	153	55	2:NOAF	2:NOAF	-35.11	1	
26	37	1369	0	24	100	137	73	2:NOAF	2:NOAF	-29.945	1	
27	38	1444	1	25	79	0	70	2:NOAF	2:NOAF	-2.755	0.953	
28	39	1521	0	26	103	147	73	2:NOAF	2:NOAF	-30.797	1	
29	39	1521	1	29	90	156	72	2:NOAF	2:NOAF	-29.143	1	
30	39	1521	1	27	87	160	80	2:NOAF	2:NOAF	-29.527	1	
31	39	1521	1	23	79	155	81	2:NOAF	2:NOAF	-29.167	1	
32	40	1600	1	20	77	129	70	2:NOAF	2:NOAF	-24.974	1	
33	40	1600	1	23	82	140	68	2:NOAF	2:NOAF	-26.715	1	
34	40	1600	0	24	93	151	68	2:NOAF	2:NOAF	-32.379	1	
35	41	1681	1	22	78	228	53	2:NOAF	2:NOAF	-43.38	1	
36	41	1681	1	32	88	157	62	2:NOAF	2:NOAF	-29.638	1	
37	42	1764	0	24	87	136	75	2:NOAF	2:NOAF	-29.179	1	
38	42	1764	1	20	82	157	66	2:NOAF	2:NOAF	-29.076	1	
39	42	1764	0	26	113	213	78	2:NOAF	2:NOAF	-40.233	1	
40	43	1849	1	29	80	162	70	2:NOAF	2:NOAF	-30.011	1	
41	43	1849	0	32	90	169	68	2:NOAF	2:NOAF	-35.287	1	
42	43	1849	0	29	100	188	80	2:NOAF	2:NOAF	-36.756	1	
43	44	1936	0	20	84	118	64	2:NOAF	2:NOAF	-26.199	1	
44	44	1936	1	24	88	146	71	2:NOAF	2:NOAF	-25.78	1	
45	44	1936	0	29	188	125	77	2:NOAF	2:NOAF	-16.818	1	
46	45	2025	1	32	77	143	72	2:NOAF	2:NOAF	-26.348	1	
47	45	2025	1	26	82	122	87	2:NOAF	2:NOAF	-20.848	1	
48	46	2116	1	38	90	155	60	2:NOAF	2:NOAF	-28.01	1	
49	46	2116	0	27	91	156	72	2:NOAF	2:NOAF	-31.518	1	
50	46	2116	1	28	84	173	69	2:NOAF	2:NOAF	-30.738	1	
51	47	2209	1	21	75	132	76	2:NOAF	2:NOAF	-23.269	1	
52	47	2209	1	21	92	187	77	2:NOAF	2:NOAF	-31.327	1	
53	47	2209	0	31	108	173	86	2:NOAF	2:NOAF	-31.88	1	
54	47	2209	0	20	79	145	49	2:NOAF	2:NOAF	-31.663	1	
55	47	2209	1	33	78	0	117	1:AF	1:AF	2.663	0.905	
56	48	2304	1	23	81	0	67	2:NOAF	2:NOAF	0.377	0.507	
57	48	2304	1	26	83	146	61	2:NOAF	2:NOAF	-25.952	1	
58	48	2304	1	25	85	176	74	2:NOAF	2:NOAF	-30.191	1	
59	48	2304	0	39	85	177	72	2:NOAF	2:NOAF	-35.896	1	
60	48	2304	0	25	91	224	102	2:NOAF	2:NOAF	-41.036	1	
61	48	2304	0	23	77	196	89	2:NOAF	2:NOAF	-38.188	1	
62	48	2304	1	34	81	0	81	1:AF	1:AF	0.784	0.592	
63	49	2401	1	21	78	0	67	2:NOAF	2:NOAF	0.415	0.502	
64	49	2401	0	26	95	157	60	2:NOAF	2:NOAF	-31.299	1	
65	49	2401	1	22	73	132	71	2:NOAF	2:NOAF	-23.354	1	
66	49	2401	1	23	94	170	72	2:NOAF	2:NOAF	-28.041	1	
67	49	2401	1	32	78	0	115	1:AF	1:AF	3.066	0.933	
68	49	2401	1	32	77	0	116	1:AF	1:AF	3.034	0.931	
69	50	2500	1	24	89	130	63	2:NOAF	2:NOAF	-21.826	1	
70	50	2500	1	29	75	125	93	2:NOAF	2:NOAF	-20.563	1	
71	50	2500	0	27	103	142	70	2:NOAF	2:NOAF	-27.006	1	
72	50	2500	0	28	94	160	68	2:NOAF	2:NOAF	-31.271	1	
73	50	2500	1	30	81	105	87	2:NOAF	2:NOAF	-16.858	1	
74	50	2500	1	41	85	151	73	2:NOAF	2:NOAF	-26.095	1	
75	50	2500	1	22	84	145	76	2:NOAF	2:NOAF	-24.034	1	
76	50	2500	1	24	75	151	68	2:NOAF	2:NOAF	-26.606	1	
77	50	2500	1	32	80	0	119	1:AF	1:AF	3.752	0.964	
78	51	2601	1	32	96	147	71	2:NOAF	2:NOAF	-23.8	1	
79	51	2601	0	28	100	145	81	2:NOAF	2:NOAF	-26.941	1	
80	51	2601	0	27	94	203	71	2:NOAF	2:NOAF	-38.466	1	
81	51	2601	1	30	79	0	118	1:AF	1:AF	3.896	0.968	
82	51	2601	1	32	81	0	81	1:AF	1:AF	1.556	0.749	

83	52	2704	1	29	78	137	69	2:NOAF	2:NOAF	-23.573	1	
84	52	2704	0	29	88	202	59	2:NOAF	2:NOAF	-39.56	1	
85	52	2704	1	43	84	217	68	2:NOAF	2:NOAF	-37.949	1	
86	52	2704	1	43	84	188	66	2:NOAF	2:NOAF	-32.919	1	
87	52	2704	1	23	67	153	98	2:NOAF	2:NOAF	-25.303	1	
88	52	2704	0	27	92	152	74	2:NOAF	2:NOAF	-29.184	1	
89	52	2704	1	32	78	0	120	1:AF	1:AF	4.038	0.972	
90	52	2704	1	32	82	0	82	1:AF	1:AF	1.922	0.809	
91	53	2809	0	28	85	157	51	2:NOAF	2:NOAF	-32.135	1	
92	53	2809	1	29	86	141	117	2:NOAF	2:NOAF	-20.143	1	
93	53	2809	1	23	86	133	80	2:NOAF	2:NOAF	-20.879	1	
94	53	2809	1	27	80	199	63	2:NOAF	2:NOAF	-34.525	1	
95	53	2809	1	31	89	0	117	1:AF	1:AF	5.155	0.99	
96	53	2809	1	31	81	0	124	1:AF	1:AF	4.833	0.987	
97	53	2809	1	31	81	0	81	1:AF	1:AF	1.995	0.817	
98	53	2809	1	31	82	0	82	1:AF	1:AF	2.159	0.84	
99	54	2916	0	32	138	163	75	2:NOAF	2:NOAF	-26.435	1	
100	54	2916	1	20	78	155	73	2:NOAF	2:NOAF	-25.722	1	
101	54	2916	1	25	82	158	54	2:NOAF	2:NOAF	-27.353	1	
102	54	2916	0	27	113	216	61	2:NOAF	2:NOAF	-39.008	1	
103	54	2916	1	26	70	182	78	2:NOAF	2:NOAF	-31.264	1	
104	54	2916	1	32	87	0	70	1:AF	1:AF	1.988	0.814	
105	54	2916	1	28	88	0	73	1:AF	1:AF	2.472	0.876	
106	55	3025	0	31	100	202	71	2:NOAF	2:NOAF	-37.152	1	
107	55	3025	0	31	87	292	64	2:NOAF	2:NOAF	-54.908	1	
108	55	3025	1	32	88	0	71	2:NOAF	1:AF	2.318	0.856	+
109	55	3025	0	25	132	184	53	2:NOAF	2:NOAF	-31.718	1	
110	55	3025	0	25	85	198	79	2:NOAF	2:NOAF	-37.1	1	
111	55	3025	1	27	93	155	67	2:NOAF	2:NOAF	-24.811	1	
112	55	3025	1	32	88	0	71	1:AF	1:AF	2.318	0.856	
113	55	3025	1	31	82	0	82	1:AF	1:AF	2.503	0.877	
114	56	3136	1	24	81	174	53	2:NOAF	2:NOAF	-29.998	1	
115	56	3136	1	24	90	164	79	2:NOAF	2:NOAF	-25.62	1	
116	56	3136	1	27	90	147	65	2:NOAF	2:NOAF	-23.659	1	
117	56	3136	0	28	81	162	79	2:NOAF	2:NOAF	-31.071	1	
118	56	3136	0	28	83	183	72	2:NOAF	2:NOAF	-35.075	1	
119	56	3136	1	32	87	0	70	1:AF	1:AF	2.308	0.853	
120	56	3136	1	32	90	0	72	1:AF	1:AF	2.734	0.899	
121	56	3136	1	33	92	0	92	1:AF	1:AF	4.203	0.975	
122	56	3136	1	30	91	0	91	1:AF	1:AF	4.18	0.974	
123	56	3136	1	31	80	0	80	1:AF	1:AF	2.329	0.855	
124	57	3249	1	26	82	181	66	2:NOAF	2:NOAF	-30.24	1	
125	57	3249	1	22	75	157	69	2:NOAF	2:NOAF	-26.268	1	
126	57	3249	0	27	82	205	107	2:NOAF	2:NOAF	-36.59	1	
127	57	3249	0	25	93	157	77	2:NOAF	2:NOAF	-28.854	1	
128	57	3249	1	32	90	0	73	1:AF	1:AF	2.942	0.914	
129	57	3249	1	32	90	0	90	1:AF	1:AF	4.064	0.97	
130	58	3364	1	26	71	136	81	2:NOAF	2:NOAF	-22.188	1	
131	58	3364	1	26	90	157	70	2:NOAF	2:NOAF	-24.79	1	
132	58	3364	0	5	87	166	70	2:NOAF	2:NOAF	-30.436	1	
133	58	3364	1	25	97	128	74	2:NOAF	2:NOAF	-18.631	1	
134	58	3364	0	25	95	145	76	2:NOAF	2:NOAF	-26.458	1	
135	58	3364	1	24	98	158	72	2:NOAF	2:NOAF	-23.958	1	
136	58	3364	1	30	85	140	71	2:NOAF	2:NOAF	-22.376	1	
137	58	3364	1	35	82	0	104	2:NOAF	1:AF	4.193	0.973	+
138	58	3364	0	25	133	148	70	2:NOAF	2:NOAF	-23.664	1	
139	58	3364	1	35	82	0	104	1:AF	1:AF	4.193	0.973	
140	58	3364	1	32	88	0	74	1:AF	1:AF	2.942	0.913	
141	58	3364	1	28	90	0	76	1:AF	1:AF	3.458	0.946	
142	58	3364	1	33	91	0	91	1:AF	1:AF	4.311	0.976	
143	58	3364	1	27	91	0	91	1:AF	1:AF	4.593	0.982	

144	58	3364	1	33	92	0	92	1:AF	1:AF	4.475	0.98	
145	59	3481	0	27	83	194	69	2:NOAF	2:NOAF	-36.794	1	
146	59	3481	0	27	108	180	60	2:NOAF	2:NOAF	-32.446	1	
147	59	3481	1	28	97	149	72	2:NOAF	2:NOAF	-22.524	1	
148	59	3481	0	24	121	0	75	2:NOAF	1:AF	1.999	0.801	+
149	59	3481	1	36	84	152	66	2:NOAF	2:NOAF	-25.104	1	
150	59	3481	1	30	83	209	75	2:NOAF	2:NOAF	-34.472	1	
151	59	3481	0	27	92	158	65	2:NOAF	2:NOAF	-29.768	1	
152	59	3481	0	20	92	128	75	2:NOAF	2:NOAF	-23.439	1	
153	59	3481	0	24	83	164	63	2:NOAF	2:NOAF	-31.709	1	
154	59	3481	0	24	121	0	75	1:AF	1:AF	1.999	0.801	
155	59	3481	1	35	83	0	105	1:AF	1:AF	4.475	0.979	
156	59	3481	1	33	83	0	107	1:AF	1:AF	4.701	0.983	
157	59	3481	1	36	86	0	86	1:AF	1:AF	3.468	0.945	
158	59	3481	1	31	91	0	91	1:AF	1:AF	4.523	0.98	
159	60	3600	1	32	93	121	80	2:NOAF	2:NOAF	-17.486	1	
160	60	3600	1	24	81	191	84	2:NOAF	2:NOAF	-30.482	1	
161	60	3600	1	27	80	144	98	2:NOAF	2:NOAF	-21.431	1	
162	60	3600	1	30	91	137	76	2:NOAF	2:NOAF	-20.7	1	
163	60	3600	0	24	120	0	74	1:AF	1:AF	1.941	0.788	
164	60	3600	1	36	84	0	105	1:AF	1:AF	4.632	0.982	
165	60	3600	1	32	90	0	90	1:AF	1:AF	4.418	0.978	
166	61	3721	0	28	95	197	80	2:NOAF	2:NOAF	-35.273	1	
167	61	3721	0	27	84	178	84	2:NOAF	2:NOAF	-32.658	1	
168	61	3721	0	24	90	174	53	2:NOAF	2:NOAF	-33.263	1	
169	61	3721	1	27	83	158	73	2:NOAF	2:NOAF	-25.185	1	
170	61	3721	1	32	147	147	56	2:NOAF	2:NOAF	-18.312	1	
171	61	3721	0	25	122	0	77	1:AF	1:AF	2.382	0.849	
172	61	3721	0	23	121	0	76	1:AF	1:AF	2.312	0.84	
173	61	3721	0	25	124	0	124	1:AF	1:AF	5.68	0.993	
174	61	3721	1	36	87	0	87	1:AF	1:AF	3.832	0.96	
175	62	3844	0	25	102	135	70	2:NOAF	2:NOAF	-23.988	1	
176	62	3844	1	23	80	185	75	2:NOAF	2:NOAF	-29.883	1	
177	62	3844	1	26	72	169	103	2:NOAF	2:NOAF	-26.112	1	
178	62	3844	0	29	110	157	66	2:NOAF	2:NOAF	-27.572	1	
179	62	3844	0	24	146	138	64	2:NOAF	2:NOAF	-20.559	1	
180	62	3844	1	32	90	172	89	2:NOAF	2:NOAF	-26.088	1	
181	62	3844	1	38	97	0	100	2:NOAF	1:AF	5.658	0.993	+
182	62	3844	0	28	95	181	70	2:NOAF	2:NOAF	-33.003	1	
183	62	3844	1	26	81	174	87	2:NOAF	2:NOAF	-27.176	1	
184	62	3844	1	26	73	177	77	2:NOAF	2:NOAF	-29.154	1	
185	62	3844	0	24	121	0	78	1:AF	1:AF	2.479	0.859	
186	62	3844	1	34	83	0	106	1:AF	1:AF	4.87	0.985	
187	62	3844	0	24	121	0	76	1:AF	1:AF	2.347	0.842	
188	62	3844	1	35	87	0	107	1:AF	1:AF	5.281	0.99	
189	62	3844	1	27	91	0	91	1:AF	1:AF	4.993	0.987	
190	63	3969	0	31	83	180	50	2:NOAF	2:NOAF	-35.392	1	
191	63	3969	1	23	79	160	75	2:NOAF	2:NOAF	-25.461	1	
192	63	3969	0	26	97	147	89	2:NOAF	2:NOAF	-25.337	1	
193	63	3969	1	29	85	165	64	2:NOAF	2:NOAF	-26.771	1	
194	63	3969	0	26	91	151	59	2:NOAF	2:NOAF	-28.617	1	
195	63	3969	1	25	79	141	63	2:NOAF	2:NOAF	-22.965	1	
196	63	3969	1	20	78	140	65	2:NOAF	2:NOAF	-22.518	1	
197	63	3969	1	24	94	175	59	2:NOAF	2:NOAF	-27.764	1	
198	63	3969	1	34	85	0	109	1:AF	1:AF	5.334	0.99	
199	63	3969	0	25	125	0	81	1:AF	1:AF	3.092	0.917	
200	63	3969	0	24	125	0	125	1:AF	1:AF	6.043	0.995	
201	63	3969	0	25	125	0	125	1:AF	1:AF	5.996	0.995	
202	63	3969	1	36	87	0	87	1:AF	1:AF	3.984	0.964	
203	63	3969	1	33	86	0	86	1:AF	1:AF	3.961	0.963	
204	63	3969	1	35	85	0	85	1:AF	1:AF	3.703	0.952	

205	63	3969	0	25	123	0	123	1:AF	1:AF	5.668	0.993	
206	64	4096	1	34	87	171	65	2:NOAF	2:NOAF	-27.754	1	
207	64	4096	1	37	82	194	85	2:NOAF	2:NOAF	-31.159	1	
208	64	4096	1	26	78	162	78	2:NOAF	2:NOAF	-25.8	1	
209	64	4096	1	31	62	160	68	2:NOAF	2:NOAF	-27.907	1	
210	64	4096	1	30	84	163	78	2:NOAF	2:NOAF	-25.578	1	
211	64	4096	0	26	85	154	70	2:NOAF	2:NOAF	-28.955	1	
212	64	4096	1	31	80	157	62	2:NOAF	2:NOAF	-26.005	1	
213	64	4096	0	21	74	0	63	2:NOAF	2:NOAF	-2.848	0.973	
214	64	4096	0	24	94	162	81	2:NOAF	2:NOAF	-28.677	1	
215	64	4096	0	23	87	131	61	2:NOAF	2:NOAF	-25.118	1	
216	64	4096	0	25	83	0	65	2:NOAF	2:NOAF	-2.022	0.94	
217	64	4096	1	23	74	0	80	1:AF	1:AF	2.917	0.899	
218	64	4096	0	23	124	0	124	1:AF	1:AF	5.984	0.995	
219	65	4225	1	28	68	200	82	2:NOAF	2:NOAF	-33.328	1	
220	65	4225	0	24	87	137	63	2:NOAF	2:NOAF	-26.055	1	
221	65	4225	0	21	85	161	78	2:NOAF	2:NOAF	-29.392	1	
222	65	4225	0	29	100	139	63	2:NOAF	2:NOAF	-25.372	1	
223	65	4225	0	22	98	199	102	2:NOAF	2:NOAF	-33.345	1	
224	65	4225	1	20	85	143	68	2:NOAF	2:NOAF	-22.064	1	
225	65	4225	1	23	74	0	82	1:AF	1:AF	3.095	0.912	
226	65	4225	0	26	122	0	78	1:AF	1:AF	2.657	0.872	
227	65	4225	1	34	87	0	87	1:AF	1:AF	4.182	0.969	
228	65	4225	0	25	126	0	126	1:AF	1:AF	6.264	0.996	
229	65	4225	1	34	88	0	88	1:AF	1:AF	4.346	0.973	
230	66	4356	0	25	87	157	57	2:NOAF	2:NOAF	-30.024	1	
231	66	4356	1	33	153	156	64	2:NOAF	2:NOAF	-18.555	1	
232	66	4356	1	23	73	0	81	2:NOAF	1:AF	2.965	0.899	+
233	66	4356	1	48	99	154	94	2:NOAF	2:NOAF	-22.216	1	
234	66	4356	0	29	86	164	88	2:NOAF	2:NOAF	-29.51	1	
235	66	4356	1	21	72	164	71	2:NOAF	2:NOAF	-26.891	1	
236	66	4356	1	26	80	188	59	2:NOAF	2:NOAF	-31.406	1	
237	66	4356	1	27	76	160	66	2:NOAF	2:NOAF	-26.399	1	
238	66	4356	1	23	73	0	81	1:AF	1:AF	2.965	0.899	
239	66	4356	1	23	77	0	77	1:AF	1:AF	3.093	0.911	
240	66	4356	0	24	123	0	123	1:AF	1:AF	5.853	0.994	
241	67	4489	0	23	90	184	81	2:NOAF	2:NOAF	-32.836	1	
242	67	4489	0	26	97	144	93	2:NOAF	2:NOAF	-24.379	1	
243	67	4489	0	23	109	175	63	2:NOAF	2:NOAF	-30.56	1	
244	67	4489	0	29	106	173	69	2:NOAF	2:NOAF	-30.384	1	
245	67	4489	1	27	87	158	61	2:NOAF	2:NOAF	-25.273	1	
246	67	4489	1	19	78	180	81	2:NOAF	2:NOAF	-28.375	1	
247	67	4489	1	24	72	0	80	1:AF	1:AF	2.776	0.879	
248	67	4489	1	26	90	0	84	1:AF	1:AF	4.71	0.98	
249	67	4489	1	33	88	0	111	1:AF	1:AF	5.967	0.994	
250	67	4489	1	24	77	0	77	1:AF	1:AF	3.068	0.907	
251	68	4624	0	27	170	192	63	2:NOAF	2:NOAF	-27.786	1	
252	68	4624	1	21	78	159	86	2:NOAF	2:NOAF	-24.391	1	
253	68	4624	0	20	79	170	69	2:NOAF	2:NOAF	-32.063	1	
254	68	4624	1	29	146	200	61	2:NOAF	2:NOAF	-27.051	1	
255	68	4624	1	25	76	0	84	1:AF	1:AF	3.395	0.929	
256	68	4624	1	23	77	0	77	1:AF	1:AF	3.125	0.909	
257	68	4624	0	25	123	0	123	1:AF	1:AF	5.838	0.993	
258	69	4761	0	24	82	145	80	2:NOAF	2:NOAF	-26.783	1	
259	69	4761	1	28	75	156	98	2:NOAF	2:NOAF	-23.69	1	
260	69	4761	1	25	74	159	81	2:NOAF	2:NOAF	-25.303	1	
261	69	4761	0	23	123	193	50	2:NOAF	2:NOAF	-33.242	1	
262	69	4761	1	25	77	0	84	1:AF	1:AF	3.491	0.934	
263	69	4761	1	25	77	0	77	1:AF	1:AF	3.029	0.899	
264	70	4900	1	35	76	187	89	2:NOAF	2:NOAF	-30.047	1	
265	70	4900	0	26	105	178	93	2:NOAF	2:NOAF	-29.653	1	

266	70	4900	1	33	76	165	88	2:NOAF	2:NOAF	-26.103	1	
267	70	4900	0	25	93	118	92	2:NOAF	2:NOAF	-20.168	1	
268	70	4900	0	22	80	149	120	2:NOAF	2:NOAF	-24.971	1	
269	70	4900	1	26	74	0	82	1:AF	1:AF	3.004	0.894	
270	70	4900	1	24	76	0	76	1:AF	1:AF	2.898	0.884	
271	71	5041	1	23	78	195	98	2:NOAF	2:NOAF	-30.143	1	
272	71	5041	1	27	82	294	68	2:NOAF	2:NOAF	-49.541	1	
273	71	5041	0	18	71	158	92	2:NOAF	2:NOAF	-29.141	1	
274	71	5041	1	30	82	182	83	2:NOAF	2:NOAF	-28.756	1	
275	71	5041	1	25	79	0	79	1:AF	1:AF	3.317	0.919	
276	71	5041	1	25	91	0	91	1:AF	1:AF	5.285	0.988	
277	71	5041	1	32	89	0	89	1:AF	1:AF	4.628	0.977	
278	72	5184	1	27	77	142	57	2:NOAF	2:NOAF	-23.739	1	
279	72	5184	0	26	90	180	71	2:NOAF	2:NOAF	-32.995	1	
280	72	5184	0	25	77	172	84	2:NOAF	2:NOAF	-31.94	1	
281	72	5184	1	25	93	177	61	2:NOAF	2:NOAF	-28.043	1	
282	72	5184	1	27	79	152	68	2:NOAF	2:NOAF	-24.597	1	
283	72	5184	0	24	85	168	58	2:NOAF	2:NOAF	-32.113	1	
284	72	5184	1	23	82	140	63	2:NOAF	2:NOAF	-22.309	1	
285	73	5329	0	23	91	154	66	2:NOAF	2:NOAF	-28.508	1	
286	73	5329	1	29	137	164	80	2:NOAF	2:NOAF	-20.401	1	
287	73	5329	1	31	82	136	103	2:NOAF	2:NOAF	-19.383	1	
288	73	5329	0	21	104	0	64	2:NOAF	2:NOAF	0.14	0.689	
289	73	5329	1	25	76	0	76	1:AF	1:AF	2.737	0.857	
290	74	5476	0	25	106	165	61	2:NOAF	2:NOAF	-29.482	1	
291	74	5476	0	23	84	175	44	2:NOAF	2:NOAF	-34.446	1	
292	75	5625	1	23	73	159	89	2:NOAF	2:NOAF	-25.043	1	
293	75	5625	1	22	81	180	65	2:NOAF	2:NOAF	-29.534	1	
294	75	5625	1	23	163	147	72	2:NOAF	2:NOAF	-15.209	1	
295	75	5625	1	28	82	176	77	2:NOAF	2:NOAF	-28.214	1	
296	76	5776	1	24	71	186	63	2:NOAF	2:NOAF	-31.894	1	
297	77	5929	0	28	98	0	59	2:NOAF	2:NOAF	-1.427	0.922	
298	78	6084	0	20	97	121	75	2:NOAF	2:NOAF	-21.741	1	
299	78	6084	1	27	79	127	75	2:NOAF	2:NOAF	-20.165	1	
300	79	6241	1	27	93	178	74	2:NOAF	2:NOAF	-28.059	1	
301	80	6400	0	28	93	183	80	2:NOAF	2:NOAF	-33.471	1	
302	80	6400	0	27	90	201	67	2:NOAF	2:NOAF	-37.78	1	
303	81	6561	1	22	86	191	76	2:NOAF	2:NOAF	-30.972	1	
304	83	6889	1	21	84	186	84	2:NOAF	2:NOAF	-30.031	1	

Table 38: Dataset containing 80 A-Fib episodes and 204 Non A-Fib cases

Raw results from WEKA tool:

Scheme: weka.classifiers.functions.Logistic -R 1.0E-8 -M -1
Relation: arrhythmia

Instances: 304

Attributes: 8

age

ageage

sex

BMI

QRSduration
PRinterval
heartrate
class
Test mode: 10-fold cross-validation

=== Classifier model (full training set) ===

Logistic Regression with ridge parameter of 1.0E-8
Coefficients...

Variable	Class AF
age	0.8203
ageage	-0.0062
sex	4.7368
BMI	-0.0471
QRSduration	0.0982
PRinterval	-0.1776
heartrate	0.0657
Intercept	-41.1751

Odds Ratios...

Variable	Class AF
age	2.2712
ageage	0.9938
sex	114.0704
BMI	0.954
QRSduration	1.1032
PRinterval	0.8372

heartrate 1.0679

=== Stratified cross-validation ===

=== Summary ===

Correctly Classified Instances	296	97.3684 %
Incorrectly Classified Instances	8	2.6316 %
Kappa statistic	0.9337	
Mean absolute error	0.046	
Root mean squared error	0.1521	
Relative absolute error	11.8332 %	
Root relative squared error	34.543 %	
Total Number of Instances	304	

=== Detailed Accuracy By Class ===

TP Rate	FP Rate	Precision	Recall	F-Measure	ROC Area	Class
0.988	0.031	0.919	0.988	0.952	0.986	AF
0.969	0.013	0.995	0.969	0.982	0.986	NOAF
0.974	0.017	0.975	0.974	0.974	0.986	Weight. Ave.

=== Confusion Matrix ===

a	b	<-- classified as
79	1	a = AF
7	217	b = NOAF

BMI calculations:

Since the Body Mass Index (BMI) depends on weight and height, we use only BMI in the model in order to avoid collinearity.

$$BMI = \frac{Weight\ (kg)}{Height^2 (m^2)}$$

No.	Height (m)	Weight (kg)	BMI Kg/m2	No.	Height (m)	Weight (kg)	BMI Kg/m2	No.	Height (m)	Weight (kg)	BMI Kg/m2
1	1.7	55	19	102	1.7	78	27	203	1.68	93	33
2	1.61	78	30	103	1.61	67	26	204	1.61	91	35
3	1.61	65	25	104	1.55	77	32	205	1.67	70	25
4	1.69	43	15	105	1.68	79	28	206	1.55	82	34
5	1.63	53	20	106	1.74	94	31	207	1.54	88	37
6	1.61	57	22	107	1.84	105	31	208	1.61	67	26
7	1.66	63	23	108	1.56	78	32	209	1.61	80	31
8	1.71	73	25	109	1.73	75	25	210	1.56	73	30
9	1.66	77	28	110	1.7	72	25	211	1.66	72	26
10	1.6	54	21	111	1.61	70	27	212	1.57	76	31
11	1.51	64	28	112	1.56	78	32	213	1.73	63	21
12	1.73	75	25	113	1.71	91	31	214	1.71	70	24
13	1.65	65	24	114	1.63	64	24	215	1.62	60	23
14	1.55	58	24	115	1.65	65	24	216	1.59	63	25
15	1.66	85	31	116	1.64	73	27	217	1.63	61	23
16	1.66	58	21	117	1.69	80	28	218	1.71	67	23
17	1.71	73	25	118	1.71	82	28	219	1.56	68	28
18	1.5	45	20	119	1.57	79	32	220	1.81	79	24
19	1.65	95	35	120	1.56	78	32	221	1.76	65	21
20	1.59	53	21	121	1.58	82	33	222	1.71	85	29
21	1.56	63	26	122	1.71	88	30	223	1.73	66	22
22	1.71	76	26	123	1.72	92	31	224	1.58	50	20
23	1.84	95	28	124	1.66	72	26	225	1.62	60	23
24	1.77	72	23	125	1.64	59	22	226	1.69	74	26
25	1.58	50	20	126	1.66	74	27	227	1.64	92	34
26	1.88	85	24	127	1.72	74	25	228	1.66	69	25
27	1.59	63	25	128	1.58	80	32	229	1.61	88	34
28	1.71	76	26	129	1.58	80	32	230	1.67	70	25
29	1.6	74	29	130	1.62	68	26	231	1.56	80	33
30	1.61	70	27	131	1.7	75	26	232	1.62	60	23
31	1.64	62	23	132	1.9	18	5	233	1.61	124	48
32	1.61	52	20	133	1.55	60	25	234	1.68	82	29
33	1.55	55	23	134	1.77	78	25	235	1.59	53	21

34	1.68	68	24	135	1.61	62	24	236	1.54	62	26
35	1.58	55	22	136	1.47	65	30	237	1.61	70	27
36	1.53	75	32	137	1.6	90	35	238	1.62	60	23
37	1.77	75	24	138	1.61	65	25	239	1.66	63	23
38	1.64	54	20	139	1.6	90	35	240	1.7	69	24
39	1.87	91	26	140	1.58	80	32	241	1.71	67	23
40	1.56	71	29	141	1.7	81	28	242	1.75	80	26
41	1.63	85	32	142	1.59	83	33	243	1.68	65	23
42	1.66	80	29	143	1.74	82	27	244	1.64	78	29
43	1.67	56	20	144	1.58	82	33	245	1.59	68	27
44	1.58	60	24	145	1.61	70	27	246	1.67	53	19
45	1.7	84	29	146	1.59	68	27	247	1.59	61	24
46	1.64	86	32	147	1.6	72	28	248	1.62	68	26
47	1.58	65	26	148	1.65	65	24	249	1.65	90	33
48	1.62	100	38	149	1.62	94	36	250	1.63	64	24
49	1.78	86	27	150	1.55	72	30	251	1.61	70	27
50	1.66	77	28	151	1.66	74	27	252	1.68	59	21
51	1.51	48	21	152	1.61	52	20	253	1.63	53	20
52	1.62	55	21	153	1.76	74	24	254	1.46	62	29
53	1.74	94	31	154	1.65	65	24	255	1.62	66	25
54	1.67	56	20	155	1.61	91	35	256	1.67	64	23
55	1.63	88	33	156	1.65	90	33	257	1.73	75	25
56	1.55	55	23	157	1.62	94	36	258	1.77	75	24
57	1.64	70	26	158	1.6	79	31	259	1.59	71	28
58	1.57	62	25	159	1.61	83	32	260	1.54	59	25
59	1.56	95	39	160	1.59	61	24	261	1.62	60	23
60	1.79	80	25	161	1.55	65	27	262	1.61	65	25
61	1.83	77	23	162	1.58	75	30	263	1.64	67	25
62	1.64	91	34	163	1.66	66	24	264	1.6	90	35
63	1.6	54	21	164	1.57	89	36	265	1.64	70	26
64	1.68	73	26	165	1.6	82	32	266	1.6	84	33
65	1.68	62	22	166	1.84	95	28	267	1.79	80	25
66	1.69	66	23	167	1.7	78	27	268	1.65	60	22
67	1.65	87	32	168	1.71	70	24	269	1.61	67	26
68	1.66	88	32	169	1.53	63	27	270	1.65	65	24
69	1.67	67	24	170	1.55	77	32	271	1.56	56	23

70	1.59	73	29	171	1.62	66	25	272	1.63	72	27
71	1.72	80	27	172	1.67	64	23	273	1.7	52	18
72	1.85	96	28	173	1.67	70	25	274	1.65	82	30
73	1.73	90	30	174	1.62	95	36	275	1.64	67	25
74	1.61	106	41	175	1.7	72	25	276	1.66	69	25
75	1.62	58	22	176	1.62	60	23	277	1.69	91	32
76	1.65	65	24	177	1.64	70	26	278	1.61	70	27
77	1.64	86	32	178	1.71	85	29	279	1.69	74	26
78	1.61	83	32	179	1.74	73	24	280	1.72	74	25
79	1.65	76	28	180	1.56	78	32	281	1.65	68	25
80	1.88	95	27	181	1.7	110	38	282	1.61	70	27
81	1.7	87	30	182	1.78	89	28	283	1.63	64	24
82	1.65	87	32	183	1.58	65	26	284	1.55	55	23
83	1.55	70	29	184	1.64	70	26	285	1.66	63	23
84	1.66	80	29	185	1.67	67	24	286	1.58	72	29
85	1.56	104	43	186	1.62	89	34	287	1.61	80	31
86	1.56	104	43	187	1.68	68	24	288	1.66	58	21
87	1.55	55	23	188	1.58	87	35	289	1.66	69	25
88	1.74	82	27	189	1.74	82	27	290	1.72	74	25
89	1.68	90	32	190	1.61	80	31	291	1.71	67	23
90	1.69	91	32	191	1.64	62	23	292	1.55	55	23
91	1.74	85	28	192	1.75	80	26	293	1.55	53	22
92	1.55	70	29	193	1.55	70	29	294	1.6	59	23
93	1.62	60	23	194	1.74	79	26	295	1.63	74	28
94	1.61	70	27	195	1.59	63	25	296	1.5	54	24
95	1.67	86	31	196	1.64	54	20	297	1.66	77	28
96	1.7	90	31	197	1.68	68	24	298	1.52	46	20
97	1.72	92	31	198	1.63	90	34	299	1.61	70	27
98	1.7	90	31	199	1.65	68	25	300	1.49	60	27
99	1.72	95	32	200	1.7	69	24	301	1.74	85	28
100	1.7	58	20	201	1.66	69	25	302	1.61	70	27
101	1.59	63	25	202	1.6	92	36	303	1.65	60	22
								304	1.62	55	21

Table 39: BMI calculations

BIBLIOGRAPHY

[1] K. Patel, C.-P. Chua, S. Fau and C.J. Bleakley. Low power real-time seizure detection for ambulatory EEG. Complex & Adaptive Syst. Lab., Univ. Coll. Dublin, Dublin, Ireland, *Pervasive Computing Technologies for Healthcare*, 2009. Pervasive Health '09. 3rd International Conference

[2] A.Y. Benbasat and J. Paradiso. A Framework for the Automated Generation of Power-Efficient Classifiers for Embedded Sensor Nodes. In *SenSys.* 2007, pp. 219–232

[3] J. Flinn and M. Satyanarayanan. Energy-Aware Adaptation for Mobile Applications. In *SOSP 1999.* Oct. 1999, pp. 48–63

[4] Y.-T. Peng and D. Sow. Data Scaling in Remote Health Monitoring Systems; In *IEEE International Symposium on Circuits and System.* (To appear) 2008

[5] P. Aghera, D. Krishnaswamy, D. Fang, A. Coskun and T. Rosing. DynAHeal. Dynamic Energy Efficient Task Assignment for Wireless Healthcare Systems. In *Proc*. 2010, pp.1661–64

[6] R.B. Schnabel, M.D. et al. Development of a Risk Score for Atrial Fibrillation (Framingham Heart Study): A Community-based Cohort Study. *The Lancet.*, Vol. 373, Issue 9665, Feb. 28, 2009, pp. 739–745

[7] I. Khalil and F. Sufi. Mobile Device Assisted Remote Heart Monitoring and Tachycardia Prediction. *Information Technology and Applications in Biomedicine*. ITAB 2008

[8] F. Bogun, D. Anh, G. Kalahasty, et al. Misdiagnosis of Atrial Fibrillation and its Clinical Consequences. *Am J Med*., 2004

[9] Z. Sankari and H. Adeli. HeartSaver: A mobile cardiac monitoring system for auto-detection of atrial fibrillation, myocardial infarction, and atrio-ventricular block. *Computers in Biology and Medicine.* Vol. 41, Issue 4, April 2011, pp. 211–220

[10] T. Soman and P.O. Bobbie. Classification of Arrhythmia Using Machine Learning Techniques. *WSEAS Transactions on Computers*. Vol.4, Issue 6, June 2005, pp. 548–552

[11] M.V. Perez, F.E. Dewey, R. Marcus, E.A. Ashley, A.A. Al-Ahmad and P.J. Wang. Electrocardiographic predictors of atrial fibrillation. *American Heart Journal*. ISSN 0002-8703, Vol. 158, Issue 4, 2009, pp. 622–28

[12] K.S. Coyne, C. Paramore, S. Grandy, M. Mercader, M. Reynolds and P. Zimetbaum. Assessing the Direct Costs of Treating Nonvalvular Atrial Fibrillation in the United States. *Value Health*. Sept.-Oct. 2006, Vol. 9, Issue 5, pp. 348–56

[13] Arrhythmia Health Center. Available at: < http://www.OmniMedicalSearch.com>, retrieved Oct. 2, 2011

[14] G.C. Fonarow. Heart Failure Society of America, *Proceedings of the Heart Failure Society of America*. 5th Annual Meeting, Washington, DC. 2001, Vol.1

[15] National cost impact report to accompany 'Atrial fibrillation: the management of atrial fibrillation'. *National Institute for Health and Clinical Excellence*. NICE Clinical Guideline No. 36, July 2006

[16] E.Q. Wu, H.G. Birnbaum, M. Mareva, E. Tuttle, A. R. Castor, W. Jackman and J. Ruskin. Economic Burden and Co-Morbidities of Atrial Fibrillation in a Privately Insured Population. Nov. 2005. *Curr Med Res Opin.* 2005, Vol. 21, Issue 10, pp.1693–1699. Available at: <http://www.medscape.com/viewarticle/515523_3>

[17] D. Dubin. *Dr. Dubin's Rapid Interpretation of EKG*, Cover Pub. Co., 1996, 342 pp. ISBN 0912912022

[18] ECG etc/Lesson III - Characteristics of the Normal ECG.htm. Available at: <http://rpw.chem.ox.ac.uk/ECG etc/Lesson III Characteristics of the Normal ECG.htm>

[19] Conditions & Diseases: Cardiovascular System: Arrhythmia. Available at: <http://www.omnimedicalsearch.com/conditions-diseases/arrhythmia-types.html >

[20] V. Fuster, L.E. Ryden, R.W. Asinger, et al. ACC/AHA/ESC guidelines for the management of patients with atrial fibrillation: executive summary. A report of the American College of Cardiology/American Heart Association Task Force on Practice Guidelines and the European Society of Cardiology Committee for Practice Guidelines and Policy Conferences (Committee to Develop Guidelines for the Management of Patients with Atrial Fibrillation): developed in collaboration with the North American Society of Pacing and Electrophysiology. *J Am Coll Cardiol.* 2001, 38, pp. 1231–1266

[21] A.S. Go, E.M. Hylek, K.A. Phillips, et al., Prevalence of diagnosed atrial fibrillation in adults: national implications for rhythm management and stroke prevention: the Anticoagulation and Risk Factors in Atrial Fibrillation (ATRIA) Study. *JAMA*. 2001, 285, pp. 2370–75

[22] Y. Miyasaka, M.E. Barnes, et al. Secular trends in incidence of atrial fibrillation in Olmsted County, Minnesota, 1980 to 2000, and implications on the projections for future prevalence. *Circulation*. 2006, 114, pp. 119–25

[23] Cardionet: Charging the monitor. Available at: <https://www.cardionet.com/patients_01_06.htm>

[24] R. Bouhenguel, I. Mahgoub, and M. Ilyas. "Bluetooth Security in Wearable Computing Applications," *Proceedings of the IEEE 5th International Symposium on High Capacity Optical Networks & Enabling Technologies* (HONET 2008). Penang, Malaysia. Nov. 2008, pp. 182–186

[25] J.L. Schiffer and A.E. Waltho. Safety Evaluation of Bluetooth Class ISM Band Transmitters on board Commercial Aircraft Revision 2. *Mobile Architecture Lab Technology & Research Labs.* Dec. 28, 2000

[26] P. Bonato. Wearable Sensors/Systems and Their Impact on Biomedical Engineering. *IEEE Engineering of Medicine and Biology*, 2003

[27] Bluetooth SIG, *Specification of the Bluetooth System*. Vol. 1, *Core*, Ver. 2.1, July 26, 2007

[28] C. Candolin. Security Issues for Wearable Computing and Bluetooth Technology, Online report. Available at: <http://www.cs.hut.fi/Opinnot/Tik-86.174/btwearable.pdf>

[29] S.I. Weiss and C. Kulikowski. Computer Systems That Learn: Classification and Prediction Methods from *Statistics, Neural Networks, Machine Learning, and Expert Systems*. San Francisco, CA, Morgan Kaufmann Publishers. 1991

[30] T. Mitchell. *Machine Learning*. McGraw Hill. 1997

[31] G. Piatetsky-Shapiro and W. J. Frawley. *Knowledge Discovery in Databases*. AAAI Press, Menlo Park, CA, 1991

[32] P. Bobbie, R. Keams, S. Suther and P. Brown. Finding Molecular Signature of Prostate Cancer: An Algorithm Approach. *Proceedings of the International Conference on Bioinformatics & Computational Biology*, Las Vegas, NV, 2006, pp. 265–269

[33] M.A. Bani-Hasan, Y.M. Kadah, M. Rasmy and F.M. El-Hefnawi. Electrocardiogram signals identification for cardiac arrhythmias using prony's method and neural network. Engineering in Medicine and Biology Society, 2009. EMBC 2009. *Annual International Conference of the IEEE*, Digital Object Identifier: 10.1109/IEMBS.2009.5333035, pp. 1893–96

[34] V. Mahesh, A. Kandaswamy, C. Vimal and B. Sathish. EKG arrhythmia classification based on logistic model tree. *Journal of Biomedical Science and Engineering (JBiSE).* Vol. 2, Issue 6, ISSN: 1937-6871, Oct. 2009, Start Page: 405

[35] ACC/AHA/ESC 2006 Guidelines for Management of Patients With Ventricular Arrhythmias and the Prevention of Sudden Cardiac Death: A Report of the American College of Cardiology/American Heart Association Task Force and the European Society of Cardiology Committee for Practice Guidelines. *Journal of the American College of Cardiology.* Vol. 48, No. 5, 2006, ISSN 0735-1097/06, Published by Elsevier Inc. Available at: <http://content.onlinejacc.org/cgi/content/full/48/5/e247>

[36] E. Simoudis. Reality check for data mining. IEEE Expert. 1996, Vol. 11, Issue 5, pp. 26–33

[37] P. Bajcsy, J. Han, L. Liu and J. Yang. "Survey of Bio-Data Analysis from Data Mining Perspective," Chapter 2 of J.T.L. Wang, M.J. Zaki, H. Toivonen, and D. Shasha (eds.), *Data Mining in Bioinformatics*. Springer Verlag, ISBN 978-1852336714, pp. 9–39

[38] C. Goutte. Note on free lunches and cross-validation. *Neural Computation*,1997, 9, pp. 1211–15, Available at: <http://eivind.imm.dtu.dk/dist/1997/goutte.nflcv.ps.gz>

[39] M. Stone. Asymptotics for and against cross-validation. *Biometrika* 64. 1977, pp. 29–35

[40] The MedStats Club: Statistics Tutorials, Calculators & Tools.

Available at: <http://medstats.org/Tutorials/Sensitivity%20and%20Specificity.htm>

[41] T.A. Lasko, J.G. Bhagwat, K.H.Zou and L. Ohno-Machado. The use of receiver operating characteristic curves in biomedical informatics. *J Biomed Inform.* 2005, 38, pp. 404–15

[42] J.A. Swets. Measuring the accuracy of diagnostic systems. *Science*. 1988, 240(4857), pp. 1285–93

[43] M.H. Zweig and G. Campbell. Receiver-operating characteristic (ROC) plots: a fundamental evaluation tool in clinical medicine. *Clin Chem.* 1993, 39(4), pp. 561–77

[44] N.A. Obuchowski. Receiver operating characteristic curves and their use in radiology. *Radiology.* 2003, 229(1), pp. 3–8

[45] J.A. Hanley and B.J. McNeil. The meaning and use of the area under a receiver operating characteristic (ROC) curve. *Radiology.* 1982, 143(1), pp. 29–36

[46] D. Faraggi and B. Reiser. Estimation of the area under the ROC curve. *Stat Med.* 2002, 21(20), pp. 3093–106

[47] M.J. Domanski. The epidemiology of atrial fibrillation. *Coronary Artery Disease.* 1995, 6, pp. 95–100

[48] W.B. Kannel and P.A. Wolf. Epidemiology of atrial fibrillation. In: *Atrial fibrillation: mechanisms and management*. .H. Falk and P.J. Podrid, editors. NY: Raven Press Ltd., 1992

[49] C.D. Furberg, B.M. Psaty, T.A. Manolio, et al. Prevalence of Atrial Fibrillation in Elderly Subjects (The Cardiovascular Health Study). *Am J Cardiol*. 1994

[50] A. Krahn, MD, J. Manfreda, MD, R. Tate, MSc, F. Mathewson, MD and T. Cuddy. The Natural History of Atria1 Fibrillation: Incidence, Risk Factors, and Prognosis in the Manitoba Follow-Up Study, MD, Winnipeg, Canada. *The American Journal of Medicine*. May 2005

[51] P.A. Wolf, W.B Kannel, D.L. McGee, et al. Duration of Atrial Fibrillation and Imminence of Stroke: The Framingham Study. *Stroke*. 1983, 14(5), pp. 664-667

[52] E.J. Benjamin, D. Levy, MD, S.M. Vaziri, MPh, R.B. D'Agostino, A.J. Belanger and P.A. Wolf. Independent Risk Factors for Atrial Fibrillation in a Population-Based Cohort. The Framingham Heart Study. *JAMA*. 1994, 271, pp. 840-844

[53] A.A. Latif and B.J. Messinger-Rapport. Should Nursing Home Residents with Atrial Fibrillation be Anticoagulated? *Cleve Clin J Med*. Jan. 2004

[54] B.P. Knight, G.F. Michaud, S.A. Strickberger, et al. Electrocardiographic Differentiation of Atrial Flutter from A-Fib by Physicians. *J Electrocardiol.* 1999

[55] J. Mant, D.A. Fitzmaurice, F.D. Hobbs, et al. Accuracy of Diagnosing Atrial Fibrillation On Electrocardiogram by Primary Care Practitioners and Interpretative Diagnostic Software: Analysis of Data from Screening for Atrial Fibrillation in the Elderly (SAFE) Trial. *BMJ*. 2007

[56] A. Shiyovich, A. Wolak, L. Yacobovich, A. Grosbard and A. Katz. Accuracy of Diagnosing Atrial Flutter and Atrial Fibrillation from a Surface Electrocardiogram by Hospital Physicians: Analysis of Data from Internal Medicine Departments. Cardiology Department, Soroka University Medical Center, Ashkelon, Israel. *Am J Med Sci*. 2010

[57] P. Reinelt, G. Karth, A. Geppert and G. Heinz. Incidence and Type of Cardiac Arrhythmias in Critically Ill Patients: a Single Center Experience in a Medical-Cardiological ICU. *Intensive Care Medicine*. Vol. 27, No. 9, pp. 1466-73

[58] HRS/EHRA/ECAS Expert Consensus Statement on Catheter and Surgical Ablation of Atrial Fibrillation: Recommendations for Personnel, Policy, Procedures and Follow-Up. Available at: <http://www.hrsonline.org/ClinicalGuidance/upload/HR-and-Euro-Copy-for-Print.pdf>

[59] J.V. Tu and C.D. Naylor. Clinical prediction rules. *J Clin Epidemiol.* 1997, 50, pp. 743–744

[60] D.R. Cox. Regression Models and Life-Tables, Journal articles in statistics and medicine. 1972

[61] V. Mahesh, et al., EKG arrhythmia classification based on logistic model tree. *Journal of Biomedical Science and Engineering (JBiSE).* Vol. 2, Issue 6, ISSN: 1937-6871, Oct. 2009, Start Page: 405

[62] WEKA. Available at: <http://www.cs.waikato.ac.nz/~ml/weka/index.html>

[63] UCI Machine Learning Repository. Available at: <http://www.ics.uci.edu/~mlearn/MLRepository.html>

[64] PhysioBank, ANSI/AAMI EC13 Test Waveforms, Available at: <http://physionet.org/physiobank/database/aami-ec13/ >

[65] J. Han and M. Kamber. *Data Mining: Concepts and Techniques*, Morgan Kaufmann Publishers, San Francisco, CA, 2001

[66] I. H. Witten and E. Frank. *Data Mining: Practical Machine Learning Tools and Techniques with Java Implementations.* Morgan Kaufmann Publishers, San Francisco, CA, 2000

[67] B. Tabachnick and L.Fidell. *Using Multivariate Statistics*, 3rd ed.. Harper Collins,1996

[68] P. Komarek and A. Moore. Fast Robust Logistic Regression for Large Sparse Datasets with Binary Outputs. In *Artificial Intelligence and Statistics*. 2003

[69] Crossbow Technology, Inc. Available at: <www.xbow.com>

[70] T. Fulford-Jones, G.-Y. Wei and M. Welsh. A Portable, Low-Power, Wireless Two-Lead EKG System. Division of Engineering and Applied Sciences, Harvard University., *Proceedings of the 26th Annual International Conference of the IEEE EMBS.* San Francisco, CA, Sept. 1-5, 2004

[71] V. Fuster (ed.), Hurst's *The Heart*, 10th ed., New York, NY, McGraw-Hill Medical Publishing, 2001, Ch. 11

[72] J. Hill, R. Szewczyk, A. Woo, S. Hollar, D.E. Culler, and K.S.J. Pister. "System architecture directions for networked sensors." In *Architectural Support for Programming Languages and Operating Systems*. 2000, pp. 93–104

[73] M. Klein, MD. Clinical Professor of Medicine at Boston University, Assessment.

[74] Xiao, Yang, Hui Chen, and Frank Haizhon Li. Handbook on sensor networks. World Scientific Publishing Company, 2010.

[75] Skynet technology. Available at: < http://www.skynetlovesyou.com/>,

[76] Duracell battery. Available at: <http://www1.duracell.com/oem/Pdf/new/MN1500_US_CT.pdf>

[77] Rim Blackberry Torch 9800 OEM Battery 1270mah F-S1

Available at: <http://us.blackberry.com/smartphones/blackberrytorch/#!phone-specifications>

<http://www.trait-tech.com/product/T-F-S1__new-rim-blackberry-torch-9800-oem-battery-1270mah-f-s1/>

[78] A. Ruigómez, S. Johansson, M.-A. Wallander, L. Alberto and G. Rodríguez. Incidence of chronic atrial fibrillation in general practice and its treatment pattern. *Journal of Clinical Epidemiology.* 2001, 55, pp. 358–363

[79] S. Stewart, C.L. Hart, D.J. Hole and J.J. McMurray. Population prevalence, incidence, and predictors of atrial fibrillation in the Renfrew/Paisley study. *Heart.* 2001, 86, pp. 516–521

[80] A. Majeed, K. Moser, and K. Carroll. Trends in prevalence and management of atrial fibrillation in general practice in England and Wales. 1994-98 GPRD. *Heart.* 2001, 86, pp. 284–288

[81] Guidelines for the Management of Atrial Fibrillation: The Task Force for the Management of Atrial Fibrillation of the European Society of Cardiology (ESC), Europace. Oct. 2010

[82]WB Kannel, PA Wolf et al. Prevalence, incidence, prognosis, and predisposing conditions for AF: population based estimates. Am J Cardiol. 1998;pp.82:2N

[83] S.S. Rathore, A.K. Berger, K.P. Weinfurt, et al. Acute myocardial infarction complicated by atrial fibrillation in the elderly: prevalence and outcomes. *Circulation*. Mar 7, 2000, 101(9), pp. 969-74

[84] G.D. Karth, P. Reinelt, A. Buberl, A. Geppert, M. Huelsmann, R. Berger and G. Heinz. Circadian variation in ventricular tachycardia and atrial fibrillation in a medical-cardiological ICU. *Intensive Care Medicine.* Vol. 29, No. 6, pp. 963-968, DOI: 10.1007/s00134-003-1735-x

[85] S. Viskin, M. Golovner, N. Malov, R. Fish, I. Alroy, Y. Vila, S. Laniado, E. Kaplinsky and A. Roth. Circadian variation of symptomatic paroxysmal atrial fibrillation, Data from almost 10, 000 episodes. *European Heart Journal* (1999) 20, pp. 1429–34, Article No. euhj.1999.1632, Available at: <http://www.idealibrary.com>

[86] E.J. Benjamin, P.A. Wolf, R.B. D'Agostino, H. Silbershatz, W.B. Kannel and D. Levy. Impact of atrial fibrillation on the risk of death: the Framingham Heart Study. *Circulation*. 98(10), Sept. 8, 1998, pp. 946-52

[87] Alive Heart and Activity Monitor, Alive Technologies Pty. Ltd. Available at: http://www.alivetec.com/products.htm

[88] R. Bouhenguel and I. Mahgoub. A Risk and Incidence Based Atrial Fibrillation Detection Scheme for Wearable Healthcare Computing Devices. *6th International Conference on Pervasive Computing Technologies for Healthcare.* In Press 2012

[89] T. Krazit. ARMed for the living room. Available at: <http://news.cnet.com/ARMed-for-the-living-room/2100-1006_3-6056729.html#ixzz1B9lKQ0bN>

[90] Detailed Technical Datasheet of RIM BlackBerry Curve 8900: Available at: <http://pdadb.net/index.php?m=specs&id=1568&view=1&c=rim_blackberry_curve_8900_rim_javelin>, retrieved 09/12/2010

[91] R. Bouhenguel, I. Mahgoub and M. Ilyas. Window-Based Energy-Aware Model for Real-Time Detection and Reporting of Progressive Development of Cardiac Atrial Fibrillation in Wearable Computing, *Proceedings of the IEEE 5th International Symposium on High Capacity Optical Networks & Enabling Technologies* (HONET 2011). Riyadh, Saudi Arabia, 2011

[92] R. Bouhenguel, I. Mahgoub and M. Ilyas. An Energy Efficient Model for Monitoring and Detecting Atrial Fibrillation in Wearable Computing. *BODYNETS2012*. Oslo, Norway. In Press, 2012

[93] Atrial Fibrillation (for Professionals). American Heart Association, Inc. 2008-12-04. Available at: <http://www.americanheart.org/presenter.jhtml?identifier=1596> Retrieved April, 14, 2010

[94] T.E. Cuddy and S.J. Connolly. Atrial fibrillation and atrial flutter. *Can J Cardiol*. 1996, 12(SupplA), pp. 9–11

[95] B.M. Psaty, T.A. Manolio, L.H. Kuller, R.A. Kronmal, M. Cushman, L.P. Fried, R. Wite, C.D. Furberg and P.M. Rautaharju. Incidence of and risk factors for atrial fibrillation in older adults. *Circulation*. 1997, 96, pp. 2455–6.

[96] A. Hansson, B. Madsen-Härdig and S.B. Olsson. Arrhythmia-provoking factors and symptoms at the onset of paroxysmal atrial fibrillation: A study based on interviews with 100 patients seeking hospital assistance. *BMC Cardiovascular Disorders.* 2004, 4:13 doi:10.1186/1471-2261-4-1

[98] R. Bouhenguel and I. Mahgoub. Cardiac Arrhythmia Monitoring and Detection Techniques in Wearable Healthcare Computing Devices, Book Chapter, Springer, 2012

[99] T. Moukabary. Willem Einthoven (1860–1927): Father of electrocardiography. *Cardiology Journal*. 2007, Vol. 14, No. 3, pp. 316–317

[100] R.J. Myerburg, A. Interian, J. Simmons and A. Castellanos. Sudden cardiac death. In: Zipes DP, ed. *Cardiac Electrophysiology: From Cell to Bedside*. 4th ed. Philadelphia: WB Saunders. 2004, pp. 720–731

[101] The ECG Learning Center, The Standard 12 Lead ECG: <http://ecg.utah.edu/lesson/1>, retrieved on 10/10/2011

[102] PC World Test Center battery life test results for 3G smartphones, <http://www.pcworld.com/article/148348/3G_iPhone_Battery_Life.html>, retrieved on 10/11/2010

[103] Agur AMR, Dalley AF, Moore KL. The thorax. *Clinically Oriented Anatomy*. 5th ed. Philadelphia, Pa: Lippincott Williams & Wilkins; 2005.

[104] Encyclopedia of Health: Electrophysiology study (EPS) - diagnostic procedure heart <http://www.beltina.org/health-dictionary/sick-sinus-syndrome-symptoms-treatment.html> retrieved on 10/11/2011

[105] L. Doherty, B.A. Warneke, B.E. Boser, and K.S.J. Pister. "Energy and performance considerations for smart dust." *International Journal of Parallel and Distributed systems and Networks*. 2001, Vol. 4, No. 3, pp. 121-33